PREcast Seismic Structural Systems

PRESSS

Volume 3 - 09

DESIGN GUIDELINES
FOR
PRECAST CONCRETE SEISMIC STRUCTURAL
SYSTEMS

by

John F. Stanton and Suzanne D. Nakaki

The University of Washington and The Nakaki Bashaw Group, Inc.

Abstract

This report describes the methods that are proposed for designing five seismic structural systems made from precast concrete. Those five systems formed the structural framing in the PRESSS Phase III test building that was tested at the University of California at San Diego in August and September 1999. Four of the five systems were based on new structural concepts, and are intended to behave quite differently from the cast-in-place concrete framing systems around which present codes are written. One of the goals of the test was to provide validation for those systems.

The four new systems were:

- A precast wall, in which the individual panels are vertically post-tensioned to the foundation and are designed to rock about their bases under seismic loading. Ductile connections crossing the vertical joints between panels dissipate energy as they deform in shear.
- An unbonded pre-tensioned frame, in which the precast beams are continuous through the joints and the columns are fabricated in one-story segments. Building drifts are accommodated by development of a single crack in the beam at the beam-column interface. The unbonded pre-tensioning remains elastic and closes the crack as soon as the lateral load is removed.
- An unbonded post-tensioned frame, in which the precast columns are continuous through the joints and the beams are fabricated in one-bay segments. Building drifts are accommodated by development of a single crack between the beam and column at their interface. The unbonded post-tensioning remains elastic and closes the crack as soon as the lateral load is removed. Deformed reinforcing bars also cross the interface, but are bonded in their ducts by grouting. They yield alternately in tension and compression and, in so doing, dissipate energy.
- A yielding "gap" frame, in which a gap is left between the beam and column over most of the beam height, except at the bottom, where a grout pad joins the two. Post-tensioning along the length of the beam line maintains a permanent clamping force between the beams and columns. Reinforcing bars cross the gap at the top of the beam and yield alternately in tension and compression. The concrete at the top of the beam never comes into contact with the column. The purpose of the system is to reduce the problem of beam elongation during cyclic loading.

In addition, a yielding frame, without gaps or pre-stressing, was incorporated in the building in order to represent existing technology. It was constructed by grouting bars into ducts to connect the beams to the columns. It develops its moment resistance by tension and compression yielding of the bars.

The behavior expected of each system is described, and step-by-step design procedures are given for the primary components of each system.

Acknowledgements

Table of Contents

List of Tables.

List of Figures.

1 INTRODUCTION

1.1 Background

PRESSS is an acronym for PREcast Seismic Structural Systems, a program of structural engineering research into precast concrete building systems suitable for seismic conditions. That research was conducted jointly by researchers from eight universities, the National Institute for Science and Technology, and the practicing engineering community. The research was funded jointly by the National Science Foundation and the precast concrete industry. Priestley [1996] provides an overview of the program. The primary goals were:

- To develop comprehensive and rational design recommendations needed for broader acceptance of precast concrete construction in different seismic zones.
- To develop new materials, concepts and technologies for precast concrete construction in different seismic zones.

The program consisted of three phases. In Phase I, fundamental concepts were developed. In Phase II, laboratory tests were conducted on connections and sub-assemblages. In Phase III, a complete building was designed, using the concepts and connections developed in the earlier phases, and was tested under lateral loading.

This report summarizes the design methods associated with the five seismic framing systems incorporated in the PRESSS Phase III test building.

That building was 60% full scale, and was two bays long, two bays wide and five stories high. Typical floor plans are shown in Figure 1.1. The building derived its lateral resistance from two perimeter frames in the north-south direction and from a central spine wall running east-west. The frame on the east side of the building contained two different framing concepts that relied on pre-stressing, while the west one consisted of two non-pre-stressed systems. The wall was post-tensioned to the foundation. Two flooring systems were used; the lower three floors were constructed from pre-topped double-tees while the upper two floors used hollow-core with a cast-in-place topping.

The precast seismic systems used in the test building possess several novel features [Nakaki et al. 1999]. First, they all take advantage of the jointed nature of precast concrete construction by concentrating the deformations in the connections. By this means the deformations in, and therefore the damage to, the members themselves is minimized. This approach opens possibilities of true performance-based design by giving the designer tools with which to control the level of damage caused by an earthquake. Second, several of the systems re-center after the lateral loading is removed, leading to essentially zero residual drift. These characteristics constitute performance that is superior to the life-safety-only requirements of traditional building codes. In particular, they provide the engineer with tools to design for low repair costs and early re-use of the building after an earthquake. Last, the systems require the use of no unfamiliar

technologies, but rely for their functioning on new arrangements of existing materials. This should help them to gain acceptance in the construction community.

Double Tee Floor
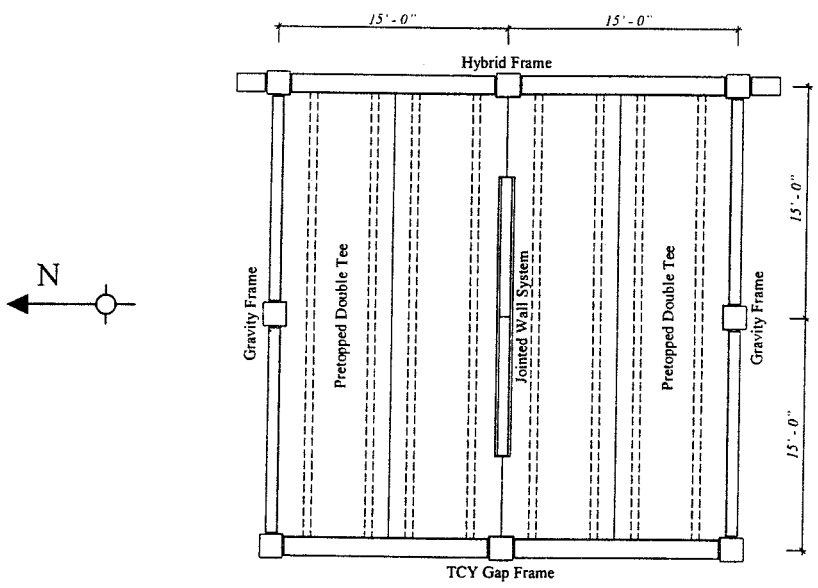
Hollowcore Floor
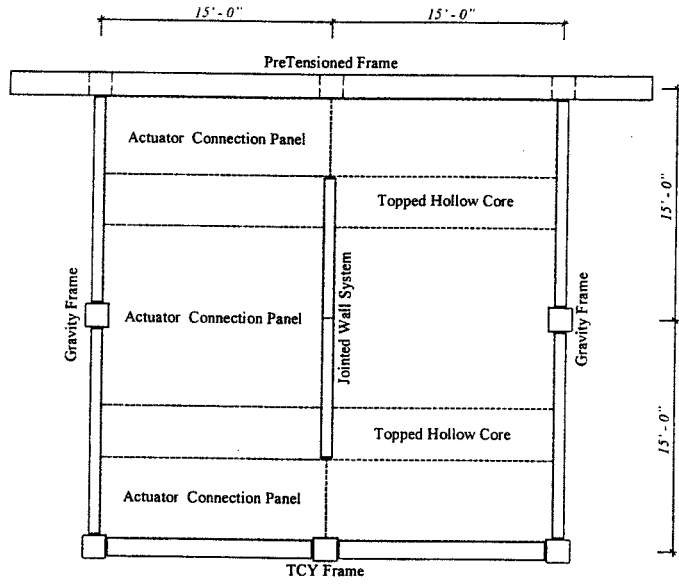
Figure 1.1: PRESSS Test Building Floor Plans
(Courtesy Prof. Sri Sritharan)

More detailed information on the design, construction and testing of the PRESSS Phase III test building may be found in the reports listed in Appendix A.

1.2 Pre-stressed Framing Systems

Some of the precast seismic framing systems contain pre-stressed reinforcement that is unbonded over part or all of its length. The pre-stressing may be achieved by pre- or post-tensioning. The frames may also contain some deformed bar reinforcement to dissipate energy through yielding in tension and compression. Thus four combinations are possible, and are illustrated in Figure 1.2. They are:

- A post-tensioned frame without damping
- A post-tensioned frame with damping
- A pre-tensioned frame without damping
- A pre-tensioned frame with damping

	Pre-tensioned	Post-tensioned
With Damping		
Without Damping		

Figure 1.2: Pre-stressed Frames with and without Damping.

The PRESSS Phase III Test Building contained only two of the four: the post-tensioned frame with damping and the pre-tensioned frame without damping. However, the results obtained from them are considered adequate to show that the basic concepts for all four types are valid.

1-3

Priestley and MacRae [1996] tested several post-tensioned frame connections without damping, and achieved satisfactory results. The post-tensioned system without damping is designed in the same way as the pre-tensioned system without damping of Chapter 4, except that the cracking moment does not need to be evaluated since the interface is pre-cracked.

At the time of writing no pre-tensioned frame with damping has been tested. However, its behavior is expected to be similar to that of damped post-tensioned precast frame described in Chapter 5, and it should be designed according to the principles presented there.

1.3 Format of the Report

This report is divided into five main chapters (Chapters 3-7), each of which describes a single system and is largely autonomous. Each of those chapters presents, for the system that it addresses, the design concept, the design procedure, important construction issues and a brief discussion.

Preceding these main chapters is Chapter 2, which discusses the derivation of earthquake loads and the appropriate limit states. That information is included because the test building was designed using displacement-based methods, which may be unfamiliar to some designers.

At the end of the report are a list of acronyms, a list of definitions, and a list of symbols. In addition, all symbols are defined in any chapter in which they are used.

1.4 Notation

The notation used in this report does not correspond to that used in any single code or standard. While much of it follows ACI notation, differences exist. There are several reasons for the divergence. First, the material contained herein must be read in conjunction with several different published documents, all of which use different notation. Second, ACI notation does not use a consistent set of subscripts. For example, pre-stressed reinforcement is sometimes indicated by the subscript "p", (as in f_{py}) and sometimes by the subscript "s" (as in f_{se}). In this report, the need to distinguish between pre-stressed and non-pre-stressed reinforcement is paramount, so such anomalies were considered unacceptable.

Inasmuch as possible, the notation adheres to the following principles. Greek symbols represent dimensionless coefficients or ratios. Roman symbols represent variables that carry dimensions. Of the latter, stresses are given by lower case letters and forces by upper case letters. Subscripts "p" and "s" refer to pre-stressed and non-pre-stressed steel reinforcement respectively. Subscripts "0" and "des" refer to the zero drift state and the design limit state respectively.

2 DEVELOPMENT OF EARTHQUAKE LOADS FOR DESIGN

The PRESSS Phase III Test Building was designed using Displacement Based Design [Priestley and Kowalsky, 2000]. This is a relatively new approach to developing seismic design loads that provides a rational alternative to the Force-Based Design procedures that are required by almost every contemporary code. In the interests of providing a background on the environment in which the design equations presented in the following chapters were developed, this chapter contains a brief discussion of Force and Displacement Based Design methodologies.

2.1 Force-Based Design

Force Based Design procedures for computing seismic loads are contained in current design codes, such as the UBC ["Uniform" 1997], the NEHRP provisions [NEHRP, 2000] and the IBC ["International", 2000]. The most commonly used approach is the Equivalent Lateral Force (ELF) procedure, in which the elastic response to the design earthquake ground motion is first computed using assumed values of stiffness, after which it is modified using empirical factors to approximate the effects of inelastic response. An estimate of the drift under the design loading is obtained by computing the drift of an elastic model of the structure under the design load, then modifying that by an empirical factor to account for the influence of inelasticity.

2.2 Displacement-Based Design

2.2.2 Overview

Displacement Based Design (DBD) embodies the philosophy that a structure should be designed to achieve a specified drift during a specified ground motion. The strength of the structure is then selected by rational means to ensure that this goal is met. The displacement is the key parameter, and the loads are derived from it. This approach is essentially the reverse of the traditional Force Based Design (FBD), in which the loads are derived first and an estimate of the drift is then obtained from the computed loads.

Priestley [2000] has described the Displacement Based Design method in some detail, so only a summary is given here. The method has its origins in the work of Gulkan and Sozen [1974] and Shibata and Sozen [1976], but has undergone considerable development since then [Priestley and Kowalsky, 2000], and is now incorporated into the SEAOC Recommended Lateral Force Requirements ["Tentative",1999] as a viable approach to determining seismic loads.

Two important assumptions underlie it:

- First, the response of the structure is dominated by a deformed shape that resembles the fundamental inelastic mode shape. This is essentially the same assumption as is made in the Equivalent Lateral Force embodiment of existing force-based design. It generally leads to a

reasonable description of the building and story drifts but, because it excludes higher mode effects, it cannot be used alone to calculate individual story forces and the corresponding floor-to-frame connection forces. The inelastic mode shape is defined in the same way as an elastic mode shape, namely the shape that leads to identical distributions of load and response. However the inelastic shape is not a mode shape in the sense of an eigenvector to a linear system, because it lacks some of the properties, such as orthogonality, of a true mode shape. The shape also varies with the intensity of the applied load. In DBD, a shape is chosen that approximates the displaced shape of the inelastic system at the design load.

- Second, the peak displacement of an inelastic SDOF system is the same as that of a viscously damped elastic system if the two have, at peak drift, the same secant stiffness and energy dissipation per cycle.

2.2.3 Notation

A_{loop}	= area of hysteresis loop
A_{rect}	= area of rectangle circumscribing hysteresis loop
$\{e\}$	= vector with elements = 1.0 in DOFs parallel to ground motion and 0.0 elsewhere
C_d	= ratio of inelastic to elastic drift
f_{pu}	= specified strength of pre-stressing tendon material
f_{py}	= specified yield strength of pre-stressing tendon material
f_{sy}	= specified yield strength of deformed reinforcement
K	= stiffness of SDOF system
K_{eq}	= secant stiffness of true hysteretic system at maximum displacement
L	= earthquake participating mass
M	= mass of SDOF system
$[M]$	= mass matrix
M^*	= generalized mass in first mode
$M_{cap,tot}$	= total moment capacity
$M_{cap,p}$	= moment capacity provided by pre-stressed reinforcement
$M_{cap,s}$	= moment capacity provided by yielding reinforcement
$M_{cap,tot}$	= total moment capacity
M_{eff}	= effective mass in first mode
$M_{s',des}$	= resisting moment provided by compression deformed reinforcement at design limit state
R	= seismic response modification factor
S_a	= spectral acceleration
S_d	= spectral displacement
T	= period of linear elastic SDOF system
T_{eq}	= period of equivalent viscously-damped linear SDOF system
V_{des}	= design base shear
V_{eq}	= design base shear of equivalent viscously-damped linear system
V_{max}	= peak shear experienced during pushover analysis
Γ	= earthquake participation factor

Δ_M	= inelastic drift of structure under reduced earthquake load in 1997 UBC
Δ_S	= elastic drift of structure under reduced earthquake load in 1997 UBC
$\Delta_{tar,MDOF}$	= target displacement for MDOF system
$\Delta_{tar,SDOF}$	= target displacement for SDOF system
θ_{des}	= design interface rotation, consistent with design moment, M_{des}
λ	= over-strength factor
λ_p	= over-strength factor for pre-stressed reinforcement in tension
λ_s	= over-strength factor for deformed reinforcement in tension
$\lambda_{s'}$	= over-strength factor for deformed reinforcement in compression
ξ	= viscous damping
ξ_{eq}	= viscous damping in equivalent linear system
$\xi_{eq,calc}$	= calculated viscous damping in equivalent linear system
$\xi_{eq,est}$	= estimated viscous damping in equivalent linear system
$\{\phi_{eq}\}$	= equivalent mode shape, or assumed deformed shape
ω	= natural frequency of SDOF system
ω_{eq}	= natural frequency of equivalent linear SDOF system

2.2.4 Procedure

The core of the DBD method may be explained most easily by considering the simplest case of a viscously damped linear Single Degree-of Freedom (SDOF) system in which the system mass and damping are assumed to be known. The objective is to design the system so that it will reach a specified displacement (the design displacement, $\Delta_{tar,SDOF}$) when subjected to a specified ground motion. The procedure is illustrated in Figure 2.1.
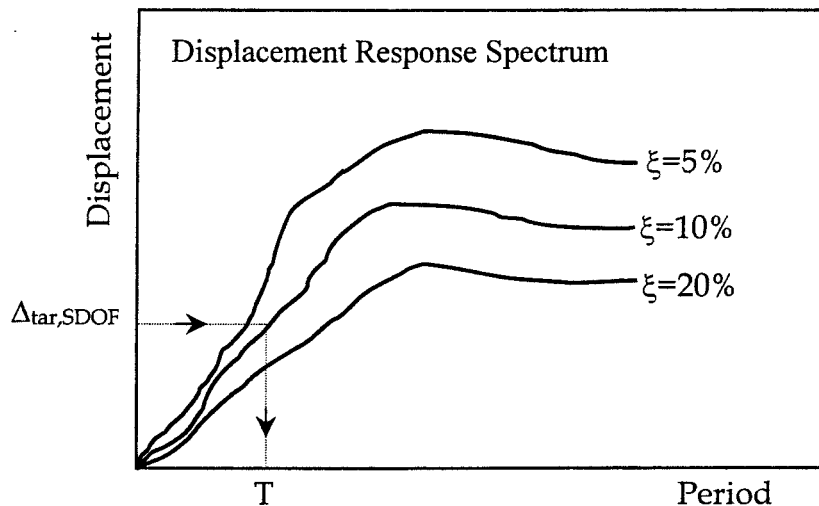
Figure 2.1: Use of DRS to Find Period Corresponding to a Target Displacement

2-3

It requires the elastic Displacement Response Spectrum (DRS) for the ground motion in question. This can easily be obtained from the traditionally used Acceleration Response Spectrum (ARS) for the motion by dividing each ordinate of the ARS by ω^2, since

$$S_d = \frac{S_a}{\omega^2} \quad\text{..(2.1)}$$

Figure 2.1 shows curves typical of a DRS for a specific ground motion. For design, the DRS is likely to be idealized by a series of smooth curves or lines, such as shown in Figure 2.2a. The conversion from ARS to DRS is illustrated for a typical design spectrum in Figure 2.2b.
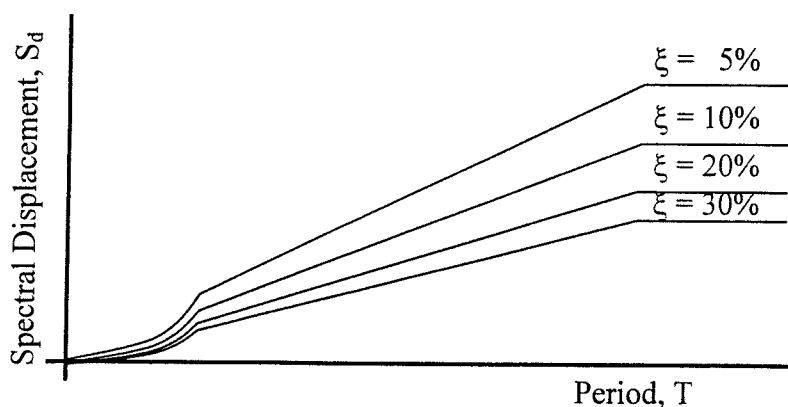
Figure 2.2a. Typical design DRS
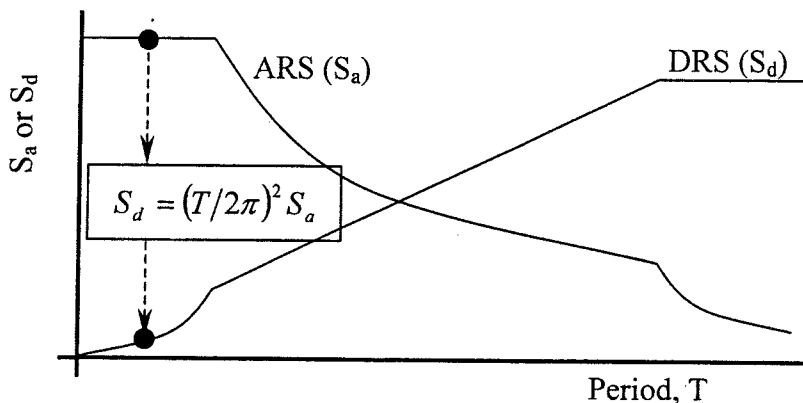
Figure 2.2b. Conversion from ARS to DRS

The design calculations consist of entering the DRS with the design displacement, $\Delta_{tar,SDOF}$, and finding the period, T, that corresponds to it. The curve corresponding to the correct damping for the system relates the displacement and the period. The required stiffness can then be obtained from the period, T, and the known mass, M, because

$$K = M\omega^2 = M\left(\frac{2\pi}{T}\right)^2 \dotfill (2.2)$$

Once the required stiffness is known, the member sizes can be selected and the design is complete.

If the true system is hysteretic, rather than elastic, the procedure must be augmented by a second step that relates inelastic and elastic behavior. The (SDOF) hysteretic system is approximated by an equivalent viscously damped one. The two are equivalent in that the stiffness of the elastic system is the same as the secant stiffness of the inelastic system at the design drift. The viscous damping is selected to give the same energy dissipation per cycle as exists in the hysteretic system at peak drift. The hysteretic energy dissipation per cycle, and therefore the equivalent damping, is assumed here to be known at the start of the design. (A modification to address the case in which it is not known is described below). The DRS is entered, as before, with $\Delta_{tar,SDOF}$ to find a period. The resulting period is T_{eq}, the period of the equivalent elastic system that, when combined with the known damping, will result in the desired $\Delta_{tar,SDOF}$. The equivalent stiffness, K_{eq}, corresponding to T_{eq}, is then computed from

$$K_{eq} = M\left(\frac{2\pi}{T_{eq}}\right)^2 \dotfill (2.3)$$

An elastic system with this stiffness will result in the desired displacement, $\Delta_{tar,SDOF}$. The required strength of the real hysteretic system can be obtained from the equivalent elastic one by reference to Figure 2.3 and Equation 2.4.
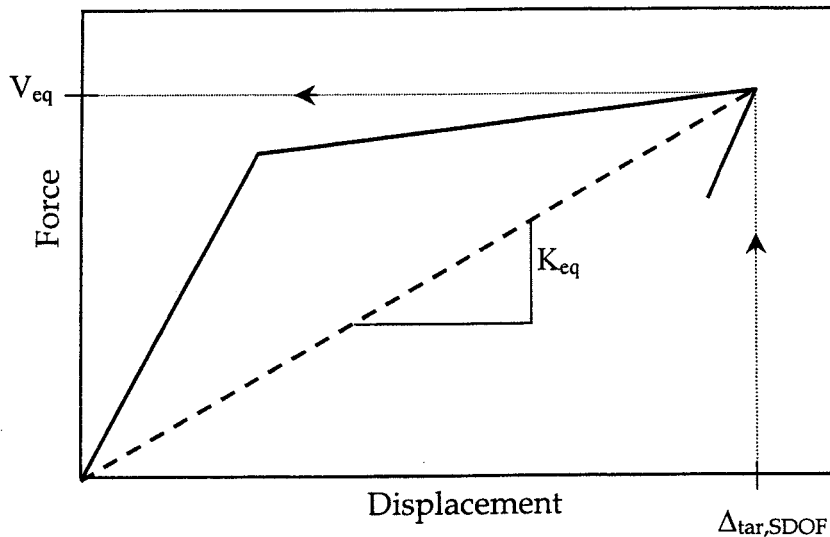
Figure 2.3 Relationship among $\Delta_{tar,SDOF}$, V_{eq} and K_{eq}.

$$V_{eq} = K_{eq}\Delta_{tar,SDOF} \dotfill (2.4)$$

Since $\Delta_{tar,SDOF}$ was selected by the designer, and is therefore known, V_{eq} can be computed directly from Equation 2.4.

Once the required strength, V_{eq}, has been computed, the member sizes can be selected and the complete load vs. displacement curve can be constructed. The area inside the hysteresis loop is equal to the energy dissipated per cycle, from which the equivalent damping can be computed. For systems with the same properties in each direction, the equivalent damping [Chopra, 1999] is given by using Equation 2.5.

$$\xi_{eq} = \frac{2}{\pi} \frac{A_{loop}}{A_{rect}} \dotfill (2.5)$$

where A_{loop} = area enclosed by the hysteresis loop
$\quad\quad A_{rect}$ = area of the rectangle circumscribing the hysteresis loop

If ξ_{eq} differs from the value assumed at the start of the analysis, the computations must be repeated with the new ξ_{eq} until convergence is achieved.

If, in addition, the system has more than one Degree of Freedom (DOF), a procedure is needed for reducing the Multi-Degree-of-Freedom (MDOF) system to an equivalent SDOF one, so that the DRS can be used. This is done using classical modal analysis procedures, except that a deformed shape, $\{\phi_{eq}\}$, is assumed for the MDOF hysteretic system and is used in place of the true first elastic mode shape. Approximate shapes are suggested by Priestley and Kowalsky [2000]. Use of this equivalent mode shape leads to

$$M^* = \{\phi_{eq}\}^T [M]\{\phi_{eq}\} \dotfill (2.6)$$

$$L = \{\phi_{eq}\}^T [M]\{e\} \dotfill (2.7)$$

$$\Gamma = \frac{L}{M^*} \dotfill (2.8)$$

$$M_{eff} = \frac{L^2}{M^*} \dotfill (2.9)$$

$$\Delta_{tar,SDOF} = \Delta_{tar,MDOF} / \Gamma \dotfill (2.10)$$

where $\{\phi_{eq}\}$ = equivalent mode shape (i.e. shape chosen by the engineer to represent the deflected shape of the structure at the design drift)
$\quad\quad$ [M] = mass matrix
$\quad\quad$ $\{e\}$ = vector with elements = 1.0 in DOFs parallel to the ground motion and 0.0 elsewhere
$\quad\quad$ Γ = earthquake participation factor

L   = earthquake participating mass
M^* = generalized mass in first mode
M_{eff} = effective mass in first mode

The equivalent mode shape, $\{\phi_{eq}\}$, should be normalized so that it has the value 1.0 at the location where the target displacement, $\Delta_{tar,MDOF}$ is measured in the MDOF system.

After computing the design base shear, V_{des}, on the basis of an assumed level of damping, and designing the corresponding member sizes and strengths, the true damping supplied by the MDOF hysteretic system must be computed. This may be done by conducting a single-cycle "pushover" analysis on the MDOF system, using imposed lateral displacements distributed in the assumed displaced shape (the equivalent mode shape). The structure should be pushed to $\Delta_{tar,MDOF}$, reversed to $-\Delta_{tar,MDOF}$, then taken back to zero displacement. Equation 2.5 can then be used to determine the equivalent damping, for symmetric systems. In Equation 2.5, A_{loop} is given by the energy dissipated by the MDOF system and A_{rect} is given by ($4\Delta_{tar,SDOF}*V_{max}$), where V_{max} is the peak base shear experienced during the pushover analysis.

For hysteretic MDOF systems, the procedure may be broken into nine steps, shown in Figure 2.4.

Step 1. *Select the target displacement, $\Delta_{tar,MDOF}$.* A possible basis for the choice is the amount of drift-induced damage to the building that is deemed to be tolerable under the intensity of ground motion being considered.

Step 2. *Estimate the equivalent viscous damping of the structure, $\xi_{eq,est}$.* The exact value is not important at this stage because it will be corrected in subsequent iterations. The value depends on the ductility demand. In the absence of better information, the following starting values may be used as a guide: 5-8% for undamped unbonded pre-stressed systems, 8-15% for unbonded pre-stressed frames and walls with damping, and 15-25% for yielding or yielding gap frames.

Step 3. *Select a deformed shape, $\{\phi_{eq}\}$.* The shape should resemble the expected deformed shape of the structure at the design drift. This shape is used as the equivalent mode shape in the analysis that follows.

Step 4. *Compute the Earthquake Participation Factor, Γ,* that converts the roof displacement of the MDOF system to the displacement of the associated SDOF system, using conventional modal techniques and treating the deformed shape of Step 3 as an elastic mode shape. If the equivalent mode shape is normalized so that the element corresponding to the roof displacement is 1.0, and if the MDOF target displacement is measured at the roof, the Earthquake Participation Factor, Γ, is defined by

$$L = \{\phi_{eq}\}^T [M]\{e\} \quad\text{..(2.11)}$$

START

Step 1
Choose the MDOF design displacement, $\Delta_{tar,MDOF}$

Step 2
Estimate $\xi_{eq,est}$ = estimated damping ratio of the structure

Step 3
Select equivalent mode shape, $\{\phi_{eq}\}$

Step 4
Reduce MDOF to SDOF system. Calculate M^*, L, M_{eff}, Γ, $\Delta_{tar,SDOF}$

Step 5
Obtain T_{eq} from $\Delta_{tar,SDOF}$ and Displacement Response Spectrum

$\xi=5\%$
$\xi=15\%$
$\xi=25\%$

$\Delta_{tar,SDOF}$

T_{eq}

Step 6
Compute $K_{eq} = \omega_{eq}^2 M^*$

Step 7
Compute design base shear $V_{des} = K_{eq} \Delta_{tar,SDOF}$

Step 8
Compute member forces corresponding to V_{des}.

Design structural members

Step 9
Calculate $\xi_{eq,calc}$ = true damping

V_{des}

$\Delta_{tar,SDOF}$

$\xi_{eq,calc} = \xi_{eq,est}$?

No

Yes

END

Figure 2.4: Flowchart for Displacement Based Design

2-8

$$M^* = \{\phi_{eq}\}^T [M]\{\phi_{eq}\} \dotfill (2.12)$$

$$\Gamma = \frac{L}{M^*} \dotfill (2.13)$$

The target drift of the SDOF system is then

$$\Delta_{tar,SDOF} = \Delta_{tar,MDOF} / \Gamma \dotfill (2.14)$$

Step 5. *Compute the Equivalent Period, T_{eq},* necessary to achieve $\Delta_{tar,SDOF}$ during the design earthquake, given the estimated damping, $\xi_{eq,est}$, and the DRS.

Step 6. *Compute the Equivalent Stiffness, K_{eq},* for the SDOF system from the equivalent period and the known mass of the structure, by

$$K_{eq} = \left(\frac{2\pi}{T_{eq}}\right)^2 M^* \dotfill (2.15)$$

Step 7. *Compute the Design Base Shear* from

$$V_{des} = K_{eq}\Delta_{tar,SDOF} \dotfill (2.16)$$

Compute the story loads using the distribution defined by the equivalent mode shape.

Step 8. *Analyze the structure* under the loads of Step 7, obtain the member forces and design the members to resist them.

Step 9. *Determine the Energy Dissipated per Cycle* (EDC) by the structure from a cyclic push-pull analysis or otherwise, and re-evaluate the equivalent viscous damping. It is given by

$$\xi_{eq,calc} = \frac{2}{\pi}\frac{A_{loop}}{A_{rect}} \dotfill (2.17)$$

If the value of $\xi_{eq,calc}$ differs significantly from the previous estimate, $\xi_{eq,est}$, repeat Steps 5-9 with the new estimate of damping.

2.2.5 Discussion of Displacement Based Design

Displacement Based Design addresses primarily the response in the fundamental mode of vibration. In almost all two-dimensional systems, this represents the vast majority of the displacement. However, local forces, such as floor-to-wall forces in a wall structure, may be

much larger than those predicted from the basic DBD procedure because of the local effect of higher modes. The same is true for the FBD procedure. Consideration of such forces is important at least in the design of connections. One approach to estimating the effects of higher modes is given by Eberhard and Sozen [1993]. It is applicable to both FBD and DBD.

One of the consequences of using DBD is that the required strength is related to the available damping. Thus, if two systems have identical stiffnesses but different damping characteristics, the one with the smaller damping will require a larger strength if both are to reach the same prescribed drift. This feature of the DBD procedure reflects the physics of the problem, but is not taken into account by FBD. As an example, if a pre-stressed frame with damping and a pre-stressed frame without damping are under consideration for a particular building, if DBD is used, and if the same drift limit is imposed for both systems, the design loads will be higher in the system without damping.

2.2.6 Comparison of Force and Displacement Based Design Procedures

The Displacement-Based Design procedure is essentially the reverse of that used in Force-Based Design. A comparison of the two procedures helps to bring out the differences between them.

The Equivalent Lateral Force (ELF) procedure is perhaps the most commonly used manifestation of FBD. In it, the structural configuration is selected and approximate member sizes are assumed, then the period of the structure is taken either from an eigenvalue analysis of an elastic model of the structure or from empirical equations in the code. The elastic response, and in particular the maximum elastic forces, are found from a simplified acceleration response spectrum and the computed period. They are applied over the height of the structure according to a code-specified distribution that approximates the first mode of vibration but that also includes an empirical allowance for higher mode effects. The design forces, which represent inelastic response, are obtained by dividing the elastic forces by an empirical factor, R [e.g., "Uniform", 1997]. That factor is based purely on the type of system, and not on the individual characteristics of the building in question.

The global displacements are estimated by applying the design (i.e. inelastic) forces to an elastic model of the structure and computing the displacements. These displacements (Δ_S in UBC 1997) have no physical meaning, but are converted to the estimated design displacements, Δ_M, by multiplying by an empirical factor of C_d ["International" 2000] or 0.7R ["Uniform" 1997]. These estimated design displacements are computed without reference to the real damping available, and depend on the validity of the empirical "Equal Displacements Rule" [Veletsos and Newmark, 1960]. Furthermore, the maximum displacement, Δ_S, is sensitive to the elastic stiffness of the structure, which in turn depends on the level of cracking assumed in the concrete. Thus the estimated design displacement, Δ_M, also depends on the assumptions that underlie the analytical model of the structure.

The primary approximations in FBD lie in the assumption that inelastic forces can be obtained satisfactorily from the response of an elastic model with a nominal 5% damping, through the use of an empirical modifying factor that is based solely on the type of vertical structure.

Computation of the displacements rely on the design forces, the properties of the elastic model of the structure, and the empirical factor that is used to relate elastic and inelastic displacement. That factor relies in part on the validity of the "Equal Displacements Rule".

In DBD, the maximum displacement is selected by the designer, then the required strength of the system is computed by assuming that the inelastic system can be represented by an equivalent elastic system with the same secant stiffness and damping. The initial elastic stiffness is comparatively unimportant for this calculation, because the only design variable that it influences is the damping, and its effect on that is small.

The primary approximation in DBD is the assumption that an inelastic system displays the same displacement response as does an elastic system with the same secant stiffness and energy dissipation per cycle.

DBD relies on none of the empirical modification factors used in FBD. It is therefore better able to take into account the particular characteristics of the structure in question. It is believed by some, e.g. [Priestley and Kowalsky 2000], to be the more rational procedure. However this view is not universally held, e.g. [Chopra and Goel, 2001].

2.3 Performance Levels and Limit States

For any structure, consideration of several different limit states is desirable. In each, response to a prescribed set of loads is compared against acceptance criteria. For example, response to loads that represent those to be expected in an earthquake with a probability of 2% in 50 years might be evaluated for the potential for collapse. Or the response to an earthquake with a probability of 50% in 50 years might be reviewed for its potential to cause non-structural damage. In making these evaluations, both demand and capacity mist be considered. Furthermore, consistent combinations of load and allowable drift should be developed separately for each limit state.

The determination of these loads, and the factors that reflect the reliability with which they can be predicted, lies outside the scope of this report. The material contained herein addresses only the matter of capacity. The purpose of the report is to provide design methods and equations that permit an engineer to establish by calculation the physical characteristics of the five systems that were used in the PRESSS Phase III test Building. Selection of the appropriate loads against which to match the computed strengths must be achieved through consensus, and that is the responsibility of code-writing bodies rather than individual authors. The same is true for other related issues, such as the amount of live load to be taken into account in a seismic analysis or design, or minimum design standards to account for other loading types.

In this report, material over-strength factors, λ, are applied to the yield strength of the reinforcement to define the stress in that reinforcement at the strain in question. This is necessary because, at the strains implicit in the design, considerable strain-hardening may have taken place. Table 2.1 contains proposed values for material over-strength factors that represent approximately the mean values to be found in the field. Separate values are given for tension

and compression. These are based on the authors' observations, so, before being incorporated into a design code they should be verified, and modified as necessary, by a comprehensive statistical study. The associated System States are provided only as a guide. The strain corresponding to a particular System State should be chosen by the designer, in accordance with the performance level desired for the particular structure.

No over-strength values are given for special items, such as the UFP shear connectors used in the walls described in Chapter 3. For such items, the designer may choose from many materials, and λ values should be selected that represent the strain-hardening characteristics of the material chosen.

Table 2.1: Over-strength Factors for Deformed Reinforcement and Pre-stressing Strand.

Suggested System State	ASTM A706 bars			Pre-stressing strand	
	strain	λ_s	$\lambda_{s'}$	strain	λ_p
First Yield	0.002	1.0	1.0	NA[1]	NA[1]
Design	0.04	1.35	1.0	0.0085	1.0
Max. Credible[2]	0.08	1.5	1.0	0.02	1.1

Notes:

1 *In systems that contain pre-stressing but no deformed reinforcement, the values for the Design System State may be used for the First Yield System State.*

2 *The Maximum Credible state corresponds to the extreme drift required by testing criteria, such as those of ACI ITG 1.1 ["Acceptance", 1999]*

The factors in Table 2.1 are not intended to reflect the fact that the true yield strength of deformed reinforcement is often significantly higher than the nominal value of 60 ksi. The difference between nominal and true yield strength needs to be taken into account if Capacity Design is to be implemented successfully. However, for the reasons stated above, the development of safety factors that reflect the true distribution of material strengths, or that address other objectives embodied in load and resistance factors in codes, lies outside the scope of this study. (For example, Section R9.3.1 of ACI 318-99 provides four different classes of uncertainty, all of which contribute to the strength reduction factors, ϕ, used in that document. The vulnerability of the systems discussed in this report to the uncertainties addressed by ACI318-99 may or may not be well represented by the strength reduction factors in that code).

2.4 Drift and Interface Rotation

For all five of the systems described in the report, the rotation at the interface between two elements plays an important role in the design procedure. That rotation is closely related, but not identical, to the drift ratio. It must be determined from the drift ratio using the geometry of the system in question.

2.5 Unbonded Pre-stressed Systems with Damping

Two of the systems described here, namely the Unbonded Post-tensioned Split Wall and the Unbonded Post-tensioned Frame with Damping, depend on a combination of unbonded pre-stressed reinforcement and bonded non-pre-stressed reinforcement. Both sets of reinforcement provide resistance to lateral load. However, the unbonded pre-stressing remains elastic and can return the structure to zero drift after the earthquake is over. By contrast, the bonded reinforcement is intended to yield cyclically, and dissipates energy by doing so, thereby helping to reduce the peak drift during the motion. The fraction of the total resistance supplied by each component may be chosen by the designer, but it affects the response, as shown schematically in Figure. 2.5.

Drift

Peak drift

Residual drift

$M_{cap,s}/M_{cap,tot}$
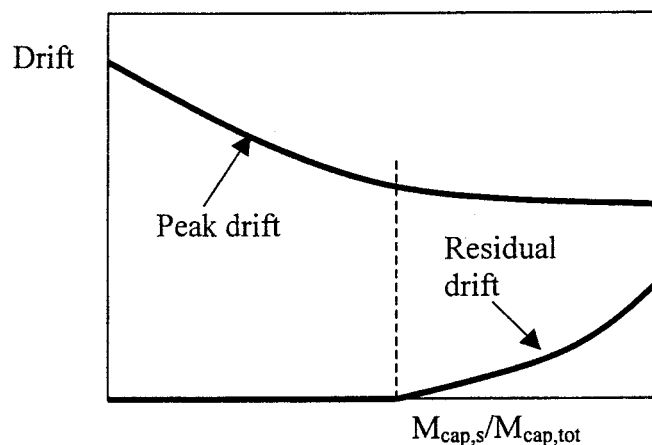
Figure. 2.5: Drift vs. Relative Strength of Resisting Elements

The total resistance to overturning moment, M_{cap}, consists of one component, $M_{cap,p}$, due to the pre-stressed reinforcement and another, $M_{cap,s}$, due to the yielding reinforcement. For low values of $M_{cap,s}/M_{cap}$, the pre-stressing as able to overcome the resistance of the yielding reinforcement and to return the structure to zero drift at the end of the earthquake. A larger contribution from the yielding reinforcement, $M_{cap,s}$, will lead to more damping and thus lower peak drift, but it could lead to a larger residual drift. The designer may select the relative proportions of the two components, and that choice will depend on the relative importance attached to peak drift and residual drift, and the limits on those drifts.

One possible design philosophy, indicated by the dashed line in Figure 2.5, is to maximize the strength of the yielding reinforcement subject to the constraint that the residual drift should still be zero. This choice will minimize the peak drift while ensuring zero residual drift. To achieve this behavior, the strength of the yielding reinforcement must be bounded above so that it supplies no more than approximately half the total moment resistance. This is the design philosophy that underlies the design equations given in Chapters 3 and 5, and it is recommended in the absence of other constraints.

3 UNBONDED POST-TENSIONED SPLIT WALLS

3.1 Concept Description

The Unbonded Post-Tensioned Split Wall is illustrated in Figure 3.1. It is composed of two or more vertical wall panels, separated by vertical joints across which shear sliding occurs during an earthquake. The wall panels are post-tensioned to the foundation. The bonded reinforcement in the wall panels has been omitted from the figure in the interests of clarity.
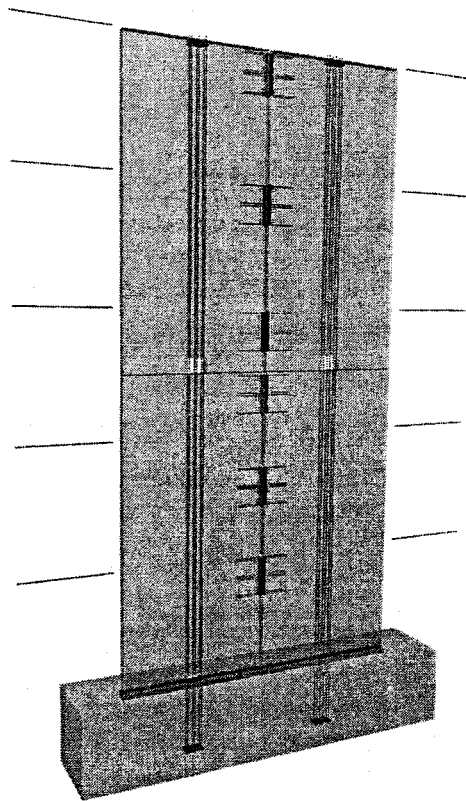
Figure 3.1: Unbonded Post-tensioned Split Wall

Each wall panel may be cast as a single element, or as several separate wall elements that are subsequently joined by rigid connections. Each wall panel is vertically post-tensioned to the foundation. The tendons may be placed at the edge or at the middle of the panel, but in most cases placement in the center will prove advantageous, because it induces the least tendon elongation for a given drift ratio.

The wall panels are connected across their vertical joints by shear connectors that dissipate energy by yielding. While other arrangements for dissipating energy are possible, the discussion in this report is restricted to the system used in the PRESSS Phase III test building. Figure 3.2

3-1

shows the locations for the post-tensioning tendons and shear connectors that were used in that building.
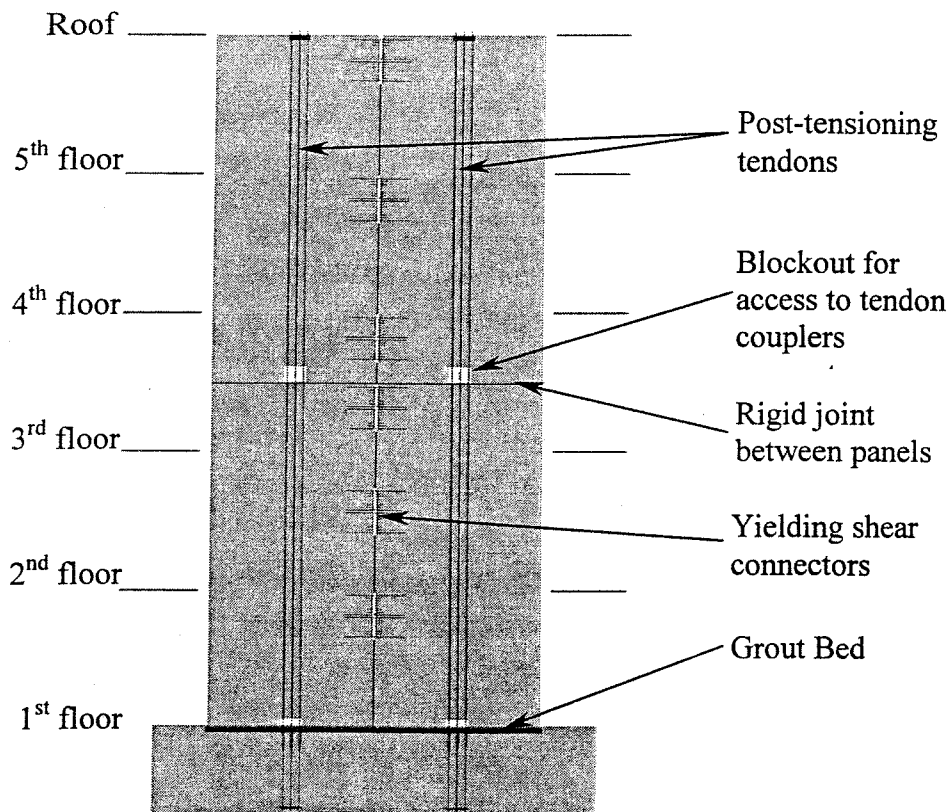
Figure 3.2: Unbonded Post-tensioned Split Wall - Location of Post-tensioning and Shear Connectors

Horizontal ground motion causes the panels to rock about their individual bases as shown in Figure 3.3. The panels move like rigid bodies and the post-tensioning tendons elongate and exert righting moments on the panels. The tendons are designed so that they remain elastic at the design limit state. Thus they act, with the gravity forces on the panel, to return the wall to its original vertical position after the ground motion stops. During the motion, the shear connectors deform inelastically. They provide resistance to lateral displacement and dissipate energy. Any rigid joints between the elements should be designed to remain elastic at all times, in order to restrict the nonlinear action to the joint at the base of the wall. The post-tensioning may be taken into account when determining the flexural strength of the rigid joints. The limit state assumed here for the design earthquake is that the post-tensioning tendon should be at incipient yield.

The system has three characteristics that distinguish it from a conventional, cast-in-place wall:

- *Essentially rigid body motion of wall panels.* The system displaces primarily by rocking of the panels and by opening of the joint at the wall base. Displacements caused by bending and shear deformations of the panels themselves are much smaller than those due to rocking. This behavior leads to much less panel damage than would be expected in a fixed-base wall that undergoes the same drift.

- *Panel rocking.* The panel properties, and in particular the aspect ratio, are selected so that the rigid body motion is rocking rather than sliding. This choice leads to high drift capacity.

- *Separation of restoring force and damping.* The post-tensioning provides an elastic restoring force while the shear connectors provide damping. This arrangement uses the same principles as are present in the suspension of an automobile, where separate elements are used for springs and shock absorbers. This separation of functions allows the wall to be designed to achieve zero residual drift after the ground motion stops.
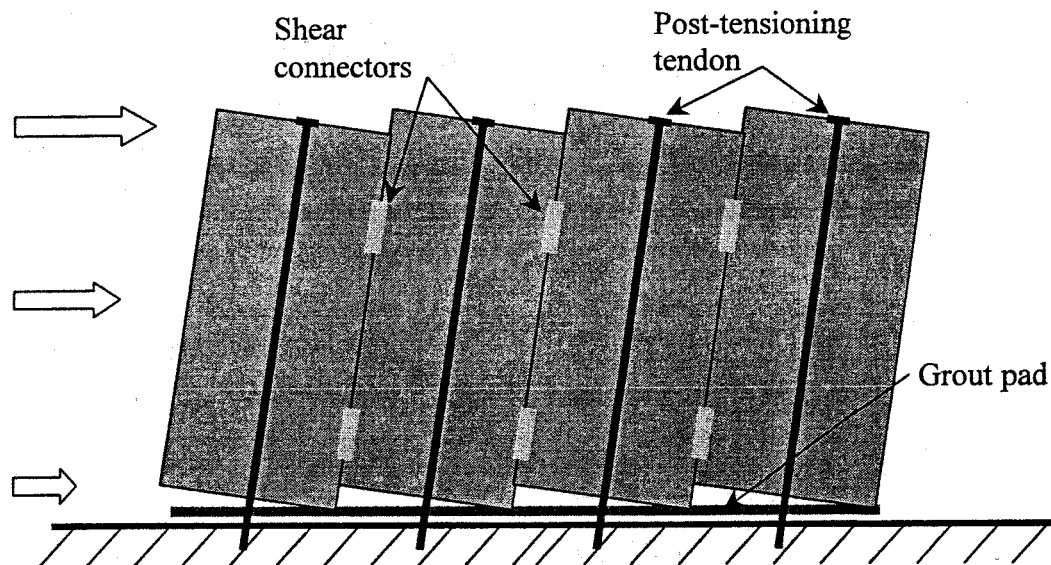
Figure 3.3: Unbonded Post-tensioned Split Wall - Components

There is no lower bound on the strength of the shear connectors. They could be omitted altogether, thereby simplifying construction, but the penalty would be larger peak drifts due to the low damping. This philosophy is adopted by Kurama et al. [1998], for example, and is commonly used in (non-pre-stressed) tilt-up panel construction.

Design procedures are given for shear connectors made from U-shaped Flexural Plates (UFPs), shown in Figure 3.4. This connector was originally proposed by Kelly et al. [1972] and is discussed further by Schultz and Magana [1996] and Galusha [1999]. Other connector types may also be used. However, the wall test [Priestley et al., 1999] that forms the basis for the comparison of predicted and measured responses contained UFPs.
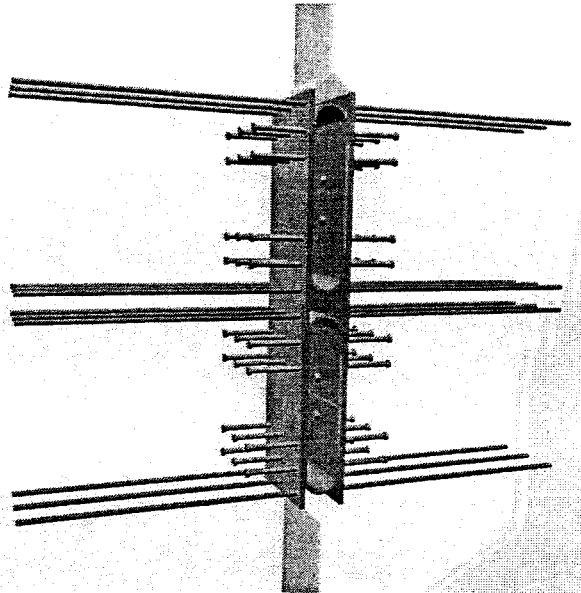
Figure 3.4: UFP Shear Connector

The UFP works by rolling like a tank track to accommodate relative shear displacement between the two panels. The bent plate dissipates energy as the different regions of it alternately bend and straighten inelastically. The shear displacement that can be accommodated is limited only by the geometry of the system, in particular by the distance by which the weld is held back from the bend in the plate.

The rocking behavior of the wall leads to less panel damage than would occur in a conventional, cast-in-place wall, because the wall panels do not deform inelastically. However, some local distress must be expected at the wall toe about which rocking occurs. Several alternative design approaches are possible for controlling that damage. The designer should select one that is consistent with the design objectives for the building and the expected level of drift. The issues to be considered include:

- damage to, and degradation of, concrete and grout
- buckling of vertical wall reinforcement
- loss of pre-stress due to vertical shortening of wall and grout pad
- horizontal sliding promoted by damaged interface materials

When the wall rocks, the local compressive stresses in the grout and concrete are high enough that some inelastic action will occur. By suitable selection of material strengths in accordance with the principles of capacity design, the designer can control the location of the inelastic action.

The inelastic action can be forced to occur in the concrete wall panel by using grout that is stronger than the concrete. Then the toe of the wall panel must be confined to prevent

compression failure of the concrete. The cover concrete, which by definition is not confined, is likely to be lost due to the large strains. However, that damage is expected to be easily repairable.

Another alternative is to make the concrete, including any reinforcement, stronger than the grout, thereby forcing the inelastic deformations into the grout bed. In this case, the strength required in the wall panels can be achieved by using stronger concrete, vertical reinforcement, confinement reinforcement, local armor, or other means. The grout can be made ductile by fiber reinforcing, by placing it in a trough below the wall, as was done in the PRESSS building, or both. This second approach is intended to reduce the damage to the panels at the expense of some grout crushing. The calculations in this chapter are based on this approach.

In extreme cases, extensive pulverization of the grout could lower the coefficient of friction and lead to premature sliding. However, sliding is controlled by the aspect ratio of the wall panels, as well as by the coefficient of friction, and in many cases sliding will not govern design, even if the grout crushes and the friction is consequently lowered.

3.2 Design Assumptions

The following assumptions are made in the development of design equations:

1. The design forces and drift limits are known. The drift limits are selected to satisfy code restrictions and user requirements. Forces may be obtained either by Force Based Design or by Displacement Based Design. Interface rotations are obtained from the drift ratio, using the geometry of the system.

2. The overall dimensions of the wall are known, having been obtained from architectural constraints and preliminary calculations.

3. The wall panels are all the same size and have a constant thickness. Design equations for other arrangements follow the same principles, but are necessarily more complex.

4. The shear connectors are treated as rigid-plastic in the interests of simplicity. Design procedures in which they are modeled as elasto-plastic would lead to the same strength, but slightly lower damping, provided that all connectors yielded prior to the design drift. Such design procedures would necessarily be more complex than those presented here. One consequence of the rigid-plastic modeling is that any relative shear displacements between panels that occur prior to the earthquake have no effect on the seismic behavior. Such displacements might be caused by differential response to pre-stress, settlement or thermal effects. Such displacements are likely to be small compared with the seismic displacements.

5. The post-tensioning tendon is at incipient yield at the design drift. If a lower tension stress is desired in the tendon at the design drift, it should be substituted for f_{py} in the equations that follow.

6. Properties of the proposed materials are known. The principal ones are:
   - strength and stiffness of post-tensioning material
   - strength of deformed reinforcement
   - strength of shear connectors
   - strength of concrete
   - strength of grout

3.3 Notation

The sign convention adopted is that forces and deformations are computed as positive quantities, regardless of whether they are tensile or compressive.

A_p	= area of pre-stressing tendon
b_{sc}	= width of UFP connector plate
C_0	= compressive reaction on one wall panel at zero drift
C_c	= compression capacity of one wall panel
C_{des}	= compressive reaction on one wall panel at design limit state
D_{sc}	= bend diameter (measured at mid-thickness of plate) in UFP connector plate
E_p	= Young's modulus of pre-stressing tendon material
f'_g	= specified grout strength at 28 days
$f_{p,des}$	= stress in pre-stressing tendon at the design limit state
f_{p0}	= stress in pre-stressing tendon, after losses, at zero drift
f_{py}	= specified yield strength of pre-stressing tendon material
$f_{sc,des}$	= stress in UFP connector plate under plastic conditions
F_{sc}	= total yield force of all shear connectors in one vertical joint
$F_{sc,left}$	= total yield force of all shear connectors in joint to left of panel
$F_{sc,net}$	= net vertical force on one panel from all shear connectors
$F_{sc,right}$	= total yield force of all shear connectors in joint to right of panel
h_{eff}	= height above foundation of lateral load resultant on wall
h_u	= unbonded length of pre-stressing tendon
h_w	= total height of wall panel (used for self-weight)
k_1	= uniform stress in Whitney rectangular equivalent stress block divided by f'_g
l_w	= length of one wall panel (horizontal dimension in plane of the wall)
$l_{w,tot}$	= total length of one wall
$M_{cap,panel}$	= moment capacity of one panel
$M_{cap,wall}$	= total moment capacity of wall
M_{des}	= moment demand at design limit state
M_{sc}	= plastic moment strength of one UFP connector
n	= number of panels per wall
n_{sc}	= number of shear connectors required per vertical joint
N_0	= total axial force on one wall panel from gravity plus post-tensioning at zero drift
N_{des}	= total axial force on one wall panel from gravity plus post-tensioning at design limit state

P_0	= force in pre-stressing tendon at zero drift
P_{des}	= force in the pre-stressing tendon at design limit state
t_{sc}	= plate thickness in UFP connector
t_w	= thickness of wall panel
$t_{w,eff}$	= thickness of wall panel effective in resisting compressive force
V_{des}	= design base shear
V_{sc}	= shear strength of one UFP shear connector
w_{floor}	= distributed vertical load on the wall, at base, from all floors
W	= total gravity load from all floors on one wall panel
W_{panel}	= self-weight of one panel

α_0	= distance from the compression face of the member to the center of the compression force, divided by the member depth, at zero drift
$\alpha_{0,ave}$	= average value, over all panels, of α_0
α_{des}	= distance from center of compressive reaction to edge of member divided by member depth, at design limit state
$\alpha_{des,ave}$	= average value, over all panels, of α_{des}
β_1	= depth of equivalent compressive stress block divided by the neutral axis depth
γ_c	= density of concrete
Δ_{fp}	= increase in stress in pre-stressing tendon between zero drift and design drift
$\Delta_{fp\infty}$	= increase in stress in pre-stressing tendon between zero drift and design drift when concrete and grout strengths are infinite
Δ_p	= deformation of pre-stressing tendon between zero drift and design drift
$\varepsilon_{sc,des}$	= strain in the UFP connector plate at the design limit state
$\varepsilon_{sc,max}$	= maximum permissible strain in UFP connector plate under cyclic loading
$\varepsilon_{sc,u}$	= strain at maximum stress in the UFP connector plate material
η_0	= distance from member compression face to neutral axis divided by member depth, at zero drift
η_{des}	= distance from member compression face to neutral axis divided by member depth, at design limit state
θ_{des}	= interface rotation at design limit state
κ_0	= ratio of design strength of shear connectors in one joint to the vertical load on one panel
μ	= coefficient of friction
ρ_{fp0}	= stress ratio to ensure that pre-stressing tendon does not yield at maximum drift
ρ_{MOM}	= demand/capacity ratio for overturning moment on panel
ρ_{ROC}	= force ratio to ensure that the panel slides rather than rocks
ρ_{UPL}	= ratio of uplift force to hold-down force on one panel
ρ_{ZRD}	= parameter ratio controlling the residual drift

3.4 Design Procedure for Critical Elements

3.4.1 Design of Post-tensioning Tendons and Shear Connectors

The following step-by-step procedure is presented in the form of analysis rather than design, because direct design, without iteration, is not possible for most cases. However, by automating the analysis procedure on a spreadsheet or similar computer application, design may be conducted quickly and easily. In the steps that follow, the lateral load is assumed to be acting to the right. Therefore the right end of the wall is the compression end, and the left end is the tension end. The wall is shown in its deformed shape in Figure 3.5. The locations of the forces are detailed in Figure 3.6.

<u>**Step 1.**</u> **Establish Material Properties**

Establish properties of materials to be used. These include:
- grout: strength, stress block coefficient β_1, coefficient of friction against concrete
- concrete: strength, density
- tendon: Young's modulus, yield strength
- connector: cyclic load-displacement relationship

In the absence of better information, the coefficient of friction, μ, between the grout and the concrete may be taken as 0.5. Hutchinson et al. [1990] measured a value of 0.6 between precast concrete and grout under cyclic loading. That value is reduced here to 0.5 to allow for variations with grout type. Roughening of the surfaces could lead to a higher value, but experimental evidence would be needed to justify its use in design.
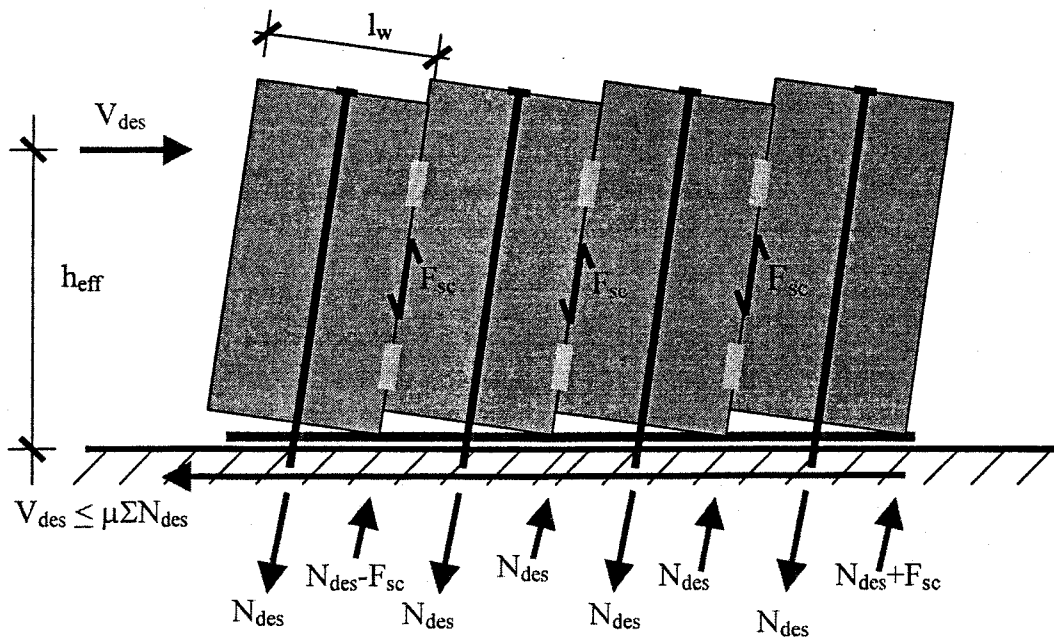
Figure 3.5: Unbonded Post-tensioned Split Wall - Deformed Configuration at Design Drift

3-8
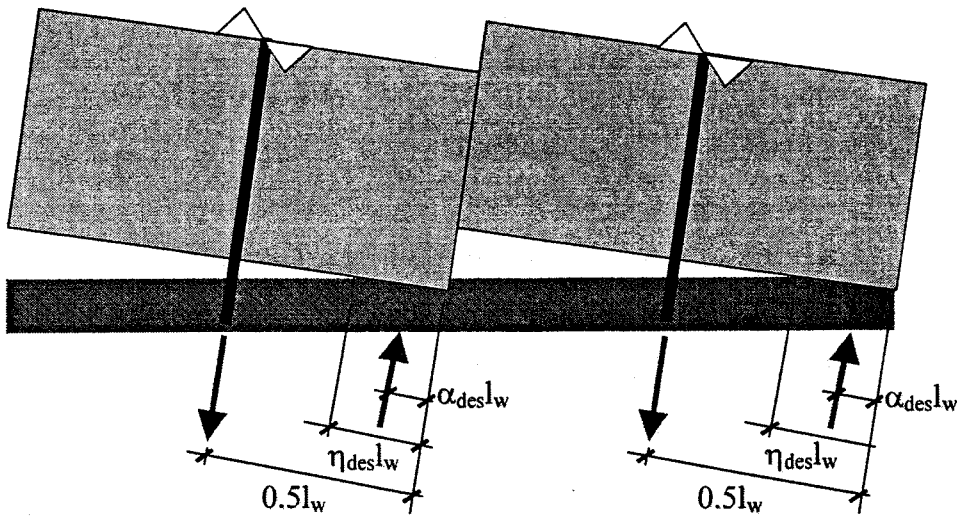
Figure 3.6: Unbonded Post-tensioned Split Wall - Locations of Forces at Design Drift

Step 2. Obtain Design Loads and Drifts.

Use DBD or FBD to obtain lateral design loads. Compute corresponding design moments and drifts. The calculations that follow are for a limit state that corresponds to incipient yielding of the post-tensioning tendon. M_{des} and θ_{des} are the corresponding overturning moment and drift ratio of the wall.

Step 3. Select Number of Panels

The wall is divided into n separate panels. The following characteristics should be taken into account when selecting n:

- wall panel aspect ratio (influences rocking vs. sliding)
- post-tensioning tendon elongation due to rocking (wider panels cause more elongation)
- lateral strength (larger n leads to lower strength, for given total area of post-tensioning)
- damping (larger n leads to slightly greater equivalent damping)

Step 4. Establish constants

$$l_w = \frac{l_{w,tot}}{n} \quad \text{...(3.1)}$$

$$\Delta f_{p\infty} = 0.5 E_p \theta_{des} \frac{l_w}{h_u} \quad \text{...(3.2)}$$

$\Delta f_{p\infty}$ has a physical meaning. It is the stress change in the tendon that would occur between zero drift and the design drift if the wall rocked about its corner. (This would require the concrete and

grout to be infinitely strong, so in practice it is impossible and the true stress change will be smaller than $\Delta f_{p\infty}$. The true stress change is given by Equation 3.18)

$$M_{des} = V_{des} h_{eff} \quad\text{(3.3)}$$

$$W_{panel} = l_w t_w h_w \gamma_c \quad\text{(3.4)}$$

$$W = W_{panel} + l_w w_{floor} \quad\text{(3.5)}$$

$$C_c = l_w t_{w,eff} \left(k_1 f'_g \right) \quad\text{(3.6)}$$

$$F_{sc,net} = F_{sc,left} - F_{sc,right} \quad\text{(3.7)}$$

In Equation 3.4, t_w is the total wall thickness, used here to compute the weight of the panel. In Equation 3.6, $t_{w,eff}$ is the thickness of wall that is effective in resisting compression. For example, if the grout strength controls the compression capacity, and the grout bed is narrower than the wall, $t_{w,eff}$ should be the width of the grout bed.

Note: Steps 5 - 10 that follow must be repeated with different input values until a combination is achieved that satisfies all the acceptance criteria in Step 10.

Step 5. Select Reinforcement

Select A_p, f_{p0}, F_{sc}. Compute $F_{sc,net}$, the net vertical force on each panel due to the shear connectors. For interior panels in a wall with more than two panels, $F_{sc,net}$ will be zero if vertical lines of connector have the same strength, as is assumed here.

Step 6. Establish Conditions Immediately after Lift-off at the Base of the Wall.

Each wall panel lifts off the base gradually. During lift-off, the stresses in the grout and concrete at the interface are initially low enough that behavior is elastic but, as lift-off progresses, the stresses rise and some inelastic behavior occurs. In the conditions addressed in this step, lift-off is assumed to have progressed far enough for the grout to behave inelastically, but the drift ratio is small enough that the tendon stress can still be taken with sufficient accuracy as f_{p0}, the value at zero drift.

$$P_0 = A_p f_{p0} \quad\text{(3.8)}$$

$$N_0 = P_0 + W \quad\text{(3.9)}$$

$$C_0 = N_0 + F_{sc,net} \quad\text{(3.10)}$$

$$\alpha_0 = 0.5 \frac{C_0}{C_c} \quad\text{...(3.11)}$$

$$\eta_0 = 2 \frac{\alpha_0}{\beta_1} \quad\text{..(3.12)}$$

$$\kappa_0 = \frac{F_{sc}}{N_0} \quad\text{...(3.13)}$$

Step 7. Establish Conditions at Design Load and Drift

P_{des}, the force in the tendon at the the design limit state, may be found by iteration. If P_{des} is estimated, then axial force equilibrium requires

$$N_{des} = P_{des} + W \quad\text{..(3.14)}$$

$$C_{des} = N_{des} + F_{sc,net} \quad\text{...(3.15)}$$

The location of the compressive force in the concrete and grout bed is $\alpha_{des} h_b$, where

$$\alpha_{des} = 0.5 \frac{C_{des}}{C_c} \quad\text{..(3.16)}$$

and the neutral axis location is given by $\eta_{des} h_b$, where

$$\eta_{des} = 2 \frac{\alpha_{des}}{\beta_1} \quad\text{.. (3.17)}$$

Figure 3.6 shows that the elongation of the tendon is

$$\Delta_p = \theta_{des} l_w (0.5 - \eta_{des}) \quad\text{...(3.18)}$$

Thus the increase in stress in the tendon is

$$\Delta f_p = E_p \frac{\Delta_p}{h_u} = \Delta f_{p\infty}(1 - 2\eta_{des}) \quad\text{..(3.19)}$$

and the total stress is

$$f_{p,des} = (f_{p0} + \Delta f_p) \le f_{py} \quad\text{...(3.20)}$$

3-11

A better estimate of P_{des} is then given by

$$P_{des} = A_p f_{p,des} \quad\text{...}(3.21)$$

Equations 3.14 to 3.21 may be solved iteratively until they converge to give the final value of P_{des}. Alternatively, those equations may be combined for a direct solution. First Equations 3.19 through 3.21 are combined and solved for η_{des}, to give

$$\eta_{des} = \frac{A_p\left(f_{p0} + \Delta f_{p\infty}\right) + W + F_{sc,net}}{\beta_1 C_c + 2A_p \Delta f_{p\infty}} \quad\text{...}(3.22)$$

This value of η_{des} is then substituted in Equations 3.19 through 3.21 to give, after some algebraic manipulation,

$$P_{des} = \frac{A_p\left\{f_{p0} + \Delta f_{p\infty}\left(1 - \dfrac{W + F_{sc,net}}{0.5\beta_1 C_c}\right)\right\}}{1 + \dfrac{A_p f_{p\infty}}{0.5\beta_1 C_c}} \leq A_p f_{py} \quad\text{..}(3.23)$$

This value of P_{des} may then be substituted in Equations 3.14- 3.19 to provide values for the other constants.

Step 8. Compute Resisting Moments of Wall Panels

$$M_{cap,panel} = l_w\left(C_{des}\left(0.5 - \alpha_{des}\right) + 0.5\left(F_{sc,left} + F_{sc,right}\right)\right) \quad\text{..................................}(3.24)$$

Equation 3.24 gives the resisting moment about the centerline of the panel. The first term represents the couple caused by the compressive force under the panel and the tendon force, and the second term represents the moment due to the shear connectors. The resisting moments of all wall panels should be computed separately, because each panel will have its own distinct value of α_{des}. In general, the panel at the tension end of the wall will have a smaller resisting moment than will the panel at the compression end. In a wall with four or more identical panels, the behavior of the interior panels will be the same.

Step 9. Compute Resisting Moment of Wall

$$M_{cap,wall} = \sum M_{cap,panel} \quad\text{..}(3.25)$$

Step 10. Check Acceptance Criteria

The following dimensionless ratios, ρ_{MOM}, etc., should be checked to ensure that the design criteria are met. Each ratio fulfills a function similar to that of a demand/capacity ratio, but it does not necessarily represent a ratio of forces.

3-12

$$\rho_{MOM} = \frac{M_{des}}{M_{cap,wall}} \le 1.0 \qquad\qquad \text{overturning} \dots\dots\dots\dots\dots\dots \text{(3.26)}$$

$$\rho_{fp0} = \frac{f_{p0}}{\left(f_{py} - \Delta f_p\right)} \le 1.0 \qquad\qquad \text{yield of post-tensioning steel} \dots \text{(3.27)}$$

$$\rho_{UPL} = \kappa_0 \le 1.0 \qquad\qquad \text{uplift of end panel} \dots\dots\dots\dots \text{(3.28)}$$

$$\rho_{ZRD} = \kappa_0 \frac{\left(n - 1 + 2\alpha_{0,ave}\kappa_0\right)}{n(0.5 - \alpha_{0,ave})} \le 1.0 \qquad\qquad \text{residual drift} \dots\dots\dots\dots\dots \text{(3.29)}$$

$$\rho_{ROC} = \frac{\kappa_0 l_w}{\mu h_{eff}} \left((0.5 - \alpha_{0,ave}) + \frac{(n - 1 - 2\alpha_{0,ave}\kappa_0)}{n} \right) \le 1.0 \quad \text{sliding vs. rocking} \dots\dots\dots \text{(3.30)}$$

where $\alpha_{0,ave}$ = average across all panels of the value of α_0.

If the acceptance criteria do not satisfy the specified limits, select new values for A_p, f_{p0} and F_{sc} and repeat Steps 5-10.

Equation 3.24 shows that the post-tensioning and the shear connectors both contribute to the resisting moment of the panel. Thus, in general, the greatest strength will be achieved by making the connector forces as large as possible. The connector forces are bounded above by the Zero Residual Drift criterion (Equation 3.29). Maximizing the connector forces will also maximize the damping.

3.4.2 Design of UFP Shear Connectors

Any ductile shear connector that has the required strength and deformation capacity may be used to connect the wall panels. The UFP connector is one example and is described here because it was used in the PRESSS Phase III building test and worked well. It consists of two flat anchorage plates, one embedded in each panel edge, and one plate bent in the shape of a "U" that is welded to the embedded plates.
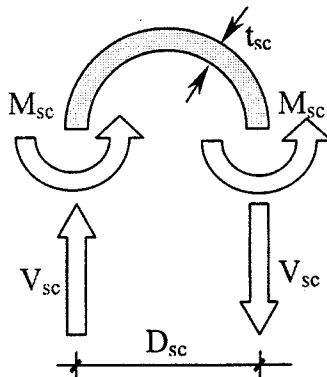
Figure 3.7: Forces on UFP under Inelastic Conditions

Equations for analysis of the UFP are presented. They may be used for design on a trial and error basis. Design is unlikely to be direct, because it is a compromise between number of connectors, plate dimensions, available plate sizes, radius of bend and material properties. A free body diagram of the curved part of the bent plate is shown in Figure 3.7. Moment equilibrium requires that

$$V_{sc} D_{sc} = 2M_{sc} \dots\dots\dots\dots\dots (3.31)$$

where M_{sc}, the plastic moment capacity of the plate, is given by

$$M_{sc} = \left(\frac{b_{sc} t_{sc}^2}{4} \right) f_{sc,des} \dots\dots\dots\dots\dots (3.32)$$

and $f_{sc,des}$ = the stress in the plate under plastic conditions, including strain-hardening.

As the straight part of the plate is bent, the strain change in the outer fiber of the UFP caused by the change in curvature is

$$\varepsilon_{sc,des} = \frac{t_{sc}}{D_{sc}} \dots\dots\dots\dots\dots (3.33)$$

Combining Equations 3.31 – 3.33 leads to

$$V_{sc} = \left(\frac{b_{sc} t_{sc}}{2} \right) \left(f_{sc,des} \varepsilon_{sc,des} \right) \dots\dots\dots\dots\dots (3.34)$$

The number of shear connectors required per vertical joint, n_{sc}, is given by

$$n_{sc} = \frac{F_{sc}}{V_{sc}} \dots\dots\dots\dots\dots (3.35)$$

In Equation 3.33, the strain $\varepsilon_{sc,des}$ should be limited to a value $\varepsilon_{sc,max}$ that can be imposed cyclically without damage to the plate. The number of cycles depends on the earthquake ground motion used for the design. In the absence of better information, a strain limit of

$$\varepsilon_{sc,max} = \frac{\varepsilon_{sc,u}}{3} \dots\dots\dots\dots\dots (3.36)$$

is proposed, where $\varepsilon_{sc,u}$ is the strain in the material at maximum stress in a static tension test. The strain change during cyclic loading is the same as the initial strain imposed in forming the plate, because the change in curvature is the same in both cases. $f_{sc,des}$ is the stress that corresponds to $\varepsilon_{sc,des}$. These strains are illustrated in Figure 3.8.
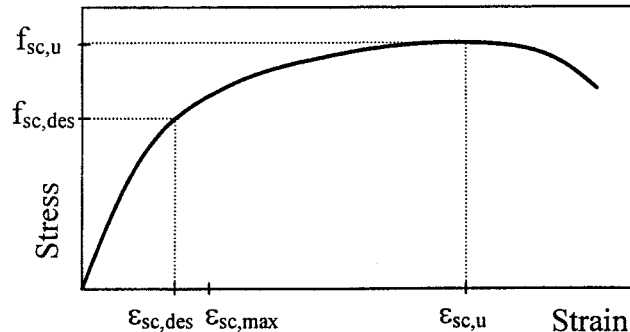
Figure 3.8: Critical Stresses and Strains in UFP Material

The value of V_{sc} in Equation 3.34 is approximately equal to one half of the work done in stretching a plate of unit length from an unstressed (and straight) condition to a tensile strain $\varepsilon_{sc,max}$. Therefore the shear capacity, V_{sc}, depends on the plate toughness, rather than simply its strength. The reason is that high stress capacity leads to a high plastic moment and high strain capacity leads to a tight bend radius, both of which are needed for a high shear capacity. This requirement has parallels with the needs for coupling beams in coupled shear walls, which also need to be both strong and ductile.

In experiments on UFPs, Schultz and Magana [1996] found that ASTM A36 steel cracked when bent to a radius that corresponds to 15% strain. They therefore used ASTM 240 type 304 stainless steel instead, because of its high strain capacity. The same was done in the PRESSS Phase III test building. No cracks occurred in the stainless steel in either test. However, most stainless steels strain-harden significantly. For example, a component test was conducted on the UFPs used in the PRESSS Phase III building test. The stress after several cycles of load was back-calculated to be approximately three times the material's nominal yield strength of 37 ksi. While this high strength is desirable, the variation in UFP resistance with cycling that it causes creates difficulties in efficiently protecting adjacent elements by Capacity Design.

An ideal steel would have high stress and strain capacities at the expected operating temperature, and limited strain hardening. Investigations to determine the most suitable steel lay outside the scope of this study. A component test should be conducted on the steel selected in order to verify the values used for design.

3.5 Design of Other Components

The Unbonded Post-tensioned Split Wall is a jointed system in which all the inelastic action is intended to take place between precast members. Therefore, the rest of the system is designed using capacity design principles.

3.5.1 Panel Reinforcement

The bonded reinforcement in the body of the wall panel should be designed to remain elastic. The influence of higher modes of vibration should be taken into account when designing the panels and any joints between them, because they may cause the effective height of the seismic loading to be smaller than suggested by the loading patterns of either the DBD analysis or the Equivalent Lateral Force procedure of FBD. For a given resistance to overturning moment, the base shear force will then increase, and local moments and shears within the panel may be larger than those caused by an approximately triangular load pattern. One method for accounting for higher mode effects is given by Eberhard and Sozen [1993].

Reinforcement should be supplied to resist the splitting and bursting stresses caused by the post-tensioning anchor. Strut-and-tie modeling is recommended for determining local design forces.

3.5.2 Confinement Reinforcement

Confinement reinforcement should be designed for the wall toes. The amount and distribution of confinement reinforcement will depend on the limit state under consideration. Relationships between the volume of confinement reinforcement and the compressive strength of the confined concrete are given by several authors, e,g., [Paulay and Priestley, 1992].

In the PRESSS Phase III building test, the wall toes were confined using a steel channel, whose depth was equal to the wall width, at each toe. The arrangement is illustrated in Figure 3.9. The web of the channel lay in a horizontal plane. At the bottom corners of each panel, vertical reinforcement was welded to the channel to ensure good transmission of compressive stress. The area of reinforcement was selected as 2% of the corresponding concrete area, and the steel was placed over the outer 25% of each panel. This reinforcement was included in the calculations of the compressive capacity of the toe of the wall.
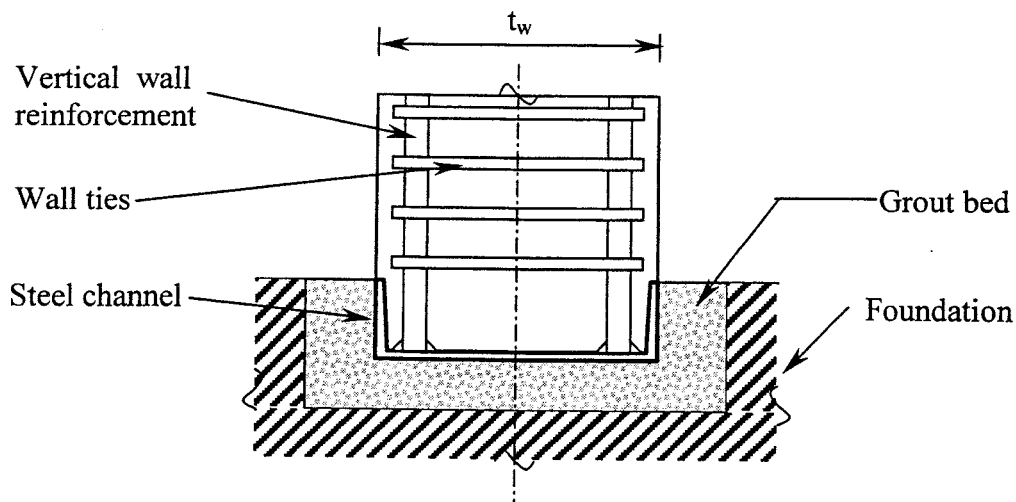
Figure 3.9: Confinement Detail at Base of Wall

Note that the grout in the joint will be considerably stronger than would a cube of the same material, because it is thin compared with its lateral dimensions and is thus confined by the wall above and the foundation below it. Conservatism in designing the wall toes is thus advisable.

3.5.3 Wall-to-Floor Connections

Connections between the wall and floor must be designed. The loads that they carry include the effects of higher modes of vibration, so these must be included in the calculation of the applied loads. The contribution of the higher modes to the global overturning moment is small. However the relative effect of higher modes on individual floor forces is larger and should be accounted for explicitly. This is true in all structures, including cast-in-place walls, and is not peculiar to precast wall systems. Guidance for selecting design forces is given by Eberhard and Sozen [1993].

The connections should also take account of any relative displacements between components that must be allowed to occur freely. Two main types of displacement exist. First, relative shear displacements occur across the interface between the sliding joint between panels, so the slab should not be attached rigidly to the wall panels close to the joint unless out of plane shear damage to the slab is acceptable. Some other means of support must be supplied in the region. Second, the center of each wall panel rises as it rocks and creates differential vertical movements between the wall and the perimeter frame. It is worth noting that a cast-in-place wall also experiences a vertical component of motion that is comparable to the one found in a precast wall.

The effects of the differential movements in the two walls are similar, but are usually ignored, perhaps because the damage to the cast-in-place wall itself is so serious that moderate cracking in the floors is viewed as relatively unimportant. Thus any methods used in a conventional cast-in-place structure are also candidates for use in a precast one.

However, measures can be taken to improve the performance of the building by designing the connections to reduce damage. One possible way of accommodating the sliding shear displacements between the panels is to install an edge beam that runs parallel to the wall and to connect it to the wall only near the centerline of each panel. In the PRESSS Phase III test building, this was achieved by bolting a steel header beam to the wall panels as shown schematically in Figure 3.10, using a single large bolt in each panel. This arrangement allowed relative rotation between the header and the wall, so the header remained horizontal at all times and no damage was done when the wall rocked. Shear forces parallel to the wall were transferred from the floor into the header and thence through the bolts into the wall.

The relative vertical displacements between the wall and the perimeter frame occur because both elements experience the same rotation, but the wall panels are wider. If the header beam is supported on both the perimeter frame and the wall, it must accommodate the differential vertical movement between them. In the PRESSS Phase III test building, this was done by introducing a joint in the header beam, because the building dimensions were such that the wall ended very close to the exterior frame and would otherwise have caused significant inelastic bending in the header beam. In a prototype structure, the likely greater horizontal separation between the wall

and the perimeter frame would permit some deformation to be accommodated by bending of the header beam and floor, thereby obviating the need for the elaborate connections used in the PRESSS Phase III test building.
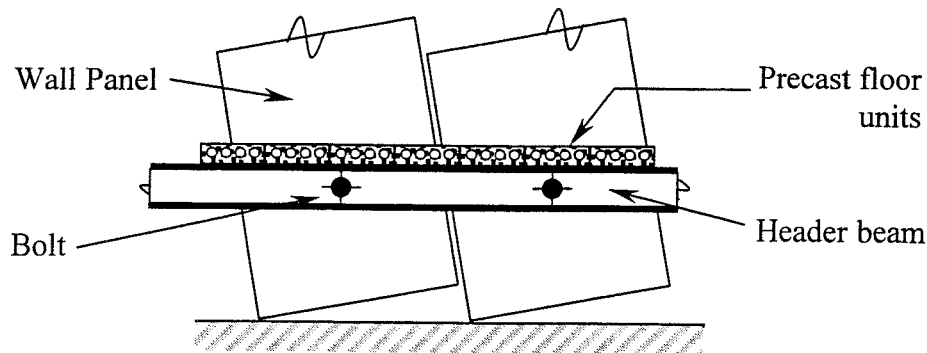
Figure 3.10: Wall-to-Floor Connection System used in PRESSS Building

3.6 Limits on Reinforcement

There is no lower limit on the quantity of post-tensioning to be used in the wall. In an extreme case of large, heavy, panels and low seismic loading, the self-weight alone may be sufficient to ensure re-centering, in which case no post-tensioning would be necessary to resist the lateral loads. However, such designs are likely to be rare.

The maximum permissible quantity of post-tensioning depends on the design objective. If the goal is to protect the panel against cover spalling, the post-tensioning must be limited so that the strains in the concrete are low enough to prevent such behavior. If cover spalling is considered acceptable during a rare, severe, earthquake, because it can be repaired easily, then the designer may use one of several different strategies, all of which are based on increasing the compressive strength of the toe of the wall. Possibilities include confinement of the wall core, adding vertical reinforcement, etc. Multiple design objectives are also possible. For example, two reasonable objectives for the same building might be no spalling under a moderate earthquake, but no failure of the core of the wall during a severe earthquake.

3.7 Construction Issues

3.7.1 Transportation Limitations

Transportation and crane limitations should be considered when selecting the wall panel and element sizes.

3.7.2 Post-tensioning Materials

Bars and strands are both acceptable forms of post-tensioning. When large tendon elongations are needed, the greater elongation capacity of strand may prove advantageous. In other cases, the ease of installing and connecting bars may offer greater benefits.

3.7.3 Post-tensioning Duct Alignment

The post-tensioning ducts must be large enough to allow installation of the tendons, and must be straight. Crooked ducts could impede installation of tendons, risk kinking of the tendons and cause friction during stressing.

3.7.4 Corrosion Protection

Measures must be taken to ensure that the unbonded post-tensioning tendons are protected against corrosion, especially at critical locations, such as anchorages and any couplings.

3.7.5 Grout Confinement

Use of fiber-reinforced grout between the foundation and wall will help to ensure that the grout does not escape from the interface when it is highly compressed. This will help to prevent deterioration in performance with cycling. Placing the grout in a pocket in the foundation, such as shown in Figure 3.9, will provide additional confinement.

3.8 Discussion

The wall in the PRESSS Phase III test building performed very well. It exhibited all the features that it was intended to possess under design loading: zero residual drift, closely predictable peak drift, and minimal damage. Figure 3.11a shows that wall after the completion of the test, during which it was displaced to 2.7% drift. The horizontal cracks in the wall were caused by out-of-plane bending, when the building was being tested in the frame direction, and so are not relevant to the in-plane performance.

The total damage caused by in-plane loading can be seen in Figure 3.11b, which shows the detail of the spalling of the cover concrete at the toe of the wall. The damage is minor in extent and could be repaired easily. The performance level of the wall would fall into the highest category of almost any classification system. The low level of damage is remarkable, especially in the light of the loading history, which included ground motions 50% larger than those consistent with the response spectrum for a UBC Zone 4 earthquake.

The design procedures outlined here have not yet been validated by the authors using the data from the PRESSS Phase III test. Therefore, they should be used only for trial designs.
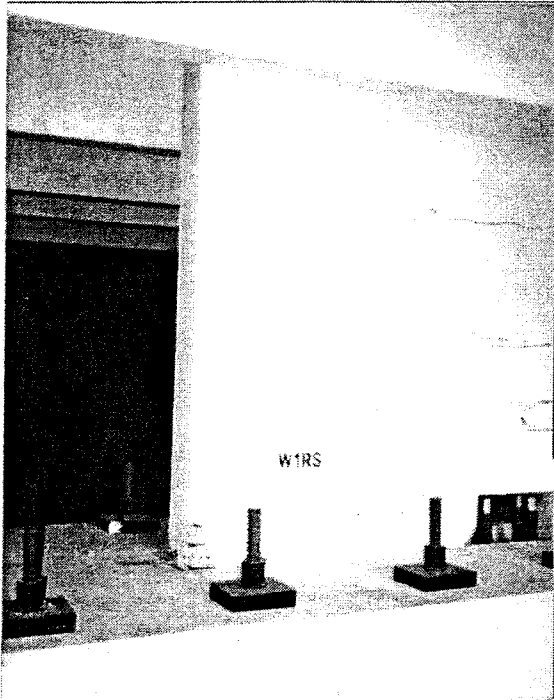
a) Wall Elevation   b) Detail of damage at Toe

Figure 3.11: Unbonded Post-Tensioned Split Wall at End of Test

4 UNBONDED PRE-TENSIONED FRAMES WITHOUT DAMPING

4.1 Concept Description

The Unbonded Pre-Tensioned Frame without Damping is illustrated in Figure 4.1.
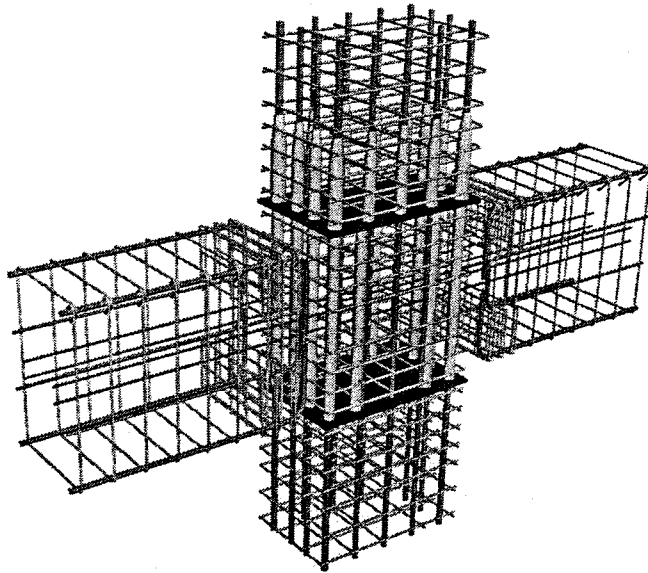
Figure 4.1: Unbonded Pre-Tensioned Frame Without Damping

The frame consists of multi-span precast pre-stressed beams that are supported by single story columns, as shown in Figure 4.2. The columns are reinforced conventionally, except that they are connected through the beams using splice sleeves. Each beam is pre-tensioned for the entire length, with the centroid of the strands at beam mid-height. If the gravity moments in the beam are significant, the tendon may be harped in the spans to counteract those moments.
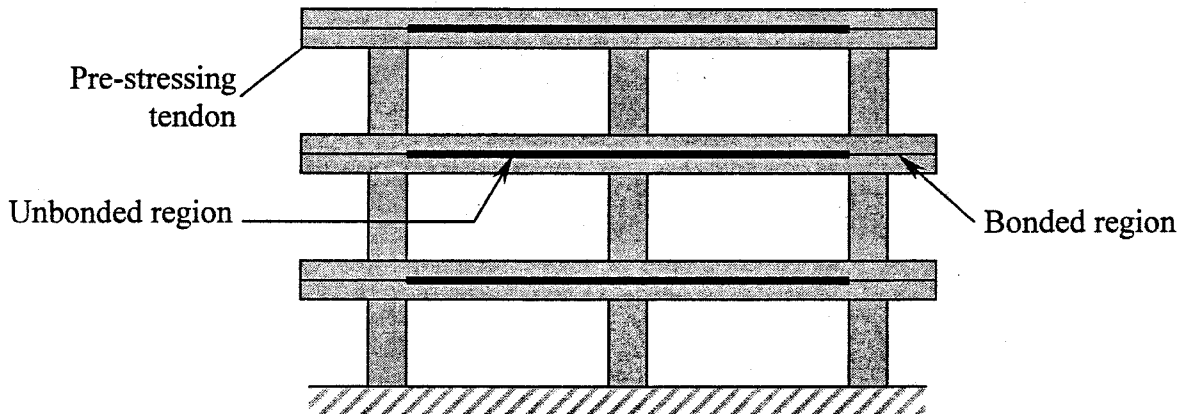
Figure 4.2: Unbonded Pre-Tensioned Frame without Damping – Layout of Elements and Primary Reinforcement

4-1

The beam also contains deformed reinforcement. However, as shown in Figure 4.3, no deformed bars cross the potential cracking plane in the beam at the column face. Crack initiators such as sharp reveals in the beams create weakened planes so that the cracks occur at the desired locations adjacent to the column faces.

When the frame experiences drift caused by lateral inertia forces, the column tilts and the beams remain approximately horizontal. The relative rotation between the beam and column is accommodated by a concentrated rotation at the interface. This rotation causes a gap to open up over part of the height of the interface, as part of the beam end separates from the column face. The pre-tensioned tendon elongates but remains elastic. It creates a couple with the compression force in the concrete, which resists the seismic load. When the load is removed, the moment from the tendon closes the gap at the interface and the frame returns to zero drift.
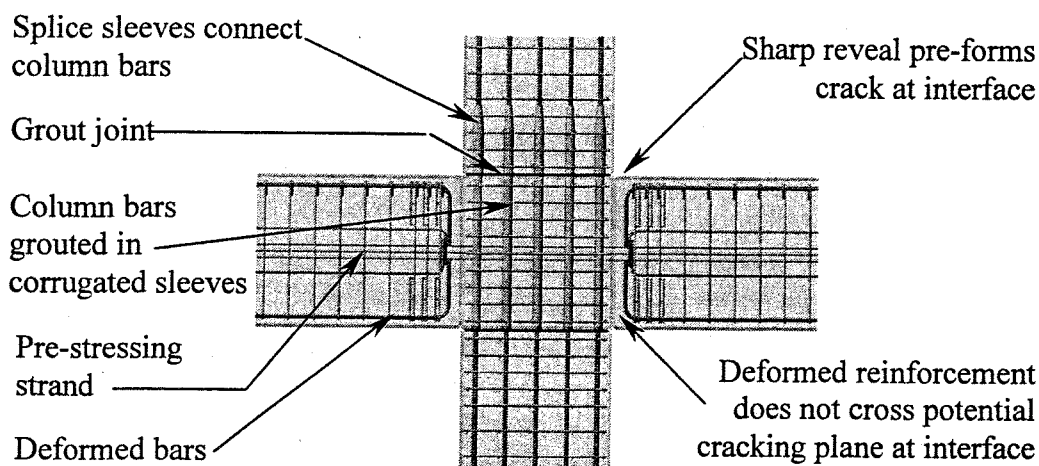
Figure 4.3: Unbonded Pre-Tensioned Frame without Damping - Components

The potential cracking plane is referred to as the interface since it is the interface between the beam and the face of the joint. This interface provides the pre-tensioned frame with jointed behavior, shown in Figure 4.4, that is different from that of a traditional monolithic concrete frame.
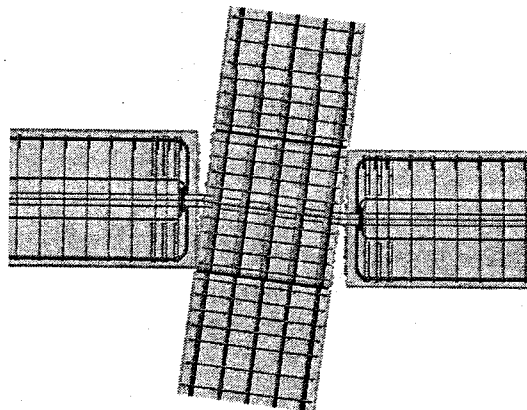
Figure 4.4: Unbonded Pre-Tensioned Frame without Damping – Deformed Configuration

The pre-tensioned strands are bonded to the concrete only at the ends of the beam length, as shown in Figure 4.2. In the central region, which must include all interfaces at which joint opening is expected, the strands are debonded by sheathing or other means. Sufficient bonded length is provided at the beam end to fully anchor the strands. If the seismic framing extends to the corner column, the beams may need to project beyond the outer face of the column in order to accommodate the strand development length. Other design alternatives include providing a mechanical anchorage to supplement the bond [Shahawy and Cai, 2001] or stopping the seismic framing short of the end bay and using a gravity-only system thereafter.

4.2 Design Assumptions

The following assumptions are made in the development of design equations:

1. The design forces and drift limits are known. The drift limits are selected to satisfy code restrictions and user requirements. Forces may be obtained either by Force Based Design or by Displacement Based Design. Interface rotations are obtained from the drift ratio, using the geometry of the system.

2. The overall dimensions of the frame members are known, having been obtained from architectural constraints and preliminary calculations.

3. The pre-tensioned beams are of constant cross section and contain pre-stressing that is the same over the full length. Each bay in the frame is of equal length.

4. Pre-stressing strands are unbonded through all columns that form part of the seismic framing. They are bonded beyond the interior face of the last column in the seismic part of the frame.

5. At each interface, the centroid of the pre-stressing strands is located at the mid-depth of the beam section.

6. The post-tensioning is at incipient yield at the design drift. If a lower tension stress is desired in the PT at the design drift, it should be substituted for f_{py} in the equations that follow.

7. Properties of the proposed materials are known. The principal ones are:
   • strength and stiffness of pre-tensioning strands
   • strength of concrete

4.3 Notation

The sign convention adopted is that forces and deformations are computed as positive quantities, regardless of whether they are tensile or compressive.

a_{des} = depth of compression stress block at design limit state

4-3

A_p = area of pre-stressing tendon

b_b = width of beam

b_{duct} = width of pre-stressing duct in joint

E_p = Young's modulus of pre-stressing tendon material

f'_c = specified concrete strength at 28 days

f_{p0} = stress in pre-stressing tendon, after losses, at zero drift

$f_{p,des}$ = stress in pre-stressing tendon at design limit state

f_{pi} = maximum tendon jacking stress minus pre-stress losses

f_{pu} = specified strength of pre-stressing tendon material

f_{py} = specified yield strength of pre-stressing tendon material

f_r = modulus of rupture of concrete

$F_{c,des}$ = force in beam concrete at beam-column interface at design limit state

$F_{p,des}$ = force in pre-stressing tendon at design limit state

h_b = depth of beam

h_c = depth of column (in plane of frame)

k_{ph} = plastic hinge length factor

l_b = total bay dimension between column centerlines

l_c = floor-to-floor story height

l_d = development length

l_n = clear span of beam between column faces

l_{ph} = plastic hinge length

l_{pu} = unbonded length of pre-stressing tendon tributary to one interface

$M_{cap,beam}$ = beam moment strength at interface at design limit state

M_{cr} = cracking moment strength at interface

M_{des} = moment demand at design limit state

v_{joint} = joint shear stress

$V_{col,des}$ = column shear force at design limit state

V_{joint} = joint shear force

V_n = nominal shear strength

V_u = factored shear demand

$V_{u,D+L}$ = factored dead and live load shear demand at interface

α_{des} = distance from center of compressive reaction to edge of member divided by member depth, at design limit state

β_1 = depth of equivalent compressive stress block divided by neutral axis depth

Δ_{fp} = increase in stress in pre-stressing tendon between zero drift and design drift

$\Delta_{fp\infty}$ = increase in stress in pre-stressing tendon between zero drift and design drift when concrete strength is infinite

Δ_p = deformation of pre-stressing tendon between zero drift and design drift

ε_c = compression strain in extreme fiber of concrete

η_{des} = distance from member compression face to neutral axis divided by member depth, at design limit state

θ_{des} = interface rotation at design limit state

μ = coefficient of friction

ϕ_v = strength reduction factor for shear

4.4 Design Procedure for Critical Elements

4.4.1 Design of Pre-stressing Tendons

The direct forces acting on the Pre-Tensioned Frame joint subject to a design interface rotation of θ_{des}, are shown in Figure 4.5. Locations of the forces are shown in Figure 4.6. The equations that follow use deformation compatibility and equilibrium to calculate these forces and the resulting moment capacity of the interface.
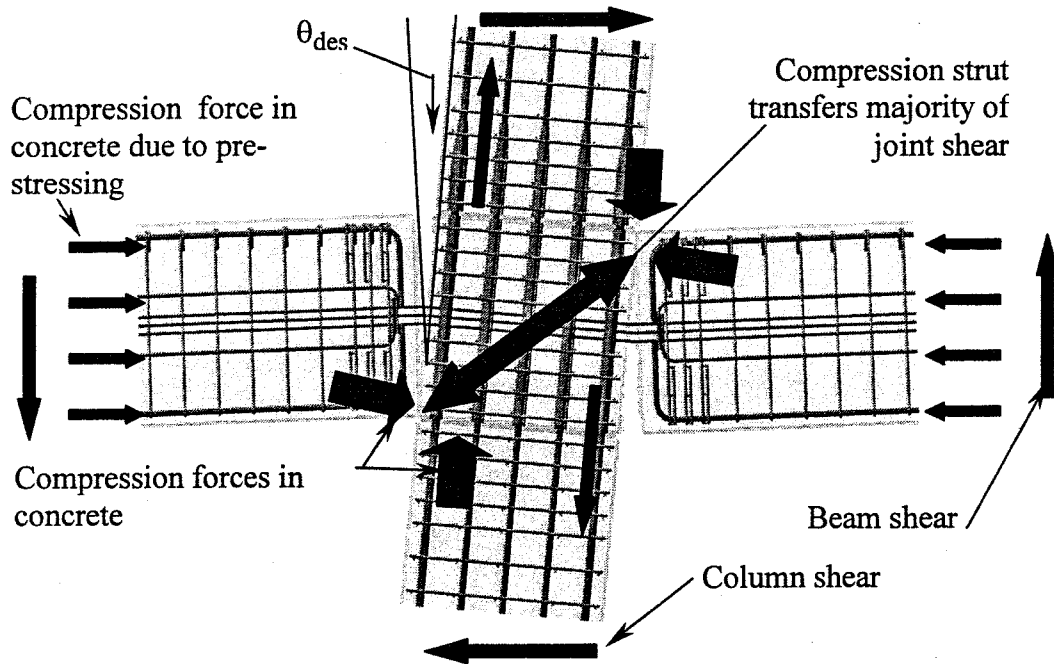
Figure 4.5: Unbonded Pre-Tensioned Frame without Damping - Forces on Connection at Design Drift

Step 1. Establish Material Properties

Establish properties of materials to be used. These include:
- Beam concrete strength and β_1
- Pre-stressed tendon strength and modulus of elasticity

Step 2. Obtain the Design Loads and Drifts

Use DBD or FBD to obtain lateral design loads. Compute corresponding design moments and drifts. The calculations that follow are for a limit state that corresponds to incipient yielding of the pre-tensioning tendon. M_{des} and θ_{des} are the corresponding interface moment and rotation.

| a) Dimensions and Displacements | b) Forces |
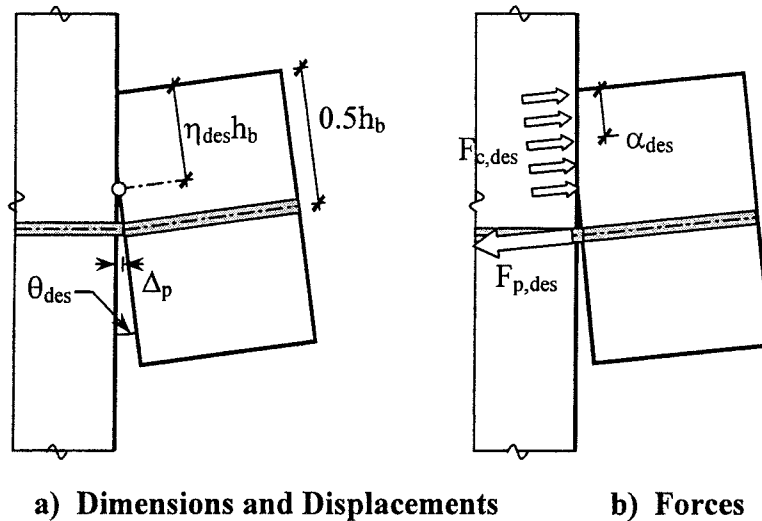
Figure 4.6: Unbonded Pre-Tensioned Frame without Damping – Locations of Forces at Design Drift

Step 3. Estimate the Frame Beam Dimensions

Frame beams that are as deep as possible are desirable because that choice leads to the smallest possible area of pre-stressing steel and the lowest shear forces in the beam-column joints. However, deeper frame beams also induce higher changes in stress in the tendon due to elongation at the design drift. Since the beam must span at least two bays, a deep section may also be heavy and present transportation and erection problems. Thus the choice of beam depth is likely to require compromise between these criteria.

Two criteria are candidates for controlling the beam depth at the interface. First is the restriction of Section 21.3.1.2 of ACI 318-99, which limits the effective depth to one quarter of the clear span. This requirement is relaxed somewhat here, for reasons explained below, to give

$$h_b \leq \frac{l_n}{3} \quad\text{...(4.1)}$$

The Commentary to ACI 318 (Section R21.3.1) states that the $l_n/4$ restriction is necessary to prevent behavior that is significantly different from that of more slender beams. That assertion is supported by a single reference, which is in Japanese. The requirement is believed to be based on the need to ensure adequate distance between the centers of rotations at the beam ends, in order to limit the plastic rotation demand. The center of rotation may be taken at the center of the plastic hinge zone. Since a plastic hinge in a monolithic frame may be as long as h_b, the implied distance between centers of rotation may be as short as $3h_b$. In the pre-tensioned system the center of rotation is at the interface, so the clear span could be $3h_b$ and still fulfill the spirit of the requirement. This reasoning forms the basis of Equation 4.1.

The second possible criterion is the need to ensure rocking rather than sliding of the beam at the interface. Ensuring that rocking behavior occurs is largely a question of selecting a low enough

depth-to-span ratio in the beam. A precise upper bound for h_n/l_n may be obtained by taking into account the shear demand and capacity, as discussed in Section 4.5.2. However, for parameter values likely in practice, that criterion is unlikely to control, and Equation 4.1 will control the maximum beam depth at the interface.

Note that h_b is the depth of the beam at the beam-column interface. If a reveal exists there to guide the crack, its dimensions must be accounted for when evaluating h_b.

The beam width should satisfy Section 21.3.1.3 of ACI 318 ["Building", 1999]

$$b_b \geq 0.3h_b \dotfill (4.2)$$

ACI 318-99 Section R21.3.1 states that this requirement is based on experience with conventional, non-pre-stressed, cast-in-place frames. Its applicability to precast, pretensioned frames is unclear. It is recommended here that Equation 4.2 be treated as advisory rather than mandatory. Use of a narrow beam could permit the beam weight to be kept low enough to overcome otherwise difficult erection problems.

Step 4. Establish Constants

$$\Delta f_{p\infty} = 0.5 E_p \theta_{des} \frac{h_b}{l_{pu}} \dotfill (4.3)$$

$\Delta f_{p\infty}$ has a physical meaning. It is the stress change in the tendon that would occur between zero drift and the design drift if the beam rocked about its corner. (This would require the concrete to be infinitely strong, so in practice it is impossible and the true stress change will be smaller. It is given by Equation 4.7)

Step 5. Estimate the Required Tendon Area, A_p

The tendon area, A_p, and initial pre-stressing stress, f_{p0}, may be computed iteratively.

If the design limit state corresponds to incipient yielding of the tendon, an initial estimate of the required tendon area can be obtained by assuming that the compression force in the beam is located $0.05h_b$ from the compression face. This assumption leads to a lever arm of $0.45h_b$ and a tendon area of

$$A_p = \frac{M_{des}}{(0.45h_b)f_{py}} \dotfill (4.4)$$

Step 6. Estimate the Neutral Axis Parameter, η_{des}, at Design Drift

The neutral axis location that is consistent with Step 5 can be obtained using Equation 4.5. The exact value assumed is unimportant, because it will be corrected during the iterative design procedure.

$$\eta_{des} = \frac{0.1}{\beta_1} \quad\text{..} (4.5)$$

Step 7. Calculate the Elongation and Stress in the Pre-stressing Tendon at θ_{des}

The elongation of the pre-stressing steel is related to both the interface rotation demand, θ_{des}, and the neutral axis depth.

$$\Delta_p = \theta_{des} h_b (0.5 - \eta_{des}) \quad\text{..} (4.6)$$

The corresponding change in stress, as the interface rotation increases from zero to θ_{des}, is

$$\Delta f_p = \frac{\Delta_p}{l_{pu}} E_p = \Delta f_{p\infty} (1 - 2\eta_{des}) \quad\text{...} (4.7)$$

The stress in the tendon must satisfy two conditions. First, at θ_{des}, it must not exceed the yield stress. Second, at zero interface rotation, it must not exceed f_{pi}, the maximum allowable initial stress. f_{pi} is given by the maximum permissible jacking stress of $0.70f_{pu}$ minus any losses. These criteria can be met by setting

$$f_{p0} = f_{py} - \Delta f_p \quad\text{...} (4.8)$$

If $f_{p0} \geq f_{pi}$

then $f_{p0} = f_{pi} \quad\text{..} (4.9)$

$$f_{p,des} = f_{p0} + \Delta f_p \quad\text{...} (4.10)$$

else
$$f_{p,des} = f_{py} \quad\text{...} (4.11)$$

Step 8. Calculate the Forces in the Pre-stressing Steel and Concrete at θ_{des}

The force in the pre-stressing tendon is

$$F_{p,des} = A_p f_{p,des} \quad\text{..} (4.12)$$

The compression force in the concrete, $F_{c,des}$, can be calculated from axial force equilibrium as

$$F_{c,des} = F_{p,des} \quad\text{..} (4.13)$$

Step 9. Calculate the Locations of the Compression Force and the Neutral Axis

The depth of the Whitney Equivalent stress block (Section 10.2.7 of ACI 318-99) in the concrete is

$$a_{des} = \frac{F_{c,des}}{0.85 f'_c b_b} \qquad \text{(4.14)}$$

The resultant compressive force on the grout is located at $\alpha_{des} h_b$ from the compression face, where

$$\alpha_{des} = \frac{a_{des}}{2h_b} \qquad \text{(4.15)}$$

and the neutral axis is located $\eta_{des} h_b$ from the compression face, where

$$\eta_{des} = \frac{a_{des}}{\beta_1 h_b} \qquad \text{(4.16)}$$

This value of η_{des} is then compared to the previous value, and Steps 7 - 9 are repeated until the computed and assumed values of η_{des} converge.

Step 10. Calculate the Moment Strength of the Section at θ_{des}

The moment strength is calculated by taking moments about the centroid of the compression force. It is given by

$$M_{cap,beam} = F_{p,des} h_b \left(0.5 - \alpha_{des}\right) \qquad \text{(4.17)}$$

This must be equal to or greater than the design moment, so

$$M_{cap,beam} \geq M_{des} \qquad \text{(4.18)}$$

If the moment capacity is too small, increase A_p and repeat Steps 6-10.

Step 11. Confine the Compression Area as Needed.

The local stress in the compressed region of the beam can become very large, especially if the interface rotation or the initial pre-stress force is large. The concrete there is expected to deform inelastically, so it must be protected against crushing and falling out of the joint by confining reinforcement. In the PRESSS Phase III test building, specially fabricated welded wire fabric was used for the purpose. It can be seen in Figure 4.1.
Since the beam end deformation is concentrated in a single crack and because the tendon is unbonded and pre-stressed, plane sections do not remain plane at the end of the beam. Thus the concrete strains cannot strictly be evaluated from the curvature within a plastic hinge length. No

4-9

completely rational method has yet been proposed for evaluating the strain field in the concrete under these circumstances.

In lieu of a more precise approach, Priestley and MacRae [1996] recommend an equivalent plastic hinge length equal to $0.04l_n$ for an unbonded post-tensioned, connection. However, this assumed plastic hinge length does not account for the level of pre-stress in the tendon. To overcome this difficulty, the plastic hinge length is taken here as a function of the compression zone depth, $\eta_{des}h_b$.

$$l_{ph} = k_{ph}\eta_{des}\,h_b \quad\text{..(4.19)}$$

where, without experimental validation, k_{ph} is taken equal to 1.0. This choice is made on the basis of St Venant's Principle [St. Venant, 1855], which implies that a local disturbance in stress dies out rapidly at distances greater than the member depth.

The average compression strain over this plastic hinge length is

$$\varepsilon_c = \frac{\theta_{des}\left(\eta_{des}h_b\right)}{l_{ph}} = \frac{\theta_{des}}{k_{ph}} \quad\text{..(4.20)}$$

If this compression strain exceeds the ultimate strain of the unconfined concrete, spalling should be expected and the compression region should be confined to ensure that the concrete can sustain higher strains without degradation. In addition, if the cover is expected to spall, a reduced beam section with dimensions equal to the confined core dimensions should be used in the above calculations.

4.5 Design of Other Components

4.5.1 Interface Cracking Strength

Section 18.8.3 of ACI 318-99 requires that the design moment strength of the beam must be greater than 1.2 times the cracking strength. The cracking moment is

$$M_{cr} = \left(f_r + \frac{A_p f_{p0}}{h_b b_b}\right)\frac{b_b\left(h_b\right)^2}{6} \quad\text{..(4.21)}$$

where f_r = modulus of rupture of the concrete = $7.5\sqrt{f'_c}$

However, the associated Commentary makes clear that this requirement is intended to prevent brittle collapse in gravity systems, and provides conditions under which the requirement need not be satisfied. If sufficient moment strength exists at mid-span to carry the gravity moments, as discussed in Section 4.5.3, cracking at the ends of the statically indeterminate beam will not lead

to collapse. It is thus recommended that the requirement of Equation 4.21 be treated as advisory and not mandatory.

4.5.2 Interface Shear Strength

Shear resistance across the interface is provided by shear friction. The normal force creating that friction is supplied by the pre-stressing. Since there is no deformed steel reinforcement crossing the interface, the compression force on the concrete is always equal to the force in the pre-stressing tendon. At zero drift, the requirement of no slip at the interface leads to

$$f_{p0} \geq \frac{V_{u,D+L}}{\phi_v \mu A_p} \quad \text{..(4.22)}$$

At the design drift, the shear friction resistance at the interface is

$$V_n = \mu A_p f_{p,des} \quad \text{..(4.23)}$$

where μ is the coefficient of friction at the cracked interface. The corresponding shear demand on the interface is determined from equilibrium on the beam.

$$V_u = V_{u,D+L} + \frac{2M_{cap,beam}}{l_n} \quad \text{..(4.24)}$$

The moment capacity for a beam with a tendon at mid-height is given by Equation 4.17. Combining Equations 4.17, 4.23 and 4.25 leads to

$$\frac{h_b}{l_n} \leq \frac{1}{(0.5 - \alpha_{des})} \left(\phi_v \mu - \frac{V_{u,D+L}}{A_p f_{p,des}} \right) \quad \text{...(4.25)}$$

ACI 318-99 permits $\mu = 1.4$ for monolithic concrete, which is the relevant condition at the interface crack. However a value lower than this should be used in order to minimize the possibility of cyclic slipping and the associated damage to the interface. A value of $\mu = 0.7$ is recommended here, albeit without experimental validation. If, as is likely, $V_{u,D+L}$ is an order of magnitude less than $A_p f_{p,des}$, the limit on h_b/l_n imposed by Equation 4.25 will be less critical than that of Equation 4.1.

4.5.3 Beam Flexure

During cyclic frame displacements, the beam end moments may become equal in magnitude and opposite in sign (i.e. both clockwise or both counter-clockwise). Their effect on the mid-span moment capacity is then zero, so moment demand at mid-span is the same as that for a simple span. This observation applies to all types of frame, including cast-in-place concrete and structural steel moment frames. Reinforcement should be selected accordingly. In particular, the

connection between the two beams at mid-span should be designed to carry the necessary positive moment if it is located near mid-span.

4.5.4 Beam Shear

The beam must be designed so that, for all possible load cases, the weakest mechanism is the moment strength at the interface. This requires the beam shear strength to be designed using Capacity Design principles. The compression force from the post-tensioning tendon in the beam improves the beam's shear capacity, and may be taken in to account by using the provisions of Section 11.3.1 of ACI318-99 and treating the pre-stressing force as an external compression.

4.5.5 Beam Torsion

Torsion at the beam-column interface is resisted almost exclusively by shear stresses in the cracked concrete. While the pre-tensioned tendon carries some shear by dowel action, the amount is uncertain. The torsional stiffness and strength at the interface are therefore much smaller than those of the beam itself, so torsional rotation is concentrated at the beam-column interface. For that reason, torsional loading on the frame beam should be minimized.

4.5.6 Bond and Anchorage

The pre-stressing tendon must be anchored past the last interface so that it is fully developed and can sustain cyclic loading. If anchorage is achieved by bond alone, the anchored length should be at least the development length required in Section 12.9 of ACI 318-99. In the PRESSS Phase III test building, the ½" dia. strands were bonded over a length of 78" (1.15 times the l_d specified by ACI) and no evidence of strand slip was seen. Mechanical anchorages, such as strand chucks, may be used to supplement the bond. Use of bond and mechanical anchorages together is discussed by Shahawy and Cai [2001].

4.5.7 Column Design

The column should be designed using Capacity Design principles to ensure that the nonlinear action occurs in the beam at the beam-column interface. Column splices should also be designed using Capacity Design principles, including consideration of higher mode effects as described in the UBC ["Uniform", 1997].

4.5.8 Joint Shear

The required joint shear strength should be determined using Capacity Design principles. The joint forces on the exterior and interior columns are different, due to both the magnitude of loading on the joint and the resistance mechanism within the joint.

The magnitude of the joint shear demand is computed here using values for the forces that are consistent with the strains expected in the members. Those forces differ from the ones used in ACI318-99, which are largely empirical, and which do not take into account pre-stressed

reinforcement. Furthermore, it is worth noting that the allowable joint shear stresses given by ACI318-99 do not represent a true Capacity Design, because considerable damage will occur to a joint that is designed in accordance with them [Mosier, 2000]. Thus the design of any joint, in a cast-in-place or a precast frame, depends on the performance desired. The requirements of ACI318-99 should be satisfied as a minimum but, if minimal joint damage is desired, a more conservative design may be necessary.

A typical interior joint is shown in Figure 4.7.
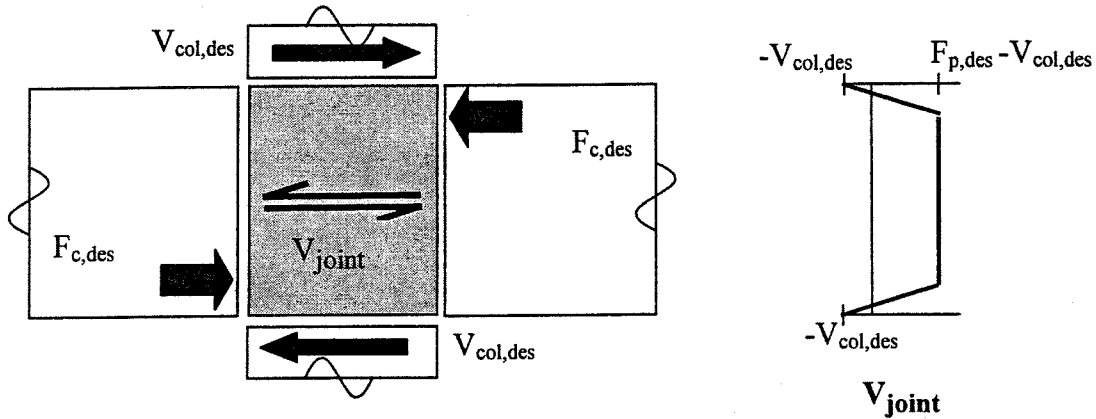
Figure 4.7: Unbonded Pre-Tensioned Frame without Damping – Interior Joint Shear Forces

Equilibrium of the joint requires a joint shear force of

$$V_{joint} = F_{c,des} - V_{col,des} = F_{p,des} - V_{col,des} \quad \dots\dots\dots\dots\dots\dots\dots\dots\dots\dots\dots\dots(4.26)$$

where $F_{p,des} = A_p f_{p,des}$

$V_{col,des}$ = the column shear force associated with development of the beam moment strength, $M_{cap,beam}$, on the beam section.

Note that the forces in Equation 4.26 are all taken as positive quantities. If the inflection points occur at mid-span of the beams and at mid-height of the columns, the column shear force is

$$V_{col,des} = \frac{2M_{cap,beam}}{l_c\left(1 - h_c/l_b\right)} \quad \dots\dots\dots\dots\dots\dots\dots\dots\dots\dots\dots\dots\dots\dots\dots(4.27)$$

The joint shear stress is then

$$v_{joint} = \frac{V_{joint}}{h_c\left(b_c - \sum b_{duct}\right)} \quad \dots\dots\dots\dots\dots\dots\dots\dots\dots\dots\dots\dots\dots\dots(4.28)$$

4-13

For an interior column, the joint shear force is the horizontal force anywhere within the joint between the top and bottom compression forces in the concrete as shown in Figure 4.7. The critical plane occurs where the net joint width is narrowest, which is therefore given by the gross joint width minus the width of the pre-tensioning sheaths or ducts. If several ducts are used, the total width of all the ducts on any horizontal plane should be used. In the absence of additional experimental validation, the allowable joint shear stresses should be kept within code limits [e.g. "Building", 1999].

For an exterior joint, the maximum joint shear force depends on the configuration of the structure and the loading on the outer face of the column. If the tendon is developed in a stub that extends beyond the column, as illustrated in Figure 4.2, and if the stub carries no vertical load, the tendon force exerts a uniform pressure on the outer face of the column joint, as shown in Figure 4.8. This causes the joint shear force to vary over the height of the joint. The shear force changes sign twice over the height of the joint, and reaches a maximum at the bottom of the compressive stress block in the beam.
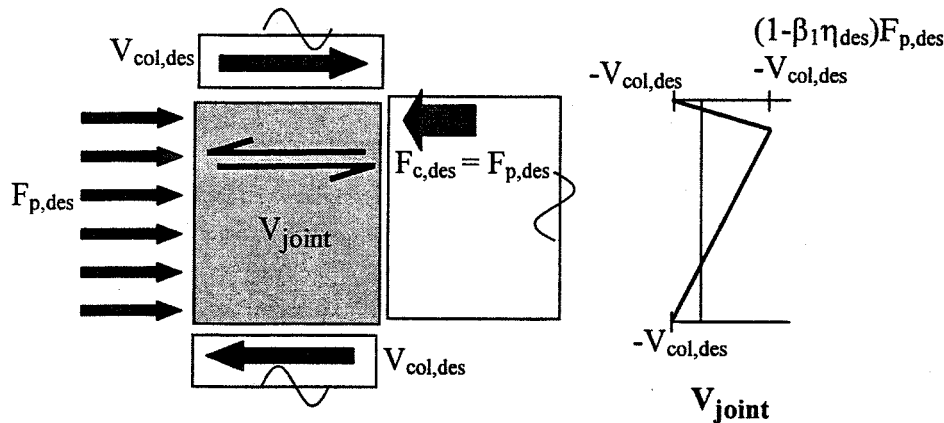
Figure 4.8: Unbonded Pre-Tensioned Frame without Damping – Exterior Joint Shear Forces

The minimum section of the joint (accounting for the voids caused by the tendon sheaths or ducts) does not coincide with the peak joint shear force, so the critical section for shear is not immediately obvious. Furthermore, joint shear failure is usually caused by diagonal tension or compression, rather than horizontal sliding at the critical plane, so an argument can be made for using an average shear stress over a region rather than the peak value. However, in the absence of a more detailed investigation, the maximum value, given by Equation 4.29, should be used.

$$V_{joint} = \left(1 - \beta_1 \eta_{des}\right) F_{p,des} - V_{col,des} \quad \text{...(4.29)}$$

$$V_{col,des} = \frac{M_{cap,beam}}{l_c \left(1 - h_c / l_b\right)} \quad \text{...(4.30)}$$

The joint shear stress is given by Equation 4.28. In the absence of experimental validation, the allowable joint shear stresses should be kept within code limits [e.g. "Building", 1999].

4.6 Limits on Reinforcement

There is no upper bound to the amount of beam reinforcement that may be used. However, as the pre-stressing force increases, the lever arm diminishes, so very heavily reinforced beams are unlikely to be economical. In heavily reinforced beams the compressive strain in the concrete will likely exceed the nominal crushing strain of 0.003 in./in, so confinement will be required.

4.7 Construction Issues

4.7.1 Beam Weight

To avoid the use of many beam connections, the beams will likely span at least two bays. Weight may then become a controlling factor in their design.

4.7.2 Erection Tolerances

The system requires accurate placement of the columns, so that the protruding column bars can be threaded through the vertical ducts in the beam.

4.8 Discussion

The Unbonded Pre-Tensioned Frame without Damping that was tested in the PRESSS Phase III test building performed very well. Figure 4.9 shows the frame at the end of the test. The only visible damage was the interface crack and slight crushing of the concrete cover on the compressive face of the beam, at the beam-column interface. While the crack formed at the interface as expected, it was not as straight as might have been desired. This occurred because the bottom of the reveal was rounded rather than sharp. In addition, a joint shear crack is visible, but it closed as soon as the loading was removed.

The Unbonded Pre-Tensioned Frame without Damping was used at the top two levels of the test building, where the flexural demands, and therefore also the capacities, were smaller than at lower levels in the same frame. However, the drift demands were still substantial, with the roof drift ratio reaching 4%. The damage to the interface was minimal, no shear slip was observed there, and there was no evidence of bond failure in the beam stubs.

In a multi-span beam using more than one beam element, the connections between beams at mid-span must resist shear and some moment. They should be rigid, and have no inelastic

deformation requirement, so many different types are possible. Examples are given in the PCI Connection Manual [PCI, 1988].

The design procedures outlined here have not yet been validated by the authors using the data from the PRESSS Phase III test. Therefore, they should be used only for trial designs.
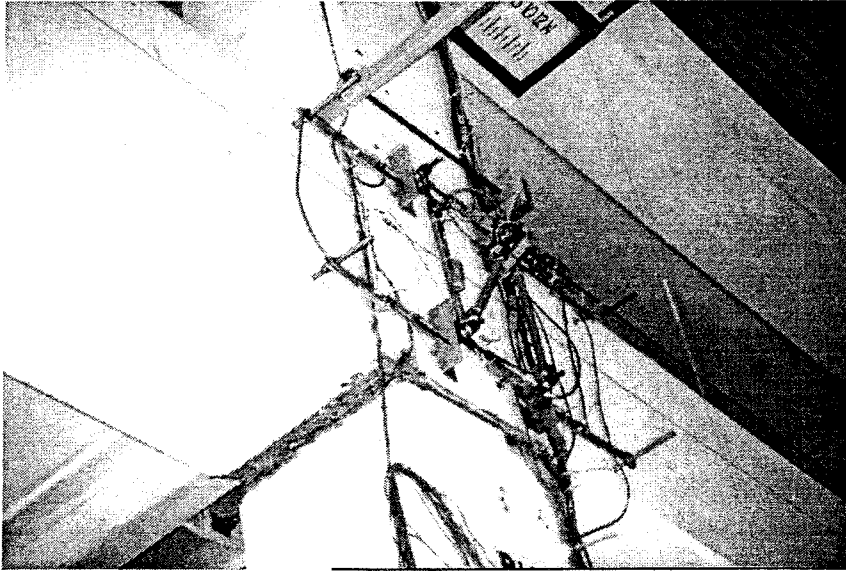
Figure 4.9: Unbonded Pre-Tensioned Frame without Damping at End of Test

5 UNBONDED POST-TENSIONED FRAMES WITH DAMPING

5.1 Concept Description

The Unbonded Post-Tensioned Frame with Damping is illustrated in Figure 5.1.
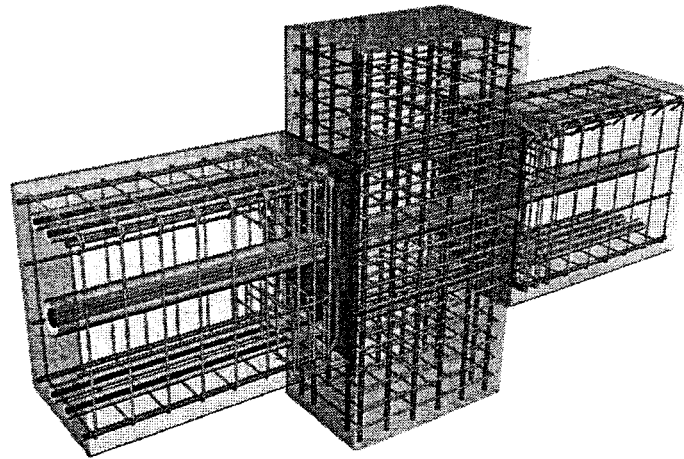
Figure 5.1: Unbonded Post-Tensioned Frame with Damping

The frame consists of multi-story precast columns, spliced as necessary, and single span beams between columns. The arrangement is shown schematically in Figure 5.2. Each beam line is post-tensioned for the entire length of the frame, at beam mid-height. The post-tensioned tendons are not grouted. Deformed bars are grouted into sleeves at the top and bottom of the beam, which extend through the column. An unbonded length of the deformed reinforcement at the interface, shown in Figure 5.3, protects the reinforcement from fracture at high drifts by limiting the strain in it.

Post-tensioning tendon (unbonded)

Post-tensioning anchorage

Deformed bars
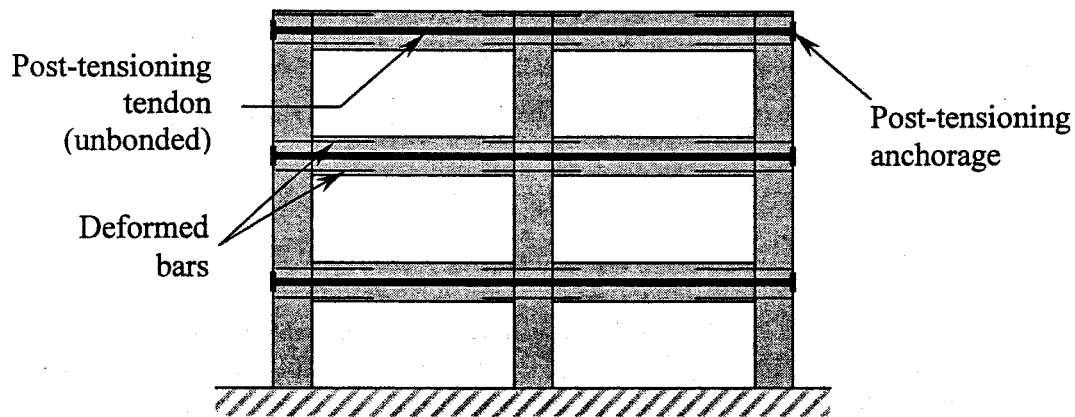
Figure 5.2: Unbonded Post-Tensioned Frame with Damping – Layout of Elements and Primary Reinforcement
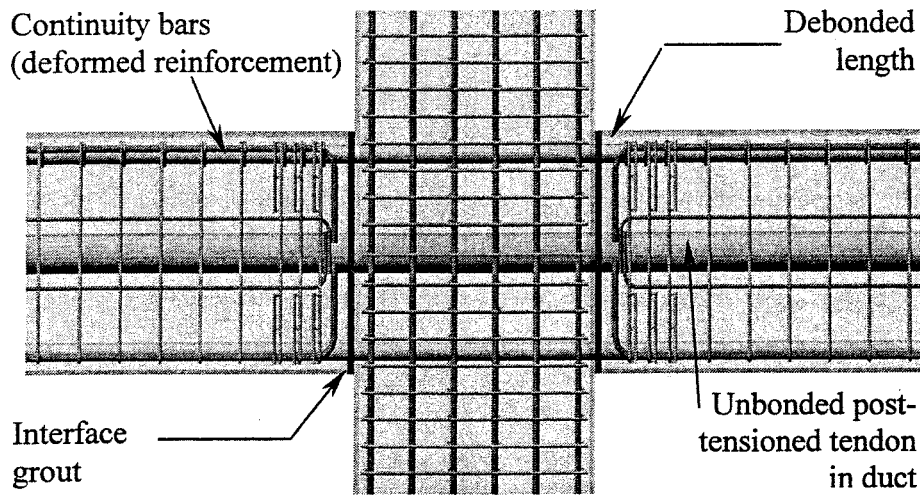
Figure 5.3: Unbonded Post-Tensioned Frame with Damping – Components

When the frame experiences drift caused by lateral inertia forces, the column tilts and the beams remain approximately horizontal. The relative rotation between the beam and column is accommodated by a concentrated rotation at the interface. This rotation causes a gap to open up over part of the height of the interface, as part of the beam end separates from the grout pad. The post-tensioning tendon elongates but remains elastic. The continuity bars in the tension region yield in tension. Each set of reinforcement creates a couple with the compression force in the grout, and the total moment resists the seismic load. When the load is removed, the moment from the post-tensioning tendon tends to close the gap at the interface. The continuity bars shorten and yield in compression, thereby resisting the closure of the gap. The frame can be made to return to zero drift by ensuring that the moment due to the post-tensioning is greater than that due to the continuity bars in compression.
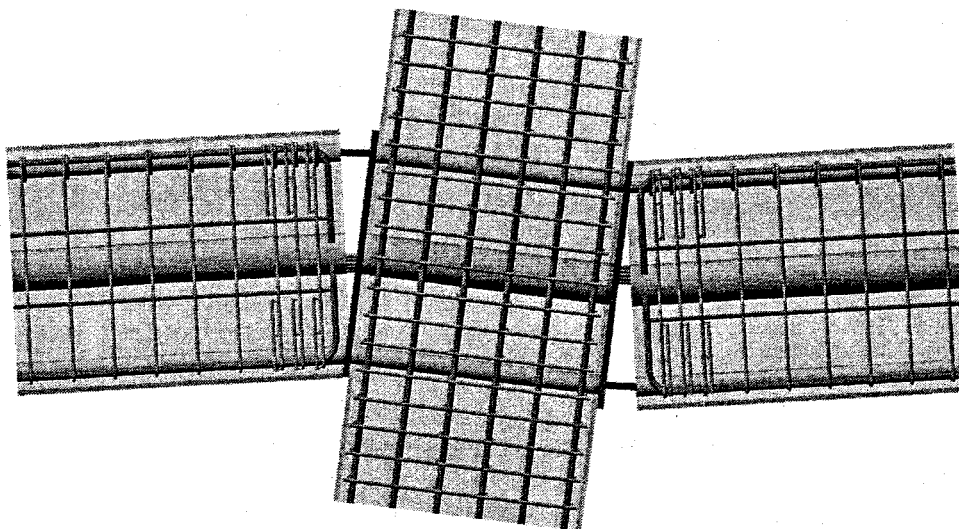
Figure 5.4: Unbonded Post-Tensioned Frame with Damping – Deformed Configuration

The grout at the interface provides an opportunity to minimize damage to the concrete beam itself. If the grout is designed to be weaker than the concrete in the beam, then the rotation at the interface is accommodated by local compression of the grout pad. In this case, grout with a high (cyclic) compressive strain capacity must be used. The calculations in this chapter are based on this approach. Alternatively, the concrete in the beam itself may be designed to be weaker than the grout. In this case the rotation at the interface is accommodated by compression of a "plastic hinge length" in the concrete. If the concrete strains are higher than the unconfined strain capacity of the concrete used in the beam, then the compression region of the beam must be confined and a reduced beam section used for the analysis, because the cover will spall.

The total resisting moment is comprised of one component from the pre-stressing tendon and another from the deformed reinforcement. The fraction of the total resistance supplied by each component may be chosen by the designer, but the choice affects the response. For a given total strength, a higher proportion of deformed reinforcement will lead to more damping and lower peak drift, but may lead to larger residual drift, and vice versa.

One possible design philosophy is to maximize the moment strength provided by the deformed reinforcement, subject to the constraint that the residual drift should still be zero. This choice will minimize the peak drift, while maintaining zero residual drift. This design philosophy is used in the following equations.

The design equations for pre-stressed systems with energy dissipation are more complex than those for beams that contain only one type of reinforcement. In the design procedure that follows, an iterative approach is taken so that the design steps are transparent and the design objective is clear.

5.2 Design Assumptions

The following assumptions are made in the development of design equations:

1. The design forces and drifts are known. The drift limits are selected to satisfy code restrictions and user requirements. Forces may be obtained either by Force Based Design, or by Displacement Based Design. Interface rotations are obtained from the drift ratio, using the geometry of the system.

2. The overall dimensions of the frame members are known, having been obtained from architectural constraints and preliminary calculations.

3. The beams are of constant cross section and contain post-tensioning that is the same over the full length. Each bay in the frame is of equal length.

4. The post-tensioning tendon is unbonded through all columns that form part of the seismic framing. It is anchored at the exterior face of the last column in the seismic part of the frame.

5. At each interface, the centroid of the post-tensioning tendon is located at the mid-depth of the beam section.

6. The post-tensioning tendon is at incipient yield at the design drift. If a lower tension stress is desired, it should be substituted for f_{py} in the equations that follow.

7. Deformed bars are grouted into ducts, with a short unbonded length at the interface. The ducts are grouted through the column. Equal top and bottom reinforcement is used.

8. The grout at the interface is reinforced with fibers to prevent grout degradation and loss under cyclic loading.

9. Properties of the proposed materials are known. The principal ones are
   - tendon material strength and modulus of elasticity
   - deformed bar yield and peak strength
   - concrete strength
   - interface grout strength and stress block coefficient β_1
   - coefficient of friction, μ, between the grout and concrete

The coefficient of friction, μ, between the grout and the concrete, may be taken as 0.5 in the absence of better information. Hutchinson et al. [1990] measured a value of 0.6 between precast concrete and grout under cyclic loading. It is reduced here to 0.5 to allow for variations with grout type. Experimental evidence would be needed to justify the use of a higher value in design.

5.3 Notation

The sign convention adopted is that forces and deformations are computed as positive quantities, regardless of whether they are tensile or compressive.

a_0	= depth of compression stress block in grout at zero drift
a_{des}	= depth of compression stress block in grout at design limit state
A_p	= area of pre-stressing tendon
A_s	= area of deformed reinforcement in one face of beam
b_c	= width column
b_{duct}	= width of pre-stressing duct in joint
b_g	= width of grout pad at beam-column interface
d_b	= diameter of deformed reinforcing bar
E_p	= Young's modulus of pre-stressing tendon material
f'_g	= specified grout strength at 28 days
f_{p0}	= stress in pre-stressing tendon, after losses, at zero drift
$f_{p,des}$	= stress in pre-stressing tendon at design limit state
f_{pi}	= maximum tendon jacking stress minus pre-stress losses
f_{pu}	= specified strength of pre-stressing tendon material
f_{py}	= specified yield strength of pre-stressing tendon material

$f_{s,des}$ = stress in tension deformed reinforcement

$f_{s',des}$ = stress in compression deformed reinforcement

f_{sy} = specified yield strength of deformed reinforcement

$F_{c,0}$ = force between beam concrete and grout at beam-column interface at zero drift

$F_{c,des}$ = force in beam concrete at beam-column interface at design limit state

$F_{p,0}$ = force in pre-stressing tendon at zero drift

$F_{p,des}$ = force in pre-stressing tendon at design limit state

F_{s0} = force in tension deformed reinforcement at zero drift

$F_{s,des}$ = force in tension deformed reinforcement at design limit state

$F_{s'0}$ = force in compression deformed reinforcement at zero drift

$F_{s',des}$ = force in compression reinforcing steel at design limit state

h_c = column depth (in plane of frame)

h_g = depth of grout pad at beam-column interface

k_{ph} = plastic hinge length factor

l_b = total bay dimension between column centerlines

l_c = floor-to-floor story height

l_n = clear span of beam between column faces

l_{ph} = plastic hinge length

l_{pu} = unbonded length of unbonded pre-stressing tendon tributary to one interface

l_{su} = length of unbonded region of deformed reinforcement at each interface

$M_{cap,beam}$ = beam moment strength at interface at design limit state

M_{des} = moment demand at design limit state

$M_{p,0}$ = resisting moment provided by pre-stressing tendon at zero drift

$M_{p,des}$ = resisting moment provided by pre-stressing tendon at design limit state

$M_{s,0}$ = resisting moment provided by tension deformed reinforcement at zero drift

$M_{s,des}$ = resisting moment provided by tension deformed reinforcement at design limit state

$M_{s'.0}$ = resisting moment provided by compression deformed reinforcement at zero drift

$M_{s',des}$ = resisting moment provided by compression deformed reinforcement at design limit state

v_{joint} = joint shear stress

$V_{col,des}$ = column shear force at design limit state

V_{joint} = joint shear force

V_n = nominal shear strength

V_u = factored shear demand

$V_{u,D+L}$ = factored dead and live load shear demand at interface

α_0 = distance from compression face of member to center of compression force, divided by member depth, at zero drift

α_{des} = distance from center of compressive reaction to edge of member divided by member depth, at design limit state

β_1 = depth of equivalent compressive stress block divided by neutral axis depth

Δ_{fp} = increase in stress in pre-stressing tendon between zero drift and design drift

$\Delta_{fp\infty}$ = increase in stress in pre-stressing tendon between zero drift and design drift when concrete and grout strengths are infinite

Δ_p = deformation of pre-stressing tendon between zero drift and design drift

Δ_s = deformation of tension deformed reinforcement

$\Delta_{s'}$ = deformation of compression deformed reinforcement

ε_c = compression strain in extreme fiber of concrete

ε_s = strain in tension deformed reinforcement

$\varepsilon_{s,max}$ = maximum strain permissible in deformed reinforcement under cyclic loading

$\varepsilon_{s'}$ = strain in compression deformed reinforcement

ζ = distance from beam deformed reinforcement to nearest face divided by h_g

η_0 = distance from member compression face to neutral axis divided by member depth, at zero drift

η_{des} = distance from member compression face to neutral axis divided by member depth, at design limit state

θ_{des} = interface rotation at design limit state

$\lambda_{s,des}$ = over-strength factor for deformed reinforcement in tension at design limit state

$\lambda_{s',des}$ = over-strength factor for deformed reinforcement in compression at design limit state

μ = coefficient of friction

ϕ_v = strength reduction factor for shear

5.4 Design Procedure for Critical Elements

5.4.1 Design of Post-tensioned Tendons and Deformed Reinforcement at Interface

The forces acting on a joint of the Unbonded Post-Tensioned Frame with Damping and corresponding to a design interface rotation of θ_{des} are shown in Figure 5.5, and the locations of the forces are given in Figure 5.6. .
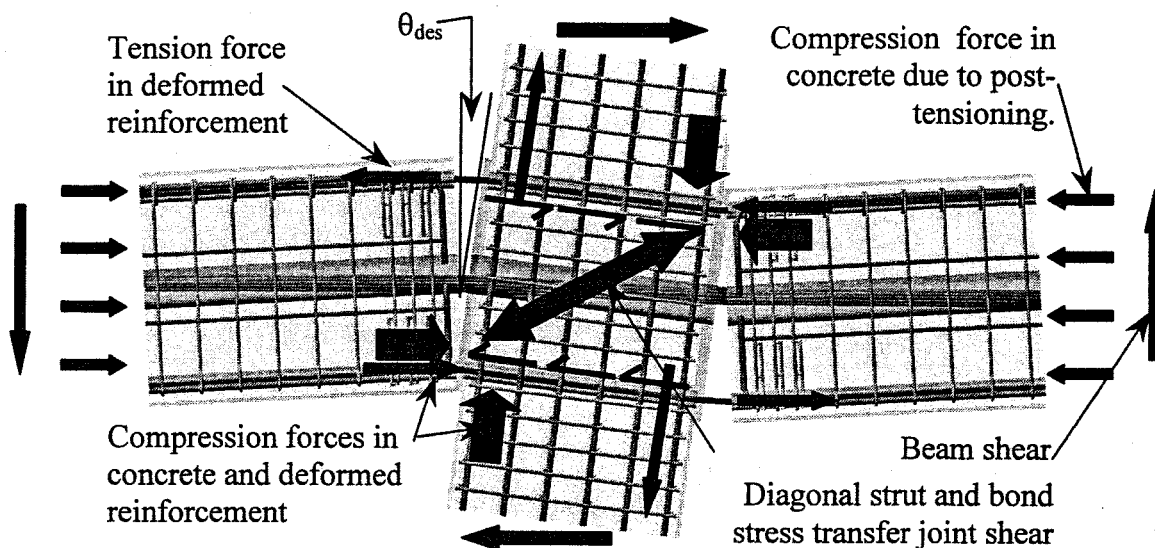
Figure 5.5: Unbonded Post-Tensioned Frame with Damping – Forces on Connection at Design Drift

a) **Dimensions and Displacements**   b) **Forces**
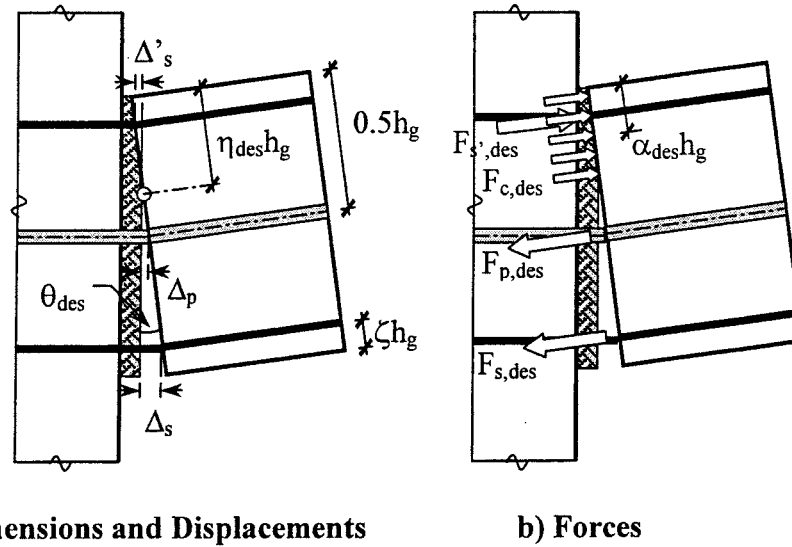
Figure 5.6: Unbonded Post-Tensioned Frame with Damping – Locations of Forces at Design Drift

The equations that follow use deformation compatibility and equilibrium to calculate the forces and the resulting moment capacity at the interface. They are presented for the limit state that corresponds to incipient yield of the post-tensioning tendon.

The moment is resisted by a combination of post-tensioning tendon and deformed reinforcement. The proportion of the total moment resisted by each may be selected to the designer, subject to certain limits. Re-centering of the frame cannot be assured if the moment resisted by the deformed reinforcement exceeds approximately one half the total. There is no lower bound on the flexural strength provided by the deformed reinforcement. In the extreme case, if it were to be omitted altogether, the frame would become a Post-Tensioned Frame Without Damping, as described in Section 1.2.

Step 1. Establish Material Properties

Establish properties of materials to be used. These include:
- beam concrete strength
- interface grout strength and corresponding β_1
- pre-stressed tendon strength and modulus of elasticity
- deformed reinforcement yield and tensile strength, and strain at maximum strength
-

Step 2. Obtain the Design Loads and Drifts

Use DBD or FBD to obtain design loads. Compute corresponding design moments and drifts. θ_{des} is the interface rotation at the design limit state.

Step 3. Estimate the Frame Beam Dimensions

Frame beams that are as deep as possible are desirable because that choice leads to the smallest possible area of pre-stressing tendon and the lowest shear forces in the beam-column joints. However, deeper frame beams also induce higher changes in stress in the tendon due to elongation at the design drift. The beam depth should be chosen with these consequences in mind.

Two criteria are candidates for controlling the beam depth at the interface. First is the restriction of Section 21.3.1.2 of ACI 318-99, which limits the effective depth to one quarter of the clear span. This requirement is relaxed somewhat here, for reasons explained below, to give

$$h_b \leq \frac{l_n}{3} \quad\text{...(5.1)}$$

The Commentary to ACI 318 (Section R21.3.1) states that the $l_n/4$ restriction is necessary to prevent behavior that is significantly different from that of more slender beams. That assertion is supported by a single reference, which is in Japanese. The requirement is believed to be based on the need to ensure adequate distance between the centers of rotations at the beam ends, in order to limit the plastic rotation demand. The center of rotation may be taken at the center of the plastic hinge zone. Since a plastic hinge in a monolithic frame may be as long as h_b, the implied distance between centers of rotation may be as short as $3h_b$. In the post-tensioned system the center of rotation is at the interface, so the clear span could be $3h_g$ and still fulfill the spirit of the requirement. This reasoning forms the basis of Equation 5.1.

The second possible criterion is the need to ensure rocking rather than sliding of the beam at the interface. Ensuring that rocking behavior occurs is largely a question of selecting a low enough depth-to-span ratio in the beam. A precise upper bound for h_n/l_n may be obtained by taking into account the shear demand and capacity, as discussed in Section 5.5.1. However, for parameter values likely in practice, the criterion is unlikely to control. In that case Equation 5.1 will control the maximum beam depth at the interface.

The beam width should satisfy Section 21.3.1.3 of ACI 318 ["Building", 1999]

$$b_b \geq 0.3h_b \quad\text{...(5.2)}$$

ACI 318-99 Section R21.3.1 states that this requirement is based on experience with conventional, cast-in-place, non-pre-stressed frames. Its applicability to precast, post-tensioned frames is unclear. It is recommended here that Equation 5.2 be treated as advisory rather than mandatory. Use of a narrow beam could permit the beam weight to be kept low enough to overcome otherwise difficult erection problems.

If the grout at the interface is held back from the face of the beam, the dimensions of the grout, rather than those of the concrete, should be used in the design.

Step 4. Establish Constants

$$\Delta f_{p\infty} = 0.5 E_p \theta_{des} \frac{h_b}{l_{pu}} \qquad (5.3)$$

$\Delta f_{p\infty}$ has a physical meaning. It is the stress change in the tendon that would occur between zero drift and the design drift if the beam rocked about its corner. (This would require the concrete and grout to be infinitely strong, so in practice it is impossible and the true stress change will be smaller. It is given by Equation 5.12)

Step 5. Determine the Proportion of Moment Strength to be Provided by Pre-stressing and Deformed Reinforcement, Respectively

In the Unbonded Post-Tensioned Frame with Damping, the two different types of reinforcement fulfill very different functions. Both provide moment strength at the interface, but the pre-stressing provides an elastic restoring force that tends to self-right the frame after the earthquake is over, whereas the deformed reinforcement provides damping. The criterion for self-righting, which is that the moment resisted by the post-tensioning tendon at zero drift be greater than the moment resisted by the deformed reinforcement, creates an upper bound on the amount of deformed reinforcement. Use of this criterion leads to designs in which slightly less than half the total moment resistance is supplied by the deformed reinforcement. The exact proportions depend on the design interface rotation, the beam span/depth ratio, the allowable jacking stress and the yield strength of the tendon. However, a reasonable initial estimate can be obtained from

$$M_{p,des} \approx 0.55 M_{des} \qquad (5.4)$$

$$M_{s,des} = M_{des} - M_{p,des} \qquad (5.5)$$

In the design equations that follow, the calculations depend on displacement compatibility between the tendon and the surrounding concrete. They are similar to those used when computing the strength of a conventional pre-stressed beam by strain compatibility and are thus iterative.

Step 6. Estimate Required the Tendon Area, A_p

If the design limit state corresponds to incipient yielding of the tendon, an initial estimate of the required tendon area can be obtained by assuming that the compression force in the beam is located $0.05h_g$ from the compression face. This assumption leads to a lever arm of $0.45h_g$ and a tendon area of

$$A_p = \frac{M_{p,des}}{(0.45 h_g) f_{py}} \qquad (5.6)$$

Step 7. Estimate the Required Area, A_s, of Deformed Reinforcement

An initial estimate of the required area of deformed reinforcement can be obtained by using the same assumptions as for Equation 5.6.

$$A_s = \frac{M_{s,des}}{(0.95 - \zeta)h_g \lambda_{s,des} f_{sy}} \quad\text{...(5.7)}$$

The value of the material stress factor, $\lambda_{s,des}$, depends on the limit state under consideration, and the corresponding allowable strain in the deformed reinforcement. Proposed values are given in Table 2.1.

Step 8. Estimate the Neutral Axis Parameter, η_{des}, at the Design Drift

The neutral axis location that is consistent with Step 7 can be obtained using Equation 5.8. The exact value assumed is unimportant, because it will be corrected during the iterative design procedure.

$$\eta_{des} = \frac{0.1}{\beta_1} \quad\text{..(5.8)}$$

Step 9. Calculate the Stress in the Tension Deformed Reinforcement

The strain in the tension deformed reinforcement exceeds the yield strain, and is given by $\varepsilon_{s,max}$ from Table 2.1. The corresponding stress is

$$f_{s,des} = \lambda_{s,des} f_{sy} \quad\text{..(5.9)}$$

Step 10. Calculate the Stress in the Compression Deformed Reinforcement

The compression deformed reinforcement is likely to be at a comparatively small net strain, because the presence of the concrete and grout prevents large compressive strains. However, the bars are also likely to have undergone significant inelastic tension strain in previous cycles, so the stress cannot be related directly to the instantaneous strain. Thus the stress is taken as

$$f_{s',des} = \lambda_{s',des} f_{sy} \quad\text{..(5.10)}$$

where $\lambda_{s',des}$ is given in Table 2.1. Its value takes into account the fact that the stress-strain curve is likely to be somewhat rounded by the Bauschinger effect. Thus $\lambda_{s',des}$ is less than $\lambda_{s,des}$.

Step 11. Calculate the Elongation and Stress in the Pre-stressing Tendon at θ_{des}

The elongation of the pre-stressing is related to both the interface rotation demand, θ_{des}, and the neutral axis depth.

$$\Delta_p = \theta_{des} h_b (0.5 - \eta_{des}) \quad \text{..(5.11)}$$

The corresponding change in stress, as the interface rotation increases from zero to θ_{des}, is

$$\Delta f_p = \frac{\Delta_p}{l_{pu}} E_p = \Delta f_{p\infty}(1 - 2\eta_{des}) \quad \text{..(5.12)}$$

The stress in the tendon must satisfy two separate upper bounds. At the start of the design it is not clear which will control. First, at θ_{des}, f_{p0} must not exceed the yield stress. Second, at zero interface rotation, f_{p0} must not exceed f_{pi}, the maximum permissible jacking stress of $0.7f_{pu}$ minus any losses. These criteria can be met by setting

$$f_{p0} = f_{py} - \Delta f_p \quad \text{..(5.13)}$$

If $\quad f_{p0} \geq f_{pi}$

then $\quad f_{p0} = f_{pi} \quad \text{..(5.14)}$

$$f_{p,des} = f_{p0} + \Delta f_p \quad \text{...(5.15)}$$

else

$$f_{p,des} = f_{py} \quad \text{...(5.16)}$$

Step 12. Calculate the Forces in the Deformed Reinforcement, Pre-stressing Tendon and Grout at θ_{des}

The forces in the various reinforcement elements are

$$F_{p,des} = A_p f_{p,des} \quad \text{...(5.17)}$$

$$F_{s,des} = A_s \lambda_{s,des} f_{sy} \quad \text{...(5.18)}$$

$$F_{s',des} = A_s \lambda_{s',des} f_{sy} \quad \text{...(5.19)}$$

The compression force between the grout and the concrete, $F_{c,des}$, can be calculated from equilibrium on the section

$$F_{c,des} = F_{p,des} + F_{s,des} - F_{s',des} \quad \text{..(5.20)}$$

Step 13. Calculate the Locations of the Compression Force and the Neutral Axis

The depth of the Whitney Equivalent stress block (Section 10.2.7 of ACI 318-99) in the grout is

$$a_{des} = \frac{F_{c,des}}{0.85 f'_g b_g} \quad \text{...(5.21)}$$

The resultant compressive force on the grout is located at $\alpha_{des} h_g$ from the compression face, where

$$\alpha_{des} = \frac{a_{des}}{2h_g} \quad \text{...(5.22)}$$

and the neutral axis is located $\eta_{des} h_g$ from the compression face, where

$$\eta_{des} = \frac{a_{des}}{\beta_1 h_g} \quad \text{...(5.23)}$$

This value of η_{des} is then compared to the previous value, and Steps 11 - 13 are repeated until the computed and assumed values of η_{des} converge.

Step 14. Calculate the Moment Strength of the Section at θ_{des}

The moment strength is calculated by taking the moments about the centroid of the compression force provided by the deformed reinforcement and pre-stressing. These are

$$M_{p,des} = F_{p,des} h_g [0.5 - \alpha_{des}] \quad \text{...(5.24)}$$

$$M_{s,des} = F_{s,des} h_g [1 - \zeta - \alpha_{des}] \quad \text{...(5.25)}$$

$$M_{s',des} = F_{s',des} h_g [\zeta - \alpha_{des}] \quad \text{..(5.26)}$$

Then the total moment strength is

$$M_{cap,beam} = M_{p,des} + M_{s,des} + M_{s',des} \quad \text{..(5.27)}$$

This must be equal to or greater than the design moment, so

$$M_{cap,beam} \geq M_{des} \quad \text{...(5.28)}$$

If the moment capacity is too small, increase A_p and A_s and repeat Steps 11-14.

Step 15. Evaluate the Restoring Properties of the Beam

In order to ensure that the frame self-rights after an earthquake, the restoring moment at zero drift provided by the pre-stressing must be large enough to overcome the resisting moment of the deformed reinforcement. Both sets of deformed reinforcement are in compression and the stress in both of them is assumed to be $\lambda_{s',des}f_{sy}$. The stresses, forces and moments in the different components are thus given by

$$F_{s0} = A_s \lambda_{s',des} f_{sy} \dotfill (5.29)$$

$$F_{s'0} = A_s \lambda_{s',des} f_{sy} \dotfill (5.30)$$

$$F_{p0} = A_p f_{p0} \dotfill (5.31)$$

$$F_{c0} = F_{p0} - F_{s0} - F'_{s0} \dotfill (5.32)$$

The depth of the Whitney equivalent stress block in the grout is

$$a_0 = \frac{F_{c0}}{0.85 f'_g b_g} \dotfill (5.33)$$

The resultant compressive force on the grout is located at $\alpha_0 h_g$ from the compression face, where

$$\alpha_0 = \frac{a_0}{2h_g} \dotfill (5.34)$$

and the neutral axis is located $\eta_0 h_g$ from the compression face, where

$$\eta_0 = \frac{a_0}{\beta_1 h_g} \dotfill (5.35)$$

At zero drift, the moments about the center of the compression force in the grout of the different components are

$$M_{p0} = F_{p0} h_g [0.5 - \alpha_0] \dotfill (5.36)$$
$$M_{s0} = F_{s0} h_g [1 - \zeta - \alpha_0] \dotfill (5.37)$$

$$M'_{s0} = F'_{s0} h_g [\zeta - \alpha_0] \dotfill (5.38)$$

To ensure self-righting,

$$M_{p0} \geq M_{s0} + M'_{s0} \quad \dotfill \quad (5.39)$$

If Equation 5.39 is not satisfied, select a higher ratio of $M_{p,des}/M_{des}$ and repeat Steps 5-15.

Step 16. Calculate the Elongation and Required Unbonded Length of the Deformed Reinforcement

The elongation of the tension deformed reinforcement is related to both the drift demand and the neutral axis depth.

$$\Delta_s = \theta_{des} h_g (1 - \zeta - \eta_{des}) \quad \dotfill \quad (5.40)$$

where ζh_g is the distance from the centroid of the tension deformed reinforcement to the tension face of the beam. In order to keep the strain in the deformed reinforcement below the maximum usable strain at the design drift, $\varepsilon_{s,max}$, given in Table 2.1, the total unbonded length must satisfy

$$l_{su} \geq \frac{\Delta_s}{\varepsilon_{s,max}} \quad \dotfill \quad (5.41)$$

High cyclic strains can cause growth in the unbonded length. The magnitude of that growth depends on the confinement provided around the bar and other parameters. For bars grouted into a pre-formed hole in the concrete, Cheok and Stone [1994] found the growth in debonded length to be $5.5d_b$ ($2.75d_b$ at each end of the intentionally debonded length) for a #3 bar. More recent testing on bars grouted in corrugated steel ducts [Stanton et al. 2000] has shown that, under those circumstances, the growth depends on bar strength, grout strength and load history, but is on the order of $1.0d_b$.

If the estimated debonded length is greater than the true one, the true bar strain will be higher than the predicted one, and the bars may fracture prematurely. If the estimated debonded length is less than the true one, the true strain will be lower than predicted and yield of the bars will be delayed. The consequences are that the bar stress, and therefore the resisting moment, at peak drift will be slightly lower, as will also be the damping. However, these changes will be very small. Because the consequences of predicting too high a growth in the debonded length are much more serious than those of a low prediction, the growth in debonded length is assumed here to be zero.

Step 16. Confine Compression Region as Needed

The local stress in the compressed region of the beam can become very large, especially if the interface rotation or the initial pre-stress force is large. That stress exists in both the concrete and the grout. The grout is expected to deform inelastically, but it is protected by fiber reinforcement against crushing and falling out of the joint. The concrete in the beam should be protected against crushing in case the grout sustains a stress higher than its cube strength. This is likely to be the case, because the dimensions of the grout pad provide excellent confinement.

Since the beam end deformation is concentrated in a single crack and because the tendon is unbonded and pre-stressed, plane sections do not remain plane at the end of the beam. Thus the concrete strains cannot strictly be evaluated from the curvature within a plastic hinge length. No completely rational method has yet been proposed for evaluating the strain field in the concrete under these circumstances.

In lieu of a more precise approach, Priestley and MacRae [1996] recommend an equivalent plastic hinge length equal to $0.04l_n$ for an unbonded post-tensioned, connection. However, this assumed plastic hinge length does not account for the level of pre-stress in the tendon. To overcome this difficulty, the plastic hinge length is taken here as a function of the compression zone depth, $\eta_{des}h_g$.

$$l_{ph} = k_{ph}\eta_{des} h_g \ \dotfill (5.42)$$

where, without experimental validation, k_{ph} is taken equal to 1.0. This choice is made on the basis of St Venant's Principle [St. Venant, 1855], which implies that a local disturbance in stress dies out rapidly at distances greater than the member depth.

The average compression strain over this plastic hinge length is

$$\varepsilon_c = \frac{\theta_{des}(\eta_{des}h_b)}{l_{ph}} = \frac{\theta_{des}}{k_{ph}} \ \dotfill (5.43)$$

If this compression strain exceeds the ultimate strain of the unconfined concrete, spalling should be expected and the compression region should be confined to ensure that the concrete can sustain higher strains without degradation. In addition, if the cover is expected to spall, a reduced beam section with dimensions equal to the confined core dimensions should be used in the above calculations.

5.5 Design of Other Components

5.5.1 Interface Shear

Shear resistance across the interface is provided by shear friction. The normal force creating that friction is supplied by the pre-stressing. Therefore, the shear resistance at the interface is

$$V_n = \mu F_{c,des} \ \dotfill (5.44)$$

The corresponding shear demand on the interface is determined from equilibrium on the beam.

$$V_u = V_{u,D+L} + \frac{2M_{cap,beam}}{l_n} \quad\text{...(5.45)}$$

5.5.2 Beam Flexure

During cyclic frame displacements, the beam end moments may become equal in magnitude and opposite in sign (i.e. both clockwise or both counter-clockwise). Their effect on the mid-span moment capacity is then zero, so moment demand at mid-span is the same as that for a simple span. Reinforcement should be selected accordingly. This observation applies to all types of frame, including cast-in-place concrete and structural steel moment frames. The post-tensioning may be taken into account in evaluating the gravity load capacity of the beam, provided that it is in place when the load occurs.

5.5.3 Beam Shear

The beam must be designed so that, for all possible load cases, the weakest mechanism is the moment strength at the interface. This requires the beam shear strength to be designed using Capacity Design principles. The compression force from the post-tensioning tendon in the beam improves the beam's shear capacity, and may be taken in to account by using the provisions of Section 11.3.1 of ACI318-99 and treating the pre-stressing force as an external compression.

5.5.4 Beam Torsion

Torsion at the beam-column interface is resisted by the couple formed by two shear forces, one in the compression region of the concrete and the other in the tension reinforcement, which resists the shear by dowel action. The torsional stiffness at the interface is much smaller than that of the beam itself, so torsional rotation is concentrated at the beam-column interface. Torsional loading on the frame beam should therefore be minimized.

5.5.5 Bond and Anchorage

The post-tensioned tendon should be anchored using mechanical anchors.

The deformed reinforcement is anchored in the grouted sleeves that extend into the beam. Care should be taken to provide sufficient development length past the end of the debonded region, including sufficient length to transfer the force from the deformed reinforcement in the ducts into the reinforcement cast directly into the beam. For these purposes, the debonded region includes both the intentionally debonded region calculated above plus any growth in the debonded region caused by cyclic bar yielding. For this calculation, it is not conservative to assume that the growth in the debonded length is zero.

The Unbonded Post-Tensioned Frame with Damping may be constructed by casting the continuity bars directly into a cast-in-place slab on a precast beam, rather than grouting them into ducts in the beam. Because the bond of bars in concrete is much less robust than bond of bars grouted into ducts, cyclic loading will cause a significant penetration of inelastic strain into the bonded region of the bars, and a significant increase in the unbonded length in the beam. The computation of the growth in debonded length should account for the appropriate bond properties of the bars.

5.5.6 Column Design

The column should be designed using Capacity Design principles to ensure that the nonlinear action occurs at the beam-column interface. Column splices should also be designed using Capacity Design principles, including consideration of higher mode effects as described in the UBC ["Uniform", 1997].

5.5.7 Joint Shear

The required joint shear strength should be determined using Capacity Design principles. The joint forces on the exterior and interior columns are different, due to both the magnitude of loading on the joint and the resistance mechanism within the joint.

The magnitude of the joint shear demand is computed here using values for the forces that are consistent with the strains expected in the members. Those forces may differ from the ones used in ACI318-99, which are largely empirical. Furthermore, it is worth noting that the allowable joint shear stresses given by ACI318-99 do not represent a true Capacity Design, because considerable damage will occur to a joint that is designed in accordance with them [Mosier, 2000]. Thus the design of any joint, in a cast-in-place or a precast frame, depends on the performance desired. The requirements of ACI318-99 should be satisfied as a minimum but, if minimal joint damage is desired, a more conservative design may be necessary.

A typical interior joint is shown in Figure 5.7. Equilibrium of the joint requires a joint shear force of

$$V_{joint} = -F_{s,des} - F_{c,des} - F_{s',des} + V_{col,des} = -F_{p,des} - 2F_{s,des} + V_{col,des} \quad \dots \dots (5.46)$$

where $F_{p,des} = A_p f_{p,des}$

$F_{s,des} = A_s \lambda_{s,des} f_{sy}$

$F_{s',des} = A_s \lambda_{s',des} f_{sy}$

$V_{col,des}$ = the column shear force associated with development of the beam moment strength, $M_{cap,beam}$, on the beam section.

Note that the forces in Equation 5.46 are all taken as positive quantities.
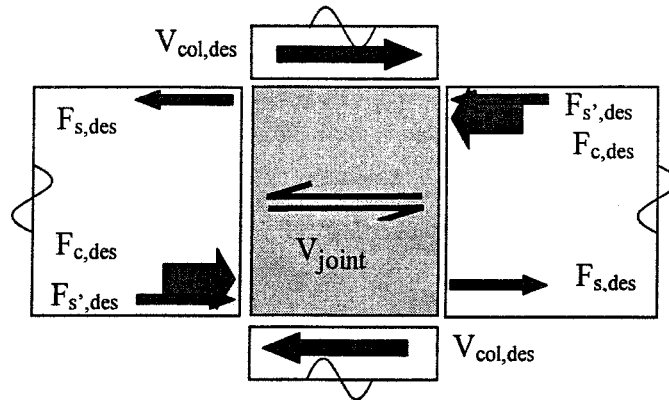
Figure 5.7: Unbonded Post-Tensioned Frame with Damping – Interior Joint Shear Forces

If the inflection points occur at mid-span of the beams and at mid-height of the columns, the column shear force is

$$V_{col,des} = \frac{2M_{cap,beam}}{l_c\left(1 - h_c/l_b\right)} \quad\text{..}(5.47)$$

The joint shear stress is then

$$v_{joint} = \frac{V_{joint}}{h_c\left(b_c - \sum b_{duct}\right)} \quad\text{..}(5.48)$$

For an interior column, the joint shear force is the horizontal force anywhere within the joint between the top and bottom deformed reinforcement as shown in Figure 5.7. The critical plane occurs where the net joint width is narrowest, which is therefore given by the gross joint width minus the width of the post-tensioning duct. If several ducts are used, the total width of all the ducts on any horizontal plane should be used. In the absence of additional experimental validation, the allowable joint shear stresses should be kept within code limits [e.g. "Building", 1999; "Uniform", 1997].

For an exterior joint, the maximum joint shear force occurs between the compression face of the beam and the pre-stressing anchorage, as shown in Figure 5.8.

Equilibrium of the joint requires a joint shear force of

$$V_{joint} = -F_{c,des} - F'_{s,des} + V_{col,des} = -F_{p,des} - F_{s,des} + V_{col,des} \quad\text{...}(5.49)$$

$$V_{col,des} = \frac{M_{cap,beam}}{l_c\left(1 - h_c/l_b\right)} \quad\text{..}(5.50)$$

At the exterior joint, the critical shear plane does not cross the plane that contains the pre-stressing duct, therefore the duct diameter does not need to be deducted from the joint width.
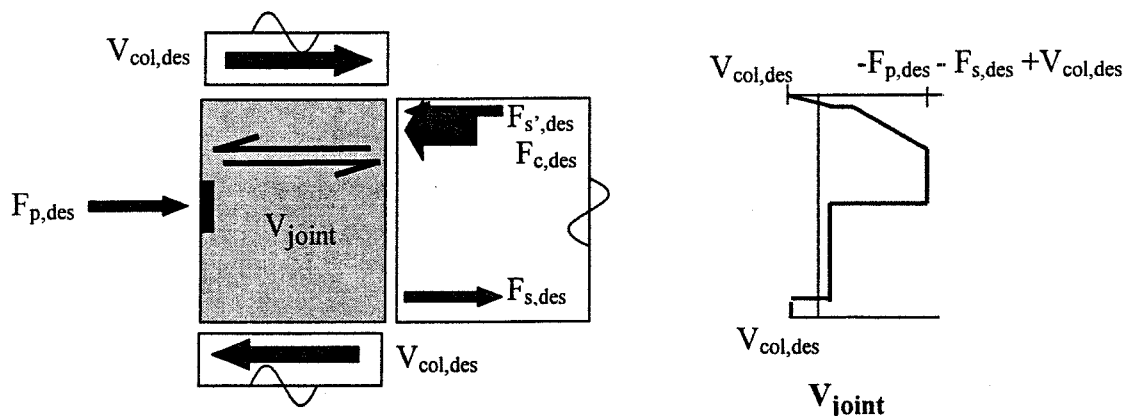
Figure 5.8: Unbonded Post-Tensioned Frame with Damping – Exterior Joint Shear Forces

The exterior joint shear stress is then

$$v_{joint} = \frac{V_{joint}}{h_c b_c} \dotfill (5.51)$$

In the absence of experimental validation, the allowable joint shear stresses should be kept within code limits.

5.6 Limits on Reinforcement

There is no upper bound to the amount of beam reinforcement that may be used. However, as the pre-stressing force increases, the lever arm diminishes, so very heavily reinforced beams are likely to be uneconomical. They are also likely to lead to highly stressed beam-column joints. These response characteristics impose natural bounds on the amount of reinforcement. The recommended lower bound is based on the criterion that the shear strength of the continuity bars in dowel action should be adequate to carry the gravity load on the beam. This leads to

$$\phi_v (2A_s)(0.5 f_{sy}) \ge V_{u,D+L} \dotfill (5.52)$$

or $$A_s \ge \frac{V_{u,D+L}}{0.5 \phi_v f_y} \dotfill (5.53)$$

5.7 Construction Issues

The seismic performance of the Post-Tensioned Frame with Damping is sensitive to several aspects of the constructed system.

5.7.1 Unbonded Deformed Reinforcement Length and Location

The debonded region of the bar must be the correct length, or the bars could fracture prematurely. It must also be located in the beam, ending at the beam-column interface. If it were to lie in the column, the bond length in the column might be inadequate to develop simultaneously the strength of the bar in tension on one side of the column and in compression on the other side.

5.7.2 Deformed Reinforcement Grouting

The grouting procedure should be selected and controlled so that the space between the bar and the duct wall is completely filled with grout. Any voids could have a detrimental effect on the bond of the bars.

5.7.3 Interface Grout

The interface grout should be reinforced with fibers to ensure that it does not degrade throughout the anticipated high strains. Research [Cheok and Stone 1994] has shown that 3 pounds of nylon fibers per cubic yard of grout is sufficient to withstand very high rotations without degradation.

5.8 Discussion

The Unbonded Post-Tensioned Frame with Damping that was tested in the PRESSS Phase III test performed very well. Minimal damage was sustained, as shown in Figure 5.9, even after the building had been deformed to 4% roof drift. In particular, the flexural cracking in the beams was minimal, and no slip was observed at any of the beam-column interfaces. The primary damage consisted of some joint cracks, which closed when the load was removed, and minor crushing at the top and bottom of the beams. The latter would have been easily repairable.

The design procedures outlined here have not yet been validated by the authors using the data from the PRESSS Phase III test building. Therefore, they should be used only for trial designs.
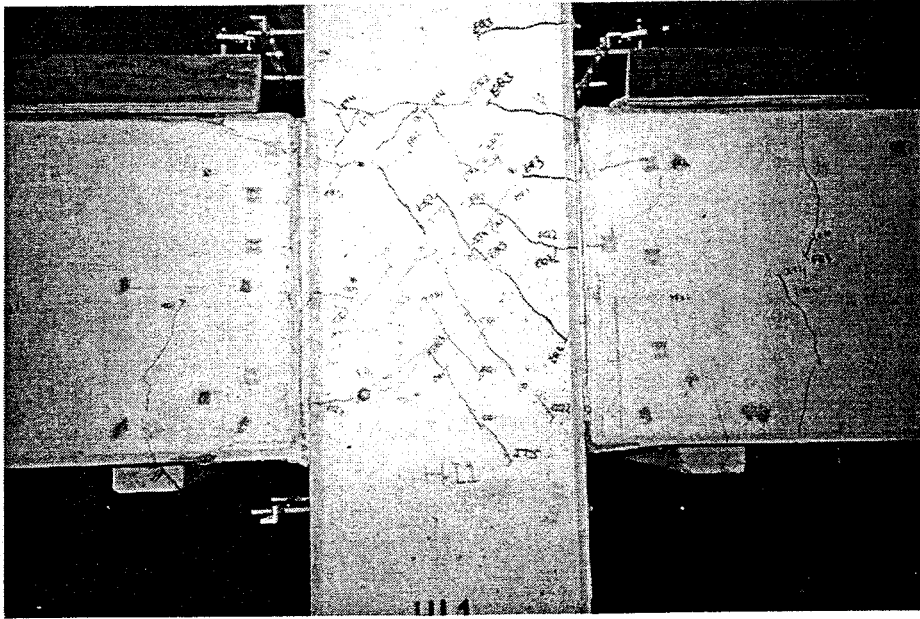
Figure 5.9: Unbonded Post-Tensioned Frame with Damping at End of Test

6 YIELDING FRAMES

6.1 Concept Description

The Yielding Frame is illustrated in Figure 6.1.

The frame consists of multi-story precast columns, spliced as necessary, and single-span beams between columns. The arrangement is shown schematically in Figure 6.2.
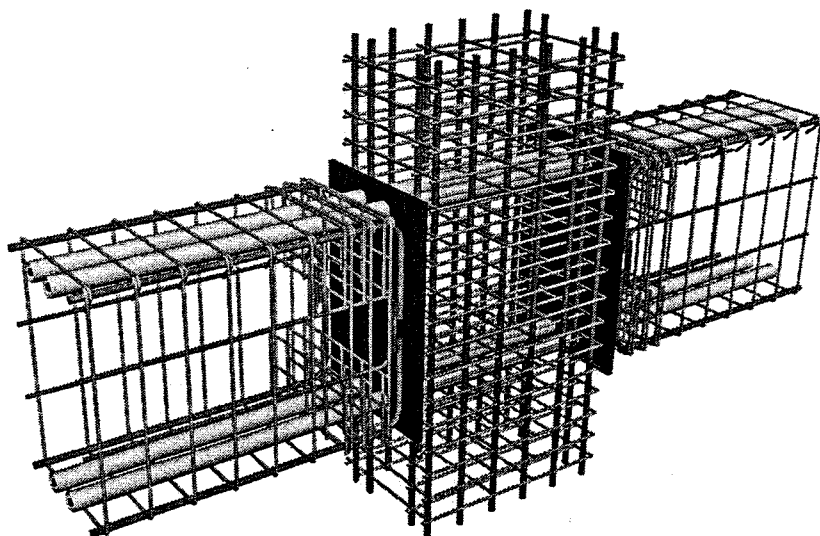
Figure 6.1: Yielding Frame
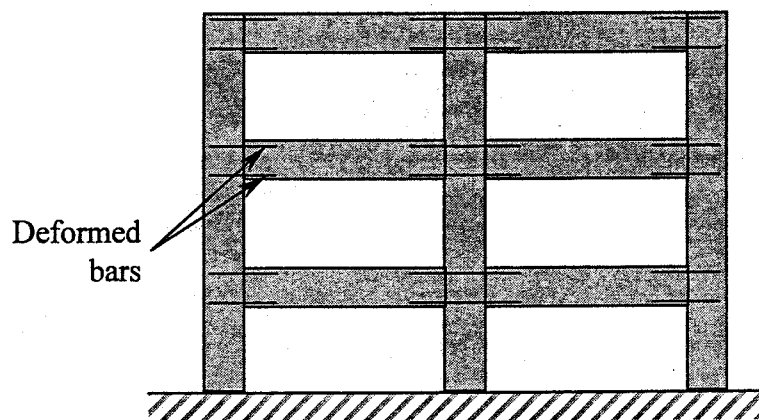
Figure 6.2: Yielding Frame – Element Layout of Elements and Primary Reinforcement

The frame derives its moment strength from tension and compression yielding of deformed reinforcing bars, which are grouted into ducts in the top and bottom of the beam and extend from the beams through the column. They are referred to here as "continuity bars". The connection

resembles, at least functionally, a conventional yielding connection of the type included in the PCI Connection Manual [PCI Committee, 1988]. As shown in Figure 6.3, the deformed reinforcement is unbonded over a short length next to the interface to limit the steel strain and protect the reinforcing from fracture at high drifts.
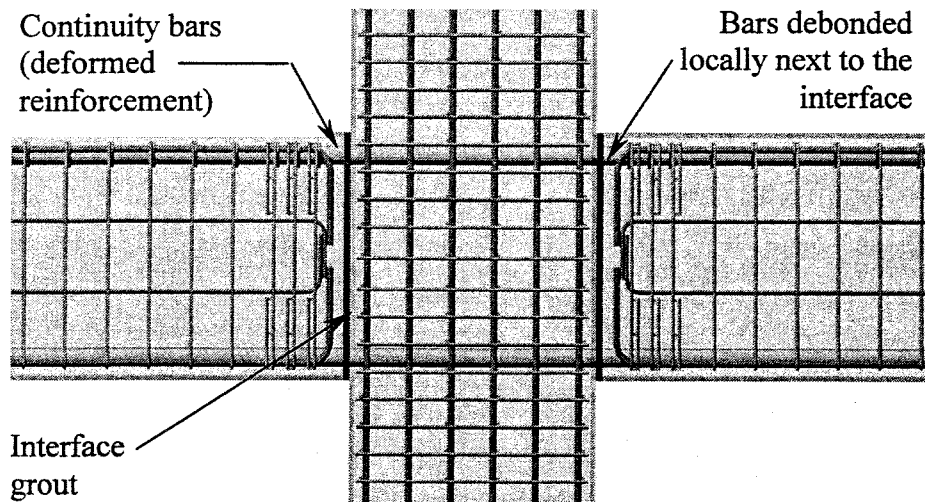
Figure 6.3: Yielding Frame - Components

The connection may be constructed by loading the bars into the beam, erecting the beam on temporary corbels, then sliding the bars through the column to their final position. The interface and the ducts are then grouted. If the slab is cast in place, or if a thick enough topping is used, the top bars may be embedded directly in it rather than being grouted in ducts in the precast beam. This construction method leads to the bars being embedded directly in cast-in-place concrete in the beam, but grouted in ducts through the column.
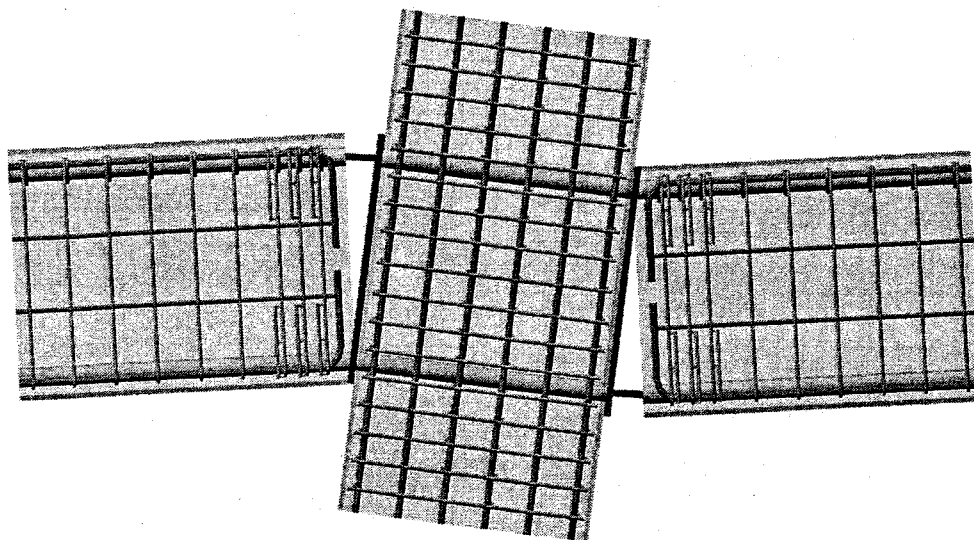
Figure 6.4: Yielding Frame - Deformed Configuration

During an earthquake, the column sways and most of its rotation is accommodated by a gap that opens between the beam and column, as shown in Figure 6.4. The bars yield in tension or compression and thereby provide a resisting moment. The connection dissipates energy during cyclic loading, but does the frame does not re-center.

The local behavior of the beam near the interface depends on the relative areas of the top and bottom bars, and on the extent to which compression is induced in the beam. If the conditions are such that an open crack can exist through the whole depth of the grout joint at the interface, the grout risks falling out, and all the shear must be carried by the bars in dowel action. The latter leads to the possibility of splitting of the concrete and kinking, and subsequent buckling, of the bars.

A full-depth crack is likely if the areas of top and bottom reinforcement are different, because the beam-column joint is likely to "walk open". This behavior is illustrated assuming that the area of top steel is the larger of the two. A large negative moment will cause the top steel to yield in tension and a crack to open at the top of the beam. When the load is reversed, the tension in the bottom steel will be too small to yield the top steel in compression, so the top crack will remain open and a bottom crack will also form.

If the areas of top and bottom steel are equal, no driving mechanism exists to open a full-depth crack. However, no closing mechanism exists either, because the forces in the bars are equal and opposite. The grout then carries no compression and so is unable to carry shear by friction. The only way that the grout can be subjected to compression is if the natural elongation of the beam, which occurs because the gap opens at the interface, is restrained by shear in the columns. This restraint has been shown to occur in cast-in-pace frames [e.g. Zerbe and Durrani, 1989], but it depends on the characteristics of the structure, and not just of the member, so it is different in every bay and is difficult to evaluate precisely. Furthermore, it is not accounted for in conventional practice. Thus it cannot be regarded as a dependable source of shear friction in the Yielding Frame. The lack of a clear mechanism for transferring the beam shear constitutes a drawback for the Yielding Frame.

6.2 Design Assumptions

The following design assumptions are made in the development of design equations:

1. The design forces and drifts are known. The drift limits are selected to satisfy code restrictions and user requirements. Forces may be obtained either by Force Based Design or by Displacement Based Design. Interface rotations are obtained from the drift ratio, using the geometry of the section.

2. The overall dimensions of the frame members are known, having been obtained from architectural constraints and preliminary calculations.

3. The beams have a constant cross section.

4. Equal top and bottom reinforcing is used.

5. The continuity bars are grouted into ducts through the column and are anchored in the beams either side.

6. The continuity bars are debonded for a short length in each beam, adjacent to the beam-column interface to limit the tension strain during an earthquake.

7. Properties of the proposed materials are known. The principal ones are:
   - strength and stiffness of deformed reinforcement
   - strength, f'_c, and stress block coefficient, β_1, of the concrete

6.3 Notation

The sign convention adopted is that forces and deformations are computed as positive quantities, regardless of whether they are tensile or compressive.

a_{des}	= depth of compression stress block in grout at design limit state
A_s	= area of deformed reinforcement in one face of beam
b_g	= width of beam at beam-column interface
d_b	= diameter of deformed reinforcing bar
f'_g	= specified grout strength at 28 days
f_{sy}	= specified yield strength of deformed reinforcement
$F_{c,des}$	= force in beam concrete at beam-column interface at design limit state
$F_{s,des}$	= force in tension deformed reinforcement at design limit state
$F_{s',des}$	= force in compression reinforcing steel at design limit state
h_b	= depth of beam
h_c	= column depth (in plane of frame)
h_g	= depth of grout pad at beam-column interface
l_b	= total bay dimension between column centerlines
l_c	= floor-to-floor story height
l_n	= clear span of beam between column faces
l_{su}	= length of unbonded region of deformed reinforcement at each interface
$M_{cap,beam}$	= beam moment strength at interface at design limit state
M_{des}	= moment demand at design limit state
v_{joint}	= joint shear stress
$V_{col,des}$	= column shear force at design limit state
V_{joint}	= joint shear force
V_u	= factored shear demand
$V_{u,D+L}$	= factored dead and live load shear demand at interface
α_{des}	= distance from center of compressive reaction to edge of member divided by member depth, at design limit state
β_1	= depth of equivalent compressive stress block divided by neutral axis depth

ε_s = strain in tension deformed reinforcement

$\varepsilon_{s,max}$ = maximum strain permissible in deformed reinforcement under cyclic loading

η_{des} = distance from member compression face to neutral axis divided by member depth, at design limit state

θ_{des} = interface rotation at design limit state

$\lambda_{s,des}$ = over-strength factor for deformed reinforcement in tension at design limit state

$\lambda_{s',des}$ = over-strength factor for deformed reinforcement in compression at design limit state

μ = coefficient of friction

ϕ_v = strength reduction factor for shear

6.4 Design Procedure for Critical Elements

The forces acting on the Yielding Frame joint subject to a design drift of θ_{des}, are shown in Figure 6.5, and the locations of the forces are given in Figure 6.6. The equations that follow are presented for the limit state that corresponds to a strain of $\varepsilon_{s,max}$ in the deformed bars.

Tension force in deformed reinforcement

Bond forces

Compression forces in concrete and deformed reinforcement

Diagonal strut and truss mechanism transfer joint shear
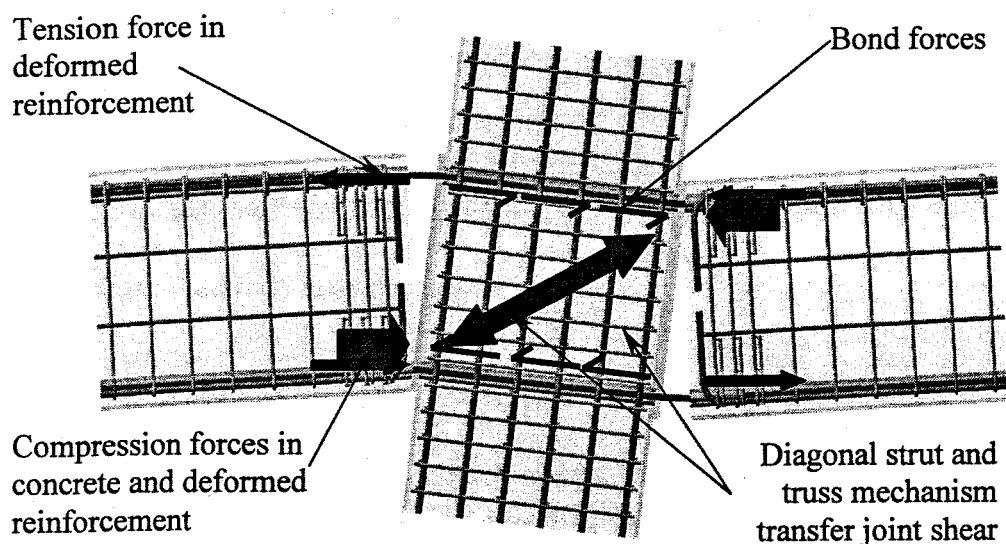
Figure 6.5: Yielding Frame – Forces on Connection

Unlike a conventional monolithic concrete frame, the inelastic action in the Yielding Frame is concentrated at the beam-column interface. Therefore the plastic hinge length is much shorter and the reinforcing must be debonded at the interface in order to avoid premature bar fracture.

6.4.1 Design of Nonlinear Hinge

<u>Step 1.</u> **Establish Material Properties**

Establish properties of materials to be used. These include:
- interface grout strength and corresponding β_1

- deformed reinforcement yield and tensile strength, and strain at maximum strength

a) Dimensions and Displacements   **b) Forces**
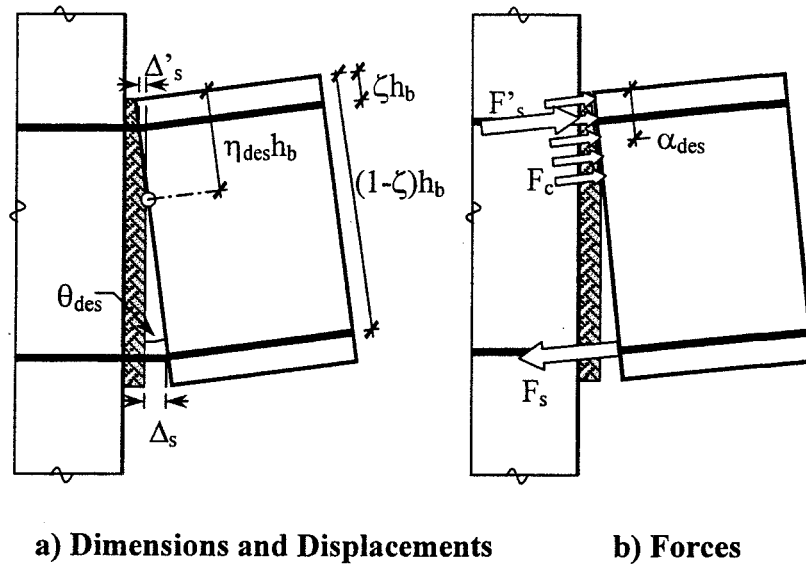
Figure 6.6: Yielding Frame – Location of Forces at Design Drift

Step 2. Obtain the Design Loads and Drifts

Use DBD or FBD to obtain design loads. Compute corresponding design moments and drifts. θ_{des} is the interface rotation at the design limit state.

Step 3. Estimate the Frame Beam Dimensions

Frame beams that are as deep as possible are desirable because that choice leads to the smallest possible area of reinforcement and the lowest shear forces in the beam-column joints.

Two criteria are candidates for controlling the beam depth at the interface. First is the restriction of Section 21.3.1.2 of ACI 318-99, which limits the effective depth to one quarter of the clear span. This requirement is relaxed somewhat here, for reasons explained below, to give

$$h_b \leq \frac{l_n}{3} \qquad\qquad\qquad (6.1)$$

The Commentary to ACI 318 (Section R21.3.1) states that the $l_n/4$ restriction is necessary to prevent behavior that is significantly different from that of more slender beams. That assertion is supported by a single reference, which is in Japanese. The requirement is believed to be based on the need to ensure adequate distance between the centers of rotations at the beam ends, in order to limit the plastic rotation demand. The center of rotation may be taken at the center of the plastic hinge zone. Since a plastic hinge in monolithic frame will never be shorter than $h_b/2$, the implied distance between centers of rotation is no larger than $3h_b$. In the precast system described

here the center of rotation is at the interface, so the clear span could then be as short as $3h_b$ and still fulfill the spirit of the requirement. This reasoning forms the basis of Equation 6.1.

The beam width should satisfy Section 21.3.1.3 of ACI 318 ["Building", 1999]

$$b_b \geq 0.3h_b \qquad \qquad (6.2)$$

ACI 318-99 Section R21.3.1 states that this requirement is based on experience with conventional, cast-in-place, non-pre-stressed frames. Its applicability to precast, post-tensioned frames is unclear. It is recommended here that Equation 6.2 be treated as advisory rather than mandatory. Use of a narrow beam could permit the beam weight to be kept low enough to overcome otherwise difficult erection problems.

Step 4. Estimate the Required Area of Reinforcement

The top and bottom reinforcement are assumed to have equal areas. End moments caused by gravity loads are addressed in Section 6.5.2.

While direct solution for the required area of reinforcement is possible, iteration provides a simpler approach and is used here. For an initial estimate of the required area of reinforcement, the lever arm is assumed to be the distance between the centroids of the two sets of reinforcement.

Thus $\qquad A_s = \dfrac{M_{des}}{\lambda_{s,des} f_{sy} h_b (1 - 2\zeta)} \qquad \qquad (6.3)$

Step 5. Calculate the Forces in the Reinforcement

The tension reinforcement is expected to undergo significant tension strain, and the stress in it is therefore taken as $\lambda_{s,des} f_{sy}$. The compression reinforcement is expected to have experienced significant tension strain during previous cycles, so, in returning to a strain close to zero, it will have also experienced a large compressive change in strain. The stress in it is therefore taken as $\lambda_{s',des} f_{sy}$. Values for $\lambda_{s,des} f_{sy}$ and $\lambda_{s',des} f_{sy}$ are proposed in Table 2.1. The forces on the different elements are then:

$$F_{s,des} = A_s \lambda_{s,des} f_{sy} \qquad \qquad (6.4)$$

$$F_{s',des} = A_s \lambda_{s',des} f_{sy} \qquad \qquad (6.5)$$

Step 6. Compute the Magnitude and Location of the Compression Force on the Concrete

The compression force between the concrete and grout, $F_{c,des}$, can be calculated from axial force equilibrium as

$$F_{c,des} = F_{s,des} - F_{s',des} \quad\text{...}(6.6)$$

The depth of the Whitney Equivalent stress block (Section 10.2.7 of ACI 318-99), assumed here to be controlled by the grout properties, is

$$a_{des} = \frac{F_{c,des}}{0.85 f'_g b_b} \quad\text{..}(6.7)$$

The resultant compressive force on the concrete is located at $\alpha_{des}h_b$ from the compression face, where

$$\alpha_{des} = \frac{a_{des}}{2h_b} \quad\text{...}(6.8)$$

The neutral axis is located at a distance $\eta_{des}h_b$ from the compression face of the beam, where

$$\eta_{des} = \frac{a_{des}}{\beta_1 h_b} \quad\text{...}(6.9)$$

The moment capacity of the beam is given by

$$M_{cap,beam} = F_{s,des}h_b\left(1 - \zeta - \alpha_{des}\right) - F_{s',des}h_b\left(\zeta - \alpha_{des}\right)\text{...}(6.10)$$

where ζ = distance from centroid of deformed reinforcement to the nearest face of the concrete, divided by h_b.

This must be greater than or equal to the design moment, so

$$M_{cap,beam} \geq M_{des} \quad\text{...}(6.11)$$

If Equation 6.11 is not satisfied, select a new A_s and repeat Steps 5 – 6 until a satisfactory solution is reached.

<u>Step 7</u>. **Select the Debonded Length for the Continuity Bars**

The debonded length of the reinforcing bars must satisfy

$$l_{su} \geq \frac{\theta_{des}h_b\left(1 - \zeta - \eta_{des}\right)}{\varepsilon_{s,max}} \quad\text{..}(6.12)$$

High cyclic strains can cause growth in the unbonded length. The amount of growth depends on the confinement provided around the bar and other parameters. For bars grouted into a pre-

formed hole in the beam, Cheok and Stone [1994] found the growth in debonded length to be $5.5d_b$ ($2.75d_b$ at each end of the intentionally debonded length) for a #3 bar. More recent testing on bars grouted in corrugated steel ducts [Stanton et al. 2002] has shown that the growth depends on bar strength, grout strength and load history, but is on the order of $1.0d_b$. The danger in assuming an additional debonded length that is larger than the true one is that the true bar strains will be higher than the predicted ones, and there is a risk of the bars fracturing prematurely. The danger in assuming an additional debonded length that is smaller than the true on is that the bars strain will be lower than expected. However, because the stress-strain curve is relatively flat at strains near $\varepsilon_{s,max}$, the resulting error in estimating the stress will be relatively small. Because the consequences of overestimating the growth in debonded length are much more serious than those of underestimating it, the growth in debonded length is assumed here to be zero.

6.5 Design of other Components

The behavior of the Yielding Frame beam is similar that of a monolithic frame beam, except that the end rotation is concentrated at the interface rather than being distributed over a finite plastic hinge length. Therefore most other features of the system, apart from the shear design of the interface, can be designed to current code requirements.

6.5.1 Interface Shear Strength

The interface beam shear must be carried largely by dowel action of the grouted bars, unless some other explicit mechanism is provided. The compression force across the interface is resisted by a combination of the compression reinforcement and the surrounding concrete. Because the compression reinforcement will have yielded, and is treated as carrying a stress of $\lambda_{s',des}f_{sy}$, the nominal shear friction capacity across the grout is given by

$$V_{n,SF} = \mu F_{c,des} = \mu\left(F_{s,des} - F_{s',des}\right) \dotfill (6.13)$$

The shear demand at the joint is

$$V_u = V_{u,D+L} + \frac{2M_{cap,beam}}{l_n} \dotfill (6.14)$$

Therefore the nominal shear strength of the bars in dowel action must satisfy

$$V_{n,dowel} \geq \frac{V_u}{\phi_v} - V_{n,SF} \dotfill (6.15)$$

Shear resistance through dowel action is not formally accounted for in conventional practice, and ACI318-99 contains no provisions for computing it. Its use also raises the possibility of kinking of the bars if the loading is cyclic. Therefore experimental evidence is needed if it is to be used in this case. It should be noted that, if more horizontal reinforcement is added to increase the

shear friction capacity given in Equation 6.13, it will be counterproductive because it will also increase the shear demand by increasing $M_{cap,beam}$, as shown by Equation 6.14.

6.5.2 Beam Flexure

During cyclic frame displacements, the beam end moments may become equal in magnitude and opposite in sign (i.e. both clockwise or both counter-clockwise). Their effect on the mid-span moment capacity is then zero, so moment demand at mid-span is the same as that for a simple span. Reinforcement should be selected accordingly. This observation applies to all types of frame, including cast-in-place concrete and structural steel moment frames.

6.5.3 Beam Shear

The beam should be designed for shear using principles of Capacity Design, as outlined in Section 21.3.4 of ACI318-99. Placing ties to carry the entire shear in the very end of the beam will help to reduce the tendency for dowel action of the continuity bars to split the concrete.

6.5.4 Beam Torsion

Torsion in the beam can be resisted only by dowel action of the bars. Therefore any slab system loading onto the beam should be designed to apply the least possible torsion.

6.5.5 Bond and Anchorage

The deformed reinforcement is anchored in the grouted sleeves that extend into the beam. Care should be taken to provide sufficient development length past the end of the debonded region, including sufficient length to transfer the force from the deformed bars into the longitudinal reinforcement that is cast into the beam. For these purposes, the debonded region includes both the intentionally debonded region calculated above plus any growth in the debonded region caused by cyclic bar yielding. For this calculation, it is unconservative to assume that the growth in the debonded length is zero. An additional length of $2d_b$ at each end of the intentionally debonded region is recommended.

The Yielding Frame may be constructed by casting the continuity bars directly into a cast-in-place slab on a precast beam, rather than grouting them into ducts in the beam. Because the bond of bars in concrete is much less robust than bond of bars grouted into ducts, cyclic loading will cause a significant penetration of inelastic strain into the bonded region of the bars, and a significant increase in the unbonded length in the beam. The development length provisions in Chapter 21 of ACI 318-99 should be used.

6.5.6 Column Design

The column should be designed using Capacity Design principles to ensure that nonlinear action occurs at the beam-column interface. Column splices should also be designed using Capacity

Design principles, including consideration of higher mode effects as described in the UBC ["Uniform", 1997].

6.5.7 Joint Shear

The magnitude of the joint shear demand is computed here using values for the forces that are consistent with the strains expected in the members. Those forces may differ from the ones used in ACI318-99, which are largely empirical. Furthermore, it is worth noting that the allowable joint shear stresses given by ACI318-99 do not represent a true Capacity Design, because considerable damage will occur to a joint that is designed in accordance with them [Mosier, 2000]. Thus the design of any joint, in a cast-in-place or a precast frame, depends on the performance desired. The requirements of ACI318-99 should be satisfied as a minimum but, if minimal joint damage is desired, a more conservative design may be necessary.

For an interior joint,

$$V_{joint} = 2F_{s,des} - V_{col,des} \quad\text{................(6.16)}$$

Note that the forces in Equation 6.16 are all taken as positive quantities. If the inflection points occur at mid-span of the beams and at mid-height of the columns, the column shear force is

$$V_{col,des} = \frac{2M_{cap,beam}}{l_c\left(1 - h_c/l_b\right)} \quad\text{................(6.17)}$$

The joint shear stress is then

$$v_{joint} = \frac{V_{joint}}{h_c b_c} \quad\text{................(6.18)}$$

For an exterior joint, the procedures are similar, but Equation 6.16 is replaced by

$$V_{joint} = F_{s,des} - V_{col,des} \quad\text{................(6.19)}$$

and $$\quad V_{col,des} = \frac{M_{cap,beam}}{l_c\left(1 - h_c/l_b\right)} \quad\text{................(6.20)}$$

6.6 Limits on Reinforcement

If the areas of the top and bottom continuity bars are equal, there is no upper limit to the amount of reinforcement used. The recommended lower bound is based on the criterion that the shear strength of the continuity bars in dowel action should be adequate to carry the gravity load on the beam. This leads to

$$\phi_v(2A_s)(0.5f_{sy}) \geq V_{u,D+L}$$

or $\quad A_s \geq \dfrac{V_{u,D+L}}{0.5\phi_v f_{sy}}$ ....(6.16)

6.7 Construction Issues

6.7.1 Placement of Bars

Some way is needed for placing the bars in the ducts. One possibility is to make the ducts run the full length of the beam and to place the bars in the ducts before lifting the beam into place. Troughs in the top and bottom of the beam, or access holes to the ducts, can then allow the bars to be moved along the duct by hand.

6.7.2 Debonded Length of Bars

The debonded region of the bar must be the correct length, and must be installed accurately, so that it occurs at the joint interface. Otherwise the bars could fracture prematurely. The debonded region should also be located in the beam. If it were to lie in the column, the bond in the column might be inadequate to develop simultaneously the strength of the bar in tension on one side of the column and in compression on the other side.

6.7.3 Deformed Reinforcement Grouting

The grouting procedure should be selected and controlled so that the space between the bar and the duct wall is completely filled with grout. Any voids could have a detrimental effect on the bond of the bars.

6.8 Discussion

Although designers may wish to use corbels to supplement the shear capacity of the connection, this approach is not recommended. First, corbels provide supplementary shear strength only in the downward direction. Second, when the beam rotates downwards, the center of rotation is at the front corner of the corbel. The end of the beam then moves upwards relative to the column face and kinks the bars at the interface. This behavior has been observed in tests and is detrimental to performance, e.g. [Stanton et al, 1987]. Corrective measures are possible for both of these behaviors, such as hold-down bolts and dapped beams, e.g. [Palmieri et al., 1996]. However the connection then becomes distinctly different from the one considered here and displays other undesirable behavior characteristics.

In the PRESSS Phase III building test, some of the continuity bars slipped through the exterior column, as shown in Figure 6.7. This behavior was most probably the result of imperfect grouting. The bars had T-heads on their ends in order to provide good tension anchorage. They appeared to yield in tension then to push through the column when the load reversed. Bond tests

on grouted bars [Stanton et al. 2002] have shown that, if the grout is properly placed and consolidated, the 18" duct length that was available in the PRESSS Phase III test building columns is easily enough to develop the bar.

The bond failure may also have contributed to the low level of damage seen in the yielding frame during the test, illustrated in Figure 6.8. The lower tension forces in the bars would have led to lower forces in the members. In particular, the interface shear would have been low, and was carried by the bars in dowel action. It is expected that, had the bars been anchored properly in the column, they would have kinked during the cyclic loading.

The Yielding Frame system was included in the PRESSS Phase III test building to act as a reference connection that represented contemporary technology. Suitable methods for carrying the cyclic shear at the interface must be developed before this connection can be recommended for use in seismic regions. Furthermore, the design procedures outlined here have not yet been validated by the authors using the data from the PRESSS Phase III test.
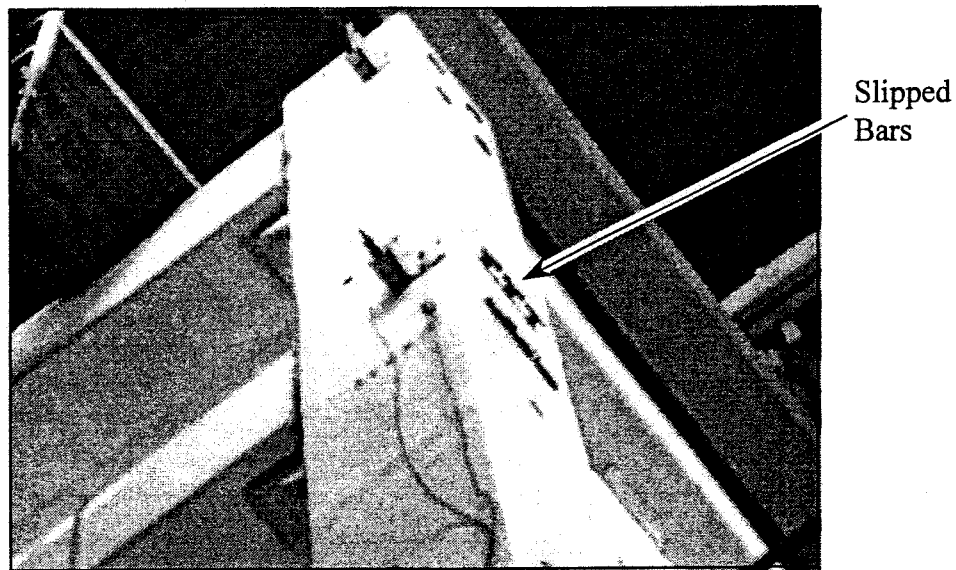
Figure 6.7: Yielding Frame - Exterior Joint, Showing Slipped Bars
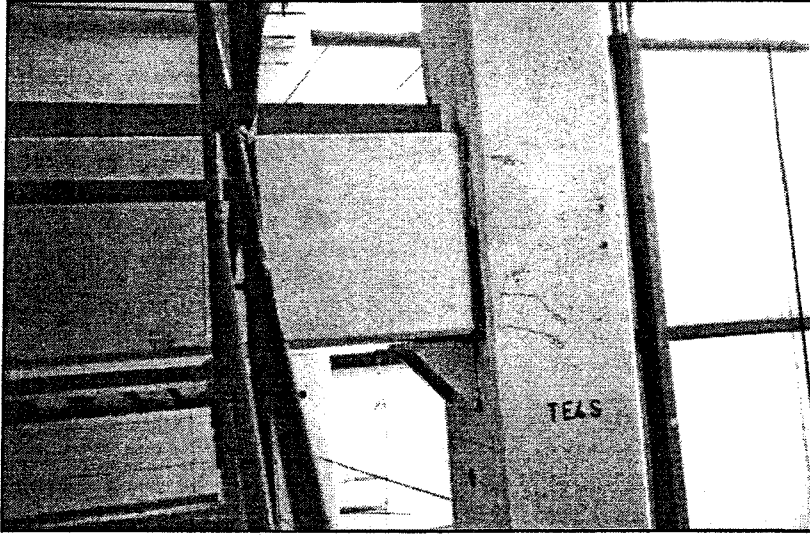
Figure 6.8: Yielding Frame - Exterior Joint after the Test

7 YIELDING GAP FRAMES

7.1 Concept Description

The Yielding Gap Frame is shown in Figure 7.1. The beam is connected to the column at the bottom by a post-tensioning tendon that passes through, and pre-compresses, a grout pad. At the top, the connection is made by deformed bars grouted into ducts. The grout pad exists only at the bottom of the beam, so there is no contact between the two concrete faces at the top of the beam. The element layout is shown in Figure 7.2 and the reinforcing details are shown in Figure 7.3
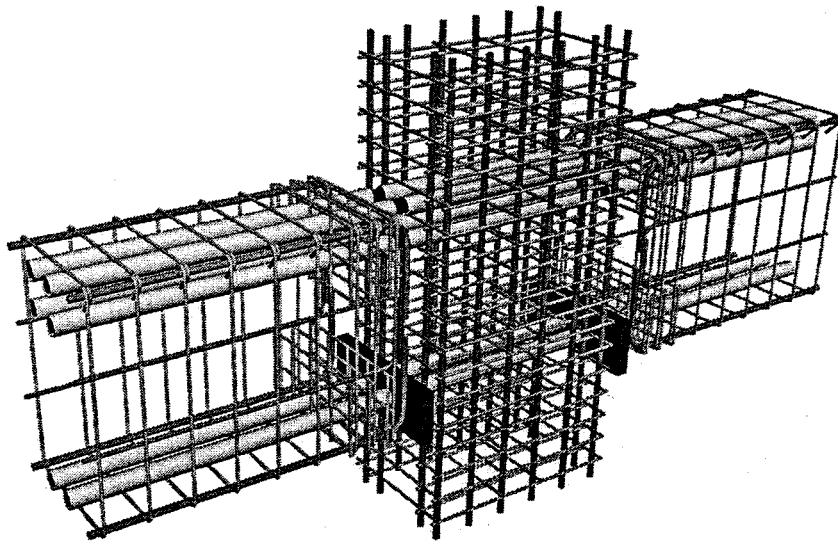
Figure 7.1: Yielding Gap Frame
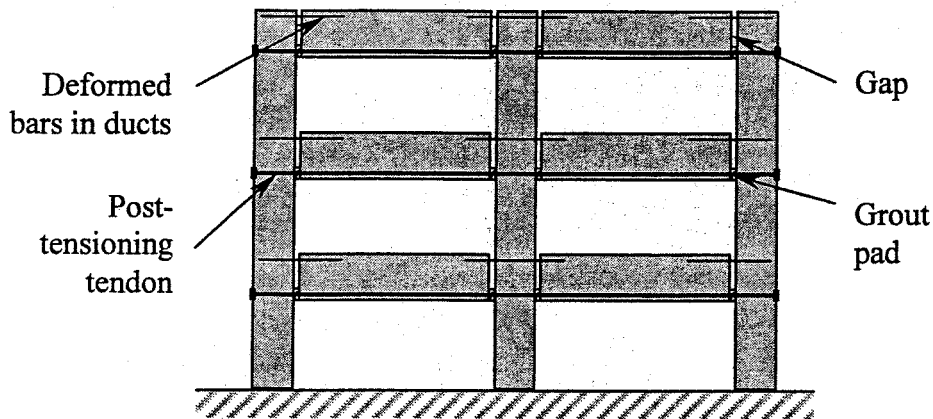
Figure 7.2: Yielding Gap Frame – Layout of Elements and Primary Reinforcement

Continuity bars
debonded locally

Continuity bars
crossing gap at
interface

Post-tensioning tendon
(remains constant length)

Grout pad
(at bottom only)
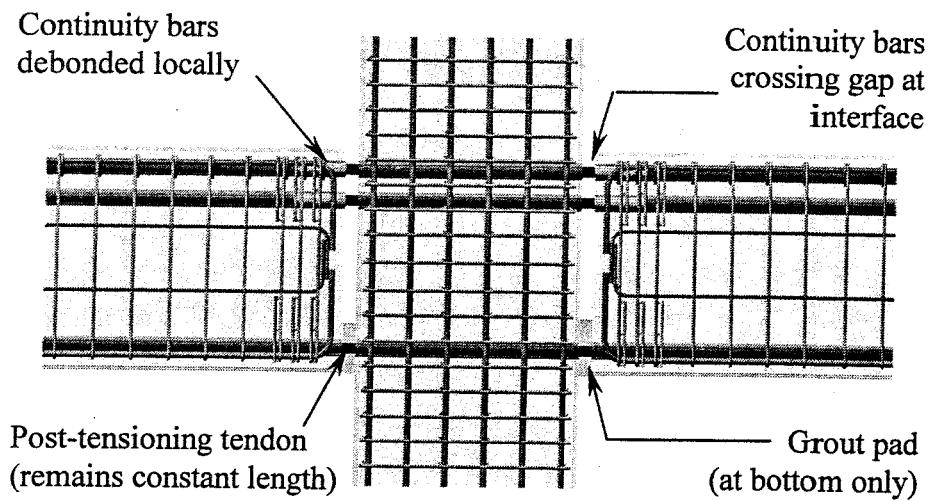
Figure 7.3: Yielding Gap Frame – Components

Figure 7.4 shows the deformed shape of the joint region caused by earthquake loading. The column tilts as the building drifts and the connections accommodate the angle change by yielding of the deformed bars in the top of the beam. The end of the beam rotates about the grout pad, which acts as a hinge. Shear is carried by friction at the grout pad, made possible by the compression force across it, which is supplied by the post-tensioning. The post-tensioning tendon never elongates and never experiences any change in stress.

Bars yield in compression
as gap closes

Beam rotates about grout pad.
Tendon does not stretch
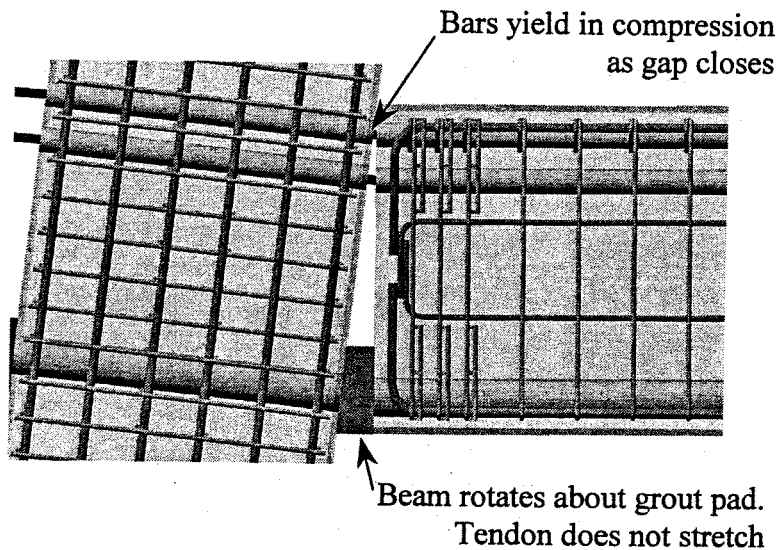
Figure 7.4: Yielding Gap Frame – Deformed Configuration

The distinguishing characteristic of the connection is that it overcomes the problems associated with the beam elongation that typically occurs under plastic rotation [Zerbe and Durrani, 1989]. That beam growth takes place in both precast and cast-in-place concrete frames and constitutes a

7-2

potential problem for precast floors, because loss of seating is a possibility. Although beam growth is more easily visualized in a precast system, in which a gap opens between the column face and the end of the beam, some researchers believe that it is more pronounced in a cast-in-place frame, because there it is caused by the continued opening under cyclic loading of the diagonal shear cracks in the plastic hinge region, [e.g. Fenwick and Megget, 1993].

By forcing the bars at the top of the beam to deform equally in tension on one side of the column and in compression on the other, the distance between the two beam ends remains unchanged during column drift. Detailing of the floors is thus much simplified, and there is no risk of losing gravity support for the floors.

The frame does not re-center, so residual drift is a possibility, as it is with conventional cast-in-place concrete moment frames and with steel moment frames.

During the PRESSS Phase III building test, the gap connections performed adequately, but the grout pads suffered some damage and the concrete at the bottom of the beams spalled. However, the shortcomings were associated with the detailed design of the connection in the test building and not with the basic concept. They are discussed in Section 7.8.

7.2 Design Assumptions

The following design assumptions are made in the development of design equations:

1. The design forces and drifts are known. The drift limits are selected to satisfy code restrictions and user requirements. Forces may be obtained either by Force Based Design or by Displacement Based Design.

2. The overall dimensions of the frame members are known, having been obtained from architectural constraints and preliminary calculations.

3. The beams are of constant cross section. Each bay in the frame is of equal length.

4. The beam continuity bars are unbonded for a short length in the beam, adjacent to the beam-column interface to prevent high strain concentrations.

5. The centroids of the grout pad and the post-tensioning tendon are coincident.

6. Properties of the proposed materials are known. The principal ones are:
   • the strength of the deformed reinforcement
   • the strength and stiffness of the post-tensioning tendon
   • the grout strength
   • the concrete strength

The coefficient of friction, μ, between the grout and the concrete, may be taken as 0.5. Hutchinson et al. [1991] measured a value of 0.6 between precast concrete and grout under cyclic shear loading. It is reduced here to 0.5 to ensure that no slip occurs. Roughening of the surfaces could lead to a higher value, but experimental evidence would be needed to justify its use in design.

7.3 Notation

The sign convention adopted is that forces and deformations are computed as positive quantities, regardless of whether they are tensile or compressive.

A_p	= area of pre-stressing tendon
A_s	= area of deformed reinforcement in one face of beam
C_g	= compressive strength of grout pad
d'	= depth from top face of beam to centroid of deformed reinforcement
d_b	= diameter of deformed reinforcing bar
d_p	= depth from top face of beam to centroid of pre-stressing tendon
f_{p0}	= stress in pre-stressing tendon, after losses, at zero drift
f_{sy}	= specified yield strength of deformed reinforcement
$F_{c,des}$	= force in beam concrete at beam-column interface at design limit state
$F_{s,des}$	= force in tension deformed reinforcement at design limit state
$F_{s',des}$	= force in compression reinforcing steel at design limit state
l_{gap}	= width of gap (in direction parallel to longitudinal axis of beam)
l_n	= clear span of beam between column faces
l_{su}	= length of unbonded region of deformed reinforcement at each interface
M_{des}	= moment demand at design limit state
$V_{u,D+L}$	= factored dead and live load shear demand at interface

$\Delta_{s'}$	= deformation of compression deformed reinforcement
$\varepsilon_{s,max}$	= maximum strain permissible in deformed reinforcement under cyclic loading
θ_{des}	= interface rotation at design limit state
$\lambda_{s,des}$	= over-strength factor for deformed reinforcement in tension at design limit state
$\lambda_{s',des}$	= over-strength factor for deformed reinforcement in compression at design limit state
μ	= coefficient of friction
ϕ_v	= strength reduction factor for shear

7.4 Design Procedure for Critical Elements

In the Yielding Gap Frame, the bending deformations of the frame occur by tension and compression yielding of the deformed bars (the "continuity bars") in the top of the beam. The grout pad carries the shear force by shear friction, so it must be permanently compressed by the post-tensioning tendon. Therefore the deformed reinforcement is designed to provide the

required flexural strength, and the post-tensioning tendon is designed to ensure a net pre-compression across the grout pad that is large enough to resist the interface shear by friction. The assumed positive directions of the forces and displacements are shown in Figure 7.5.

a) Dimensions and Displacements   b) Forces
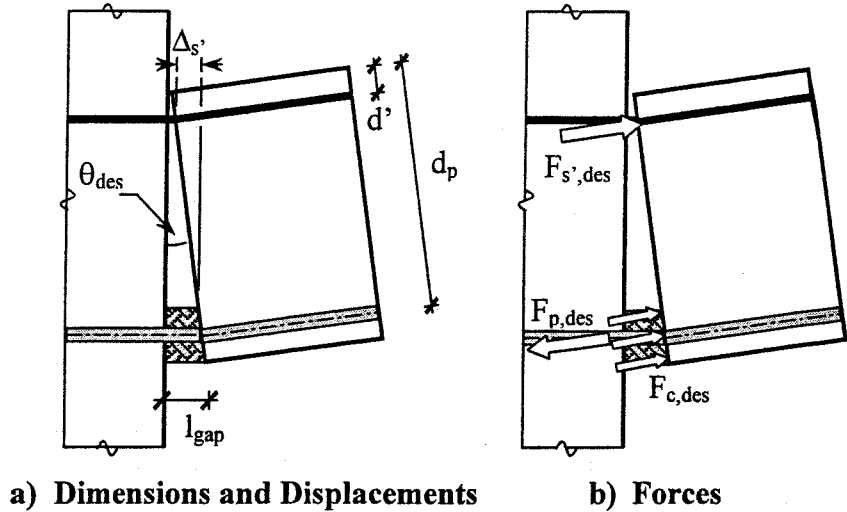
Figure 7.5: Yielding Gap Frame – Location of Forces at Design Drift

7.4.1 Design of Nonlinear Hinge

Step 1. Establish the Material Properties

Establish properties of materials to be used. These include:
- beam concrete strength
- interface grout strength and corresponding β_1
- pre-stressed tendon strength and modulus of elasticity
- deformed reinforcement yield and tensile strength, and strain at maximum strength

Step 2 Select the Gap Size

The gap size depends on the drift to be accommodated. Proper functioning of the connection requires that no contact occur between the beam and column faces at top of the interface. Therefore the gap must satisfy

$$l_{gap} \geq \theta_{des} d_p \dots\dots\dots\dots\dots\dots\dots\dots\dots\dots\dots\dots\dots(7.1)$$

Step 3 Select the Area of Deformed Reinforcement

The continuity bars grouted into the ducts must satisfy

$$A_s \geq \frac{M_{des}}{(d_p - d')0.5(\lambda_{s,des} + \lambda_{s',des})f_{sy}} \quad\quad\quad (7.2)$$

The average $\lambda_{s,des}$ value is used in Equation 7.2 because at one end of the beam the continuity bars will be in tension, whereas at the other they will be in compression. Use of the average material overstrength factor allows the structure to be analyzed assuming the strength of the beam is the same in negative and positive bending. The value of the material stress factor, $\lambda_{s,des}$, depends on the limit state under consideration, and the corresponding allowable strain in the bar reinforcement. Suitable values are given in Table 2.1. The value required in Equation 7.2 is the one that corresponds to the design limit state.

Step 4 Select the Debonded Length for the Bars

The bars must be debonded locally to prevent fracture through excessive strain. The bar may be debonded locally by wrapping or sleeving. The debonded length should be in the beam, not the column. The total debonded length must satisfy

$$l_{su} \geq \frac{\theta_{des}(d_p - d')}{\varepsilon_{s,max}} \quad\quad\quad (7.3)$$

High cyclic strains can cause growth in the unbonded length. The magnitude of that growth depends on the confinement provided around the bar and other parameters. For bars grouted into a pre-formed hole in the concrete, Cheok and Stone [1994] found the growth in debonded length to be $5.5d_b$ ($2.75d_b$ at each end of the intentionally debonded length) for a #3 bar. More recent testing on bars grouted in corrugated steel ducts [Stanton et al. 2002] has shown that, under those circumstances, the growth depends on bar strength, grout strength and load history, but is on the order of $1.0d_b$.

If the estimated debonded length is greater than the true one, the true bar strain will be higher than the predicted one, and the bars may fracture prematurely. If the estimated debonded length is less than the true one, the true strain will be lower than predicted and yield of the bars will be delayed. The consequences are that the bar stress, and therefore the resisting moment, at peak drift will be slightly lower, as will also be the damping. However, these changes will be very small. Because the consequences of predicting too high a growth in the debonded length are much more serious than those of a low prediction, the growth in debonded length is assumed here to be zero.

Step 5 Select the Post-tensioned Reinforcement

The force in the post-tensioning tendon must be large enough to resist the compression in the reinforcing bars and still provide sufficient clamping force to resist vertical shear across the grout pad by shear friction. The post-tensioning tendon must satisfy all three of Equations 7.4 – 7.6, each of which addresses a different condition. If the seismic shear adds to the gravity shear, (i.e. the continuity bars are in tension)

$$A_p f_{p0} \geq \frac{V_{u,D+L}}{\phi_v \mu} + \left(\frac{d_p - d'}{\phi_v \mu l_n}\right)\left(F_{s,des} + F_{s',des}\right) - F_{s,des} \quad \text{.....................................(7.4)}$$

If the seismic and gravity shears oppose each other, and the gravity shear is less than the seismic shear,

$$A_p f_{p0} \geq \frac{-V_{u,D+L}}{\phi_v \mu} + \left(\frac{d_p - d'}{\phi_v \mu l_n}\right)\left(F_{s,des} + F_{s',des}\right) + F_{s,des} \quad \text{.....................................(7.5)}$$

If the seismic and gravity shears oppose each other, and the gravity shear is larger than the seismic shear,

$$A_p f_{p0} \geq \frac{V_{u,D+L}}{\phi_v \mu} - \left(\frac{d_p - d'}{\phi_v \mu l_n}\right)\left(F_{s,des} + F_{s',des}\right) + F_{s,des} \quad \text{.....................................(7.6)}$$

where $F_{s,des} = A_s \lambda_{s,des} f_{sy}$ ....(7.7)

$F_{s',des} = A_s \lambda_{s',des} f_{sy}$ ....(7.8)

The forces $F_{s,des}$ and $F_{s',des}$ are positive quantities, regardless of whether they are tensile or compressive. In most cases, Equation 7.5 will control the tendon design.

The post-tensioning tendon does not elongate during lateral displacement of the frame, so the stress in it may be based on initial stressing conditions and losses. Stress limits are given in Section 18.5.1 of ACI 318-99.

Step 6 Design the Grout Pad

The compressive strength, C_g, of the grout pad must satisfy

$$C_g \geq A_p f_{p0} + \lambda_{s,des} A_s f_{sy} \quad \text{...} (7.9)$$

Under seismic loading, the grout pad experiences compression that varies from $\left(A_p f_{p0} - \lambda_{s',des} A_s f_{sy}\right)$ to $\left(A_p f_{p0} + \lambda_{s,des} A_s f_{sy}\right)$. In addition, the beam end rotates, so the grout pad will be subjected to compression plus bending. In order to minimize the adverse effects of the bending, the pad should be kept small and made of high strength material. It should also be well confined both in order to increase its strength and to provide it with some ductility. This may be achieved by suitable reinforcement, for example with fibers. Because the grout pad is a critical element, a relatively high dosage of fiber, such as 1% by volume of stainless steel fibers, is recommended.

7.5 Design of other components

7.5.1 Interface Shear

The most critical element for interface shear transfer is the pre-compression across the grout pad, which is controlled by the post-tensioning tendon and is described in Step 4. If the calculation does not account for the true compression capacity of the continuity bars, represented here by the $F_{s,des}$ and $F_{s',des}$ values, the friction at the interface may be inadequate to resist the shear.

7.5.2 Beam Flexure

The primary reinforcement cast into the top of the beam should be designed not to yield, even when the continuity bars in the ducts have strain-hardened. In this way, the cracks in the beam may be kept fine and damage may be minimized.

During cyclic frame displacements, the beam end moments may become equal in magnitude and opposite in sign (i.e. both clockwise or both counter-clockwise). Their effect on the mid-span moment capacity is then zero, so moment demand at mid-span is the same as that for a simple span. Reinforcement should be selected accordingly. Pretensioning may be used if desired. The post-tensioning may be taken into account in evaluating the gravity load capacity of the beam, provided that it is in place when the load occurs.

7.5.3 Beam Shear

The beam shear conditions at the interface are different depending whether the force acts up or down, as shown in Fig 7.6.
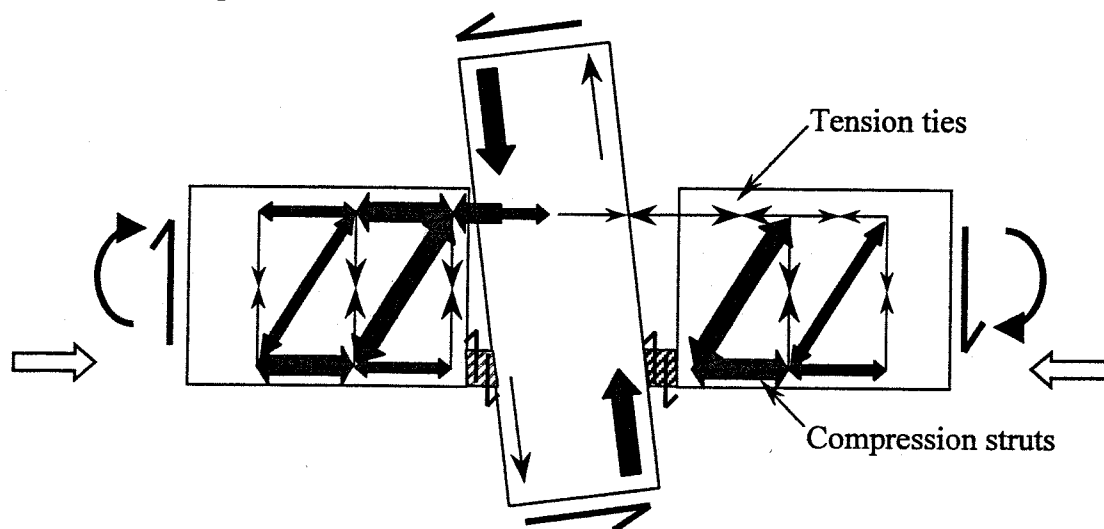
Figure 7.6: Yielding Gap Frame – Beam Shear Truss Models

7-8

For upward shear, a strut and tie model shows that, at the very end of the beam, a set of stirrups is needed that will carry the entire shear force. This is so because the shear must be transferred through the grout pad and not through the compression bars. For downward shear, the strut starts at the grout pad and propagates diagonally upward into the beam, so the behavior is comparable to that of a cast-in-place beam.

7.5.4 Beam Torsion

The beam-column interface can resist little torsion because the gap there is always open. The floor system should therefore be designed so as to minimize the torsional demand on the beam.

7.5.5 Bond and Anchorage

The minimum permissible length for the ducts in the beam depends on the transfer of force from the duct to the adjacent bar embedded directly in the beam. The maximum available length of the ducts is most likely controlled by the method of installation of the bars. They may be loaded into the duct before the beam is placed, then slid along the duct, through the column, once the beam is in place on temporary corbels. Sliding the bar requires access to it, which may be gained by means of a trough or opening in the beam, which is best located near mid-span. The presence of such a trough may limit the available duct length. The effect of the additional debonded length described in Step 3 should be taken into account. When computing the anchorage length, the additional debonded length should be assumed to have its maximum probable value. This may be taken as $2d_b$ at each end of the deliberately debonded region for bars grouted in ducts.

7.5.6 Column Design

Column design, other than the joint region, is conducted using conventional procedures. The column may be pre-tensioned for handling if desired. If it is, the bending strength provided by the pre-tensioning should be accounted for. Attention should be paid to the space needed for horizontal ducts, which may influence the arrangement of longitudinal column bars.

7.5.7 Joint Shear

The beam-column joint should be designed by conventional means, but the amount of joint steel may differ from that required by Section 21.4.4.1 of ACI 318-99. Detailed study of the joint shear behavior of a Yielding Gap frame joint has yet not been conducted. It is likely that the horizontal pre-compression due to the post-tensioning will improve the joint resistance [Pantazopoulou and Bonacci, 1992], but the fact that all the force is introduced by bar bond, rather than by direct concrete compression, may detract from it. Direct compression loading of the joint tends to cause more of the force to be carried by the main diagonal strut, whereas forces introduced through bar bond tend to be carried by the truss mechanism that includes the ties [Priestley and Paulay 1992]. Further investigation of the joint shear behavior of this system is desirable.

8 SUMMARY AND CONCLUSIONS

8.1 Summary

Guidelines are presented for the structural design of five different precast concrete seismic framing systems. The behavior expected of each system is described, and step-by-step procedures are given for establishing the capacities of the primary components of each system.

The five systems were included in the PRESSS Phase III test building, tested at the University of California at San Diego in August and September 1999. Those tests were conducted using pseudo-dynamic loading and a variety of different intensities. The most severe loading was equivalent to 150% of the Zone 4 design earthquake embodied in the 1997 UBC. Details of the tests are provided by Priestley et al. [1999].

The test building performed very well, maintaining good lateral resistance to a peak roof drift of approximately 4% in the frame direction and 3% in the wall direction. Damage was much less than would be expected in a comparable conventional reinforced concrete SMRF structure subjected to the same loading. In the frame direction, the loading was arranged so that the building did not twist. Therefore the residual drift was the same on both sides of the building. It was also very small. It is believed that the self-centering characteristics of the pre-stressed frame provided most of the benefits. In a prototype structure without the restraint against twisting, the two types of frame would likely have displayed different residual drifts. In the wall direction, the residual drift was approximately 0.0006 radians, or approximately 2% of the peak drift during the testing, and the damage was minimal. From the points of view of alignment, plumb, and structural damage, the building was fully serviceable directly after the test.

8.2 Conclusions

The following conclusions can be drawn from the study:

1. The three pre-stressed systems (the Unbonded Post-Tensioned Frame with Damping, the Unbonded Pre-tensioned Frame and particularly the Unbonded Post-Tensioned Split Wall) all represent structural systems that can be expected to provide good structural performance. They offer a characteristic that is not available in the framing systems presently recognized in the 1997 UBC, namely zero residual drift. The choice of conferring this characteristic on the building lies within the control of the designer.

2. Local debonding near the interface allows the deformed reinforcement to yield and to provide inelastic deformations, without inflicting significant damage on the surrounding concrete.

3. The Yielding Frame may be expected to provide good flexural ductility, but it will not on its own re-center. A further disadvantage is that vertical shear at the beam-column interface must be transferred by dowel action. That action risks kinking the main bars and leading to their premature fracture. This behavior was not observed in the test because the bars lost bond and did not develop large enough forces, but it is likely to occur in the field. Without a rational design procedure for the interface shear, and experimental verification of good response, the Yielding Frame cannot be recommended for use.

4. The Yielding Gap frame incurred some damage, but maintained its load-carrying capability throughout the testing. However, the damage was attributed to a shortcoming in the detailed design, rather than any error in the basic concept. Thus, while the Yielding Gap Frame cannot be recommended for use now, it merits further development because it has the potential for eliminating the undesirable effects of beam growth.

5. Displacement Based Design offers a viable method for determining the required lateral strength of the structure. It allows the designer to take full advantage of the special characteristics of the systems described here, whereas Force Based Design does not. It also allows the designer a means of designing simply and straightforwardly for different levels of performance in all structural systems.

8.3 Recommendations

1. A series of detailed design examples should be prepared for each of the systems described in this report and should be communicated to the design community through workshops or other means.

2. Studies are needed to correlate the design capacities described in this report with design loads specified in codes, such as NEHRP [2000], for different performance levels.

3. Further development and testing should be conducted on the Yielding Gap Frame system. It shows considerable promise of solving the problems of beam growth due to plastic hinging that occur in both cast-in-place frames and precast frames without gaps at the joint.

4. A study should be undertaken to determine the appropriate compressive deformation limits and confining strategies for concrete reinforced with partially unbonded reinforcement, both pre-stressed and non-pre-stressed, in which the flexural rotation is concentrated at a single crack.

9 REFERENCES

"Building Code Requirements for Reinforced Concrete (ACI 318-99) and Commentary". ACI, Farmington Hills, MI.

Cheok, G.S. and Stone, W.C. (1994). "Performance of 1/3 Scale Model Precast Concrete Beam-Column Connections Subjected to Cyclic Inelastic Loads – Report No. 4". Report No. NISTIR 5436, NIST, Gaithersburg, MD, June.

Cheok, G.S., Stone, W.C. and Nakaki, S.D. (1996). "Simplified Design Procedure for Hybrid Precast Connections". Report No. NISTIR 5765, NIST, Gaithersburg, MD, Feb.

Chopra, A.K. (1999). "Dynamics of Structures: Theory and Applications to Earthquake Engineering". 2nd ed. Prentice Hall.

Chopra, A.K. and Goel, R.K. (2001). "Direct Displacement-Based Design: Use of Inelastic vs. Elastic Design Spectra. " Earthquake Spectra, 17(1), Feb., pp 47-64.

Eberhard, M.O. and Sozen, M.A.. (1993) "A Behavior-Based Method to Determine Design Shear in Earthquake-Resistant Walls," *ASCE. Jo. Struct. Eng.*, 119(2), Feb., pp. 619-640.

Fenwick, R.C. and Megget, L.M. (1993). "Elongation and Load-Deflection Characteristics of Reinforced Concrete Members Containing Plastic Hinges". *Bulletin of the New Zealand National Society for Earthquake Engineering*, 26(1), Jan, pp. 28-41.

Galusha, J.G. (1999). "Precast, Post-tensioned Concrete Walls Designed to Rock". MSCE Thesis, University of Washington, Seattle, WA, 103 p.

Gulkan, P. and Sozen, M.A. (1974). "Inelastic Response of Reinforced Concrete Structures to Earthquake Motions". ACI Jo., ACI, Detroit, MI. pp. 604-610.

Hutchinson, R.L., Rizkalla, S.H., Lau, M. and Heuvel, S. (1990). "Horizontal Post-tensioned Wall Connections for Precast Concrete Load-Bearing Shear Wall Panels". *PCI Jo*. 36(6), Nov-Dec, pp. 64-76.

"International Building Code". (2000). International Code Council, Falls Church, VA.

Kelly, J.M., Skinner, I., and Heine, A.J. (1972). "Mechanisms of Energy Absorption in Special Devices for Use in Earthquake Resistant Structures". *Bulletin of the New Zealand National Society for Earthquake Engineering*, 5(3), pp. 63-68.

Kurama, Y., Pessiki, S., Sause, R., Lu, L.-W. and Sheikh, M. (1998). "Analytical Modeling and Lateral Load Behavior of Unbonded Post-Tensioned Precast Concrete Walls." Report No. EQ-96-02, Lehigh University, Bethlehem, PA.

Meinheit, D.F. and Jirsa, J.O., (1977). "The Shear Strength of Reinforced Concrete Beam-Column Joints". CESRL Repot No. 77-1, Dept. of Civil Engineering, University of Texas at Austin, Austin, TX, Jan, 271 p.

Mosier, W.G. "Seismic Assessment of Reinforced Concrete Beam-Column Joints". MSCE Thesis, Dept. of Civil Engineering, University of Washington, 2000. 218 p.

Nakaki, S.D, Stanton, J.F. and Sritharan, S., (1999). "An Overview of the PRESSS Five Story Precast Test Building". *PCI Jo.*, 44(2), Mar.-Apr., pp. 28-39.

"NEHRP Recommended Provisions for Seismic Regulations for New Buildings and Other Structures: Part I, Provisions (FEMA 368) and Part II, Commentary (FEMA 369)". (2000). Building Seismic Safety Council, Washington DC.

Palmieri, L., Saqan, E., French, C. and Kreger, M. (1996). "Ductile Connections for Precast Concrete Frame Systems". Paper No. SP 162-13, *Mete A. Sozen Symposium, SP-162*, ACI, Farmington Hills, MI, pp. 312-355.

Pantazopoulou, S. and Bonacci, J. (1992). "Consideration of Questions about Beam-Column Joints". *ACI Str. Jo.,* 89(1), Jan.-Feb., pp. 27-36.

Paulay, T. and Priestley, M.J.N. (1992*). "Seismic Design of Reinforced Concrete and Masonry Structures".* Wiley.

PCI Committee on Connection Details. (1988). "Manual on Design and Detailing of Connections for Precast and Prestressed Concrete". PCI, Chicago, IL.

Priestley, M.J.N., (1996). "The PRESSS Program – Current Status and Plans for Phase III*". PCI Jo.,* 41(2), Mar.-Apr., pp. 22-40.

Priestley, M.J.N. (2000) " Performance-Based Seismic Design". State-of-the-Art Plenary Session 2, *12WCEE,* Auckland, New Zealand, Jan.

Priestley, M.J.N. and Kowalsky, M.J., (2000) "Displacement-Based Design for Multi-Degree of Freedom Systems". *Bulletin of the New Zealand National Society for Earthquake Engineering.* 33(4), pp. 421-444.

Priestley, M.J.N., Kowalsky, M.J., Ranzo, G. and Benzoni, G. (1996) "Preliminary Development of Direct Displacement-Based Design for Multi-Degree of Freedom Systems". *Proc. SEAOC Annual Conference,* Oct.

Priestley, M.J.N., and MacRae, G.A., (1996). "Seismic Tests of Precast Beam-to-Column Joint Subassemblages With Unbonded Tendons," *PCI Jo.*, 41(1), Jan.-Feb. pp. 64-81

Priestley, M.J.N, Sritharan, S., Conley, J. and Pampanin, S. (1999) "Preliminary Results form the PRESSS Five Story Test Building". *PCI Jo.,* 46(6), Nov-Dec. pp. 42-67.

Saint Venant, B. (1855). "Memoire des Savants Etrangers". *Journal de Mathematique,* Liouville, taille 14.

Schultz, A.E. and Magana, R.A. (1996). "Seismic Behavior of Connections in Precast Concrete Walls". Paper No. SP 162-12, *Mete A. Sozen Symposium, SP-162,* ACI, Farmington Hills, MI, pp. 273-311.

Shahawy, M. and Cai., C.S. (2001). "Enhancement of the Performance of Prestressed Concrete Bridge Girders Using Strand Anchorage". PCI Jo. 46(5), Sept.-Oct., pp. 82-97.

Shibata, A. and Sozen, M.A. (1976). "Substitute-Structure Method for Seismic Design in R/C". *ASCE Str. Jo.,* 102(ST1), Jan., pp. 1-18.

Stanton, J.F., Raynor, D. and Lehman, D.E. (2002). "Bond Characteristics of Reinforcing Bars Grouted in Ducts". Accepted for publication by *ACI Str. Jo.*

Stanton, J.F., Anderson, R.G., Dolan, C.W. and McCleary, D.E. (1987). "Moment Resistant Connections and Simple Connections". *PCI Jo.* 32(2), Mar.-Apr. pp. 62-74.

Stone, W.C., Cheok, G.S. and Stanton, J.F. (1995). "Beam-Column Connection Subjected to Seismic Loads". *ACI Str. Jo.,* 92(2), Mar.-Apr., pp. 229-249.

"Tentative Guidelines for Performance-Based Engineering" (1999). In Appendix I, *Recommended Lateral Force Requirements and Commentary,* Structural Engineers Association of California, Sacramento, CA.

"Uniform Building Code" (1997). International Conference of Building Officials, Whittier, CA.

Veletsos, A.S. and Newmark, N.M. (1960), "Effect of Inelastic Behavior on the Response of Simple Systems to Earthquake Motions". *Proc. 2WCEE,* Tokyo and Kyoto, 1960. pp. 895-912.

Zerbe, H.E. and Durrani, A.J. (1989). "Seismic Response of Connections in 2-Bay R/C Frame Subassemblies". *ASCE, Jo. Str. Eng.,* 115(11), pp. 2829-2844.

10 DEFINITIONS

Capacity Design - A design process whereby one group of structural elements is protected against damage by designing it to be stronger than the neighboring elements through which the load must be transmitted.

Continuity Bars - Deformed reinforcing bars grouted into ducts or cast into site-cast concrete that provide structural continuity between the ends of a beam and the adjoining framing elements.

Deformed Reinforcement - Deformed reinforcing bars, bar mats, deformed wire, welded plain and deformed wire fabric conforming to the requirements of ACI 318-99.

Design Displacement – Total lateral displacement expected for the Design Basis Earthquake.

Dowel action – Carriage of transverse shear force by a reinforcing bar by means of shear stresses in the bar.

Equivalent Mode Shape – An assumed deformed shape of the structure that is used in Displacement Based Design in lieu of the true elastic first mode shape.

Essentially Rigid Body Motion – Motion in which the rigid body component is significantly greater than the deformation component.

Interface – The meeting point of two elements that undergo nonlinear action during seismic loading.

Monolithic Frame – A cast-in-place concrete seismic frame that is reinforced with deformed reinforcement only.

Tendon – Strand or high strength bars that are used for pre-stressing.

Wall Element – Part of a wall that is cast in a single piece.

Wall Panel – Part of a wall, which may be composed of several wall elements, that is designed to exhibit essentially rigid body motion and to undergo shear displacement relative to any adjacent wall panels.

11 ACRONYMS

ACI   = American Concrete Institute
ARS   = Acceleration Response Spectrum
ASTM   = American Society for Testing Materials
DBD   = Displacement Based Design
DOF   = Degree-of-freedom
DRS   = Displacement Response Spectrum
EDC   = Energy dissipated per cycle
ELF   = Equivalent Lateral Force
FBD   = Force Based Design
IBC   = International Building Code
MDOF   = Multi-degree-of-freedom
NEHRP = National Earthquake Hazards Reduction Program
NIST   = National Institute for Standards and Technology
NSF   = National Science Foundation
PCI   = Precast/Prestressed Concrete Institute
PRESSS = Precast Seismic Structural Systems
PT   = Post-tensioning
SDOF   = Single-degree-of freedom
SEAOC = Structural Engineers Association of California
SMRF   = Special Moment Resisting Frame (as defined in UBC 1997)
UBC   = Uniform Building Code
UFP   = U-shaped flexural plate

12 NOTATION

a_0 = depth of compression stress block in grout at zero drift

a_{des} = depth of compression stress block at design limit state

A_{loop} = area of hysteresis loop

A_p = area of pre-stressing tendon

A_{rect} = area of rectangle circumscribing hysteresis loop

A_s = area of deformed reinforcement in one face of beam

b_b = width of beam

b_c = width of column

b_{duct} = width of pre-stressing duct in joint

b_g = width of grout pad at beam-column interface

b_{sc} = width of UFP connector plate

C_0 = compressive reaction on one wall panel at zero drift

C_c = compression capacity of one wall panel

C_d = ratio of inelastic to elastic drift

C_{des} = compressive reaction on one wall panel at design limit state

C_g = compressive strength of grout pad

d' = depth from top face of beam to centroid of deformed reinforcement

d_b = diameter of deformed reinforcing bar

d_p = depth from top face of beam to centroid of pre-stressing tendon

D_{sc} = bend diameter (measured at mid-thickness of plate) in UFP connector plate

$\{e\}$ = vector with elements = 1.0 in DOFs parallel to ground motion and 0.0 elsewhere

E_p = Young's modulus of pre-stressing tendon material

f'_c = specified concrete strength at 28 days

f'_g = specified grout strength at 28 days

f_{p0} = stress in pre-stressing tendon, after losses, at zero drift

$f_{p,des}$ = stress in pre-stressing tendon at design limit state

f_{pi} = maximum tendon jacking stress minus pre-stress losses

f_{pu} = specified strength of pre-stressing tendon material

f_{py} = specified yield strength of pre-stressing tendon material

f_r = modulus of rupture of concrete

$f_{s,des}$ = stress in tension deformed reinforcement

$f_{s',des}$ = stress in compression deformed reinforcement

$f_{sc,des}$ = stress in UFP connector plate under plastic conditions

f_{sy} = specified yield strength of deformed reinforcement

$F_{c,0}$ = force between beam concrete and grout at beam-column interface at zero drift

$F_{c,des}$ = force in beam concrete at beam-column interface at design limit state

$F_{p,0}$ = force in pre-stressing tendon at zero drift

$F_{p,des}$ = force in pre-stressing tendon at design limit state

F_{s0} = force in tension deformed reinforcement at zero drift

$F_{s,des}$ = force in tension deformed reinforcement at design limit state

$F_{s'0}$ = force in compression deformed reinforcement at zero drift

$F_{s',des}$ = force in compression reinforcing steel at design limit state

F_{sc} = total yield force of all shear connectors in one vertical joint

$F_{sc,left}$ = total yield force of all shear connectors in joint to left of panel

$F_{sc,net}$ = net vertical force on one panel from all shear connectors

$F_{sc,right}$ = total yield force of all shear connectors in joint to right of panel

h_b = depth of beam

h_c = depth of column (in plane of frame)

h_{eff} = height above foundation of lateral load resultant on wall

h_g = depth of grout pad at beam-column interface

h_u = unbonded length of pre-stressing tendon

h_w = total height of wall panel (used for self-weight)

k_1 = uniform stress in Whitney rectangular equivalent stress block divided by f'_g

k_{ph} = plastic hinge length factor

K = stiffness of SDOF system

K_{eq} = secant stiffness of true hysteretic system at maximum displacement

l_b = total bay dimension between column centerlines

l_c = floor-to-floor story height

l_d = development length

l_{gap} = width of gap (in direction parallel to longitudinal axis of beam)

l_n = clear span of beam between column faces

l_{ph} = plastic hinge length

l_{pu} = unbonded length of pre-stressing tendon tributary to one interface

l_{su} = length of unbonded region of deformed reinforcement at each interface

l_w = length of one wall panel (horizontal dimension in plane of wall)

$l_{w,tot}$ = total length of one wall

L = earthquake participating mass

M = mass of SDOF system

$[M]$ = mass matrix

M^* = generalized mass in first mode

$M_{cap,beam}$ = beam moment strength at interface at design limit state

$M_{cap,panel}$ = moment capacity of one panel

$M_{cap,p}$ = moment capacity provided by pre-stressed reinforcement

$M_{cap,s}$ = moment capacity provided by yielding reinforcement

$M_{cap,tot}$ = total moment capacity

$M_{cap,wall}$ = total moment capacity of wall

M_{cr} = cracking moment strength at interface

M_{des} = moment demand at design limit state

M_{eff} = effective mass in first mode

$M_{p,0}$ = resisting moment provided by pre-stressing tendon at zero drift

$M_{p,des}$ = resisting moment provided by pre-stressing tendon at design limit state

$M_{s,0}$ = resisting moment provided by tension deformed reinforcement at zero drift

$M_{s,des}$ = resisting moment provided by tension deformed reinforcement at design limit state

$M_{s',0}$ = resisting moment provided by compression deformed reinforcement at zero drift

$M_{s',des}$ = resisting moment provided by compression deformed reinforcement at design limit state

M_{sc} = plastic moment strength of one UFP connector

n = number of panels per wall

n_{sc} = number of shear connectors required per vertical joint

N_0 = total axial force on one wall panel from gravity plus post-tensioning at zero drift

N_{des} = total axial force on one wall panel from gravity plus post-tensioning at design limit state

P_0 = force in pre-stressing tendon at zero drift

P_{des} = force in pre-stressing tendon at design limit state

R = seismic response modification factor

S_a = spectral acceleration

S_d = spectral displacement

t_{sc} = plate thickness in UFP connector

t_w = thickness of wall panel

$t_{w,eff}$ = thickness of wall panel effective in resisting compressive force

T = period of linear elastic SDOF system

T_{eq} = period of equivalent viscously-damped linear SDOF system

v_{joint} = joint shear stress

$V_{col,des}$ = column shear force at design limit state

V_{des} = design base shear

V_{eq} = design base shear of equivalent viscously-damped linear system

V_{joint} = joint shear force

V_{max} = peak shear experienced during pushover analysis

V_n = nominal shear strength

V_{sc} = shear strength of one UFP shear connector

V_u = factored shear demand

$V_{u,D+L}$ = factored dead and live load shear demand at interface

w_{floor} = distributed vertical load on wall, at base, from all floors

W = total gravity load from all floors on one wall panel

W_{panel} = self-weight of one panel

α_0 = distance from compression face of member to center of compression force, divided by member depth, at zero drift

$\alpha_{0,ave}$ = average value, over all panels, of α_0

α_{des} = distance from center of compressive reaction to edge of member divided by member depth, at design limit state

$\alpha_{des,ave}$ = average value, over all panels, of α_{des}

β_1 = depth of equivalent compressive stress block divided by neutral axis depth

γ_c = density of concrete

Γ = earthquake participation factor

Δ_{fp} = increase in stress in pre-stressing tendon between zero drift and design drift

$\Delta_{fp\infty}$ = increase in stress in pre-stressing tendon between zero drift and design drift when concrete and grout strengths are infinite

Δ_M = inelastic drift of structure under reduced earthquake load in 1997 UBC

Δ_p = deformation of pre-stressing tendon between zero drift and design drift

Δ_s = deformation of tension deformed reinforcement

Δ_S = elastic drift of structure under reduced earthquake load in 1997 UBC

$\Delta_{s'}$ = deformation of compression deformed reinforcement

$\Delta_{tar,MDOF}$ = target displacement for MDOF system

$\Delta_{tar,SDOF}$ = target displacement for SDOF system

ε_c = compression strain in extreme fiber of concrete

ε_s = strain in tension deformed reinforcement

$\varepsilon_{s,max}$ = maximum strain permissible in deformed reinforcement under cyclic loading

$\varepsilon_{s'}$ = strain in compression deformed reinforcement

$\varepsilon_{sc,des}$ = strain in UFP connector plate at design limit state

$\varepsilon_{sc,max}$ = maximum permissible strain in UFP connector plate under cyclic loading

$\varepsilon_{sc,u}$ = strain at maximum stress in UFP connector plate material

ζ = distance from beam deformed reinforcement to nearest face divided by h_b

η_0 = distance from member compression face to neutral axis divided by member depth, at zero drift

η_{des} = distance from member compression face to neutral axis divided by member depth, at design limit state

θ_{des} = interface rotation at design limit state

κ_0 = ratio of design strength of shear connectors in one joint to vertical load on one panel

λ = over-strength factor

λ_p = over-strength factor for pre-stressed reinforcement in tension

λ_s = over-strength factor for deformed reinforcement in tension

$\lambda_{s,des}$ = over-strength factor for deformed reinforcement in tension at design limit state

$\lambda_{s'}$ = over-strength factor for deformed reinforcement in compression

$\lambda_{s',des}$ = over-strength factor for deformed reinforcement in compression at design limit state

μ = coefficient of friction

ξ = viscous damping

ξ_{eq} = viscous damping in equivalent linear system

$\xi_{eq,calc}$ = calculated viscous damping in equivalent linear system

$\xi_{eq,est}$ = estimated viscous damping in equivalent linear system

ρ_{fp0} = stress ratio to ensure that pre-stressing tendon does not yield at maximum drift

ρ_{MOM} = demand/capacity ratio for overturning moment on panel

ρ_{ROC} = force ratio to ensure that panel slides rather than rocks

ρ_{UPL} = ratio of uplift force to hold-down force on one panel

ρ_{ZRD} = parameter ratio controlling residual drift

$\{\phi_{eq}\}$ = equivalent mode shape, or assumed deformed shape

ϕ_v = strength reduction factor for shear

ω = natural frequency of SDOF system

ω_{eq} = natural frequency of equivalent linear SDOF system

Appendix A.

List of planned PRESSS Phase III Reports.

Volume 3-1: Seismic Design
Volume 3-2: Construction
Volume 3-3: Test Procedures and Instrumentation
Volume 3-4: Frame Direction Response
Volume 3-5: Wall Direction Response
Volume 3-6: Test Database
Volume 3-7: Response Predictions
Volume 3-8: Analytical Parameter Studies
Volume 3-9: Design Guidelines
Volume 3-10: Summary Volume